Chapter 1

Historical and Review Papers

THIS chapter contains a collection of review and historical papers on quasi-optical and active antenna techniques for power combining and beam control. In addition to their archival value, the papers in this chapter have been selected to provide a general tutorial introduction to the subject, a theoretical background, an explanation of basic concepts, and a summary of recent trends. This chapter was intended to serve as a useful stand-alone overview of the topical area, without the technical detail provided in the chapters to follow.

The first paper in this chapter, "Quasi-optical power combining: A perspective," has been written specifically for this book by Mink, Steer, and Wiltse. It summarizes recent trends in the field, which have occurred since the publication of Mink's seminal paper in 1986 [1]. In addition to specific references, an extensive general bibliography has also been included. It is written in a style to be useful to the general reader and the engineer entering the new field. This paper is followed by Mink's 1986 paper, in which the concept of quasi-optical power combining was successfully quantified for the first time.

Several different architectural structures have been utilized for the design of quasi-optical power combining circuits. Quasi-optical techniques have been used to interface arrays of oscillators with a modal electromagnetic field and arrays of amplifiers with a traveling electromagnetic field. The near-term industrial and military emphasis is on amplifier arrays, because good low-power tunable sources of high-purity signals are available that can be amplified quasi-optically to high-power levels. The architecture introduced by Mink in his 1986 paper combined an array of oscillators in an open resonant cavity. The third paper in this chapter describes the quasi-optical power combining in oscillator and amplifier grid arrays. In grid array architecture, devices are spaced much closer than a wavelength, with the metallic connectors acting collectively as a large antenna structure. An alternative structure uses an array of unit cells, each containing an amplifier or oscillator circuit and a separate resonant antenna element. This type of architecture is described in later chapters. A third alternative architecture is a relatively recent, emerging development, a two-dimensional combining structure, which is described in detail in Chapter 8.

One potential advantage of quasi-optical power combining over other combining techniques is the ease with which higher order functionality, such as beam control, external injection locking, frequency multiplication, and frequency mixing can be introduced. An excellent review paper by York [2] discusses injection locking and beam steering of oscillator arrays by control of oscillator phase and frequency but could not be included in this volume. An alternative beam control technique is a beam steering quasi-optical grid, discussed in Chapter 5. The fourth paper in this chapter is a review of quasi-optical mixer approaches and also describes some frequency multiplication applications.

Most quasi-optical arrays based on semiconductor technology utilize active antennas or active antenna elements in the unit cell. The active antenna element is usually a printed planar antenna incorporating an active semiconductor device directly integrated with the antenna structure. As a result this antenna element minimizes transmission line losses and provides quasi-optical arrays with the potential for very high efficiency power combining. In addition to its application in arrays, individual active antennas can provide functionality not available from conventional passive antennas. Paper 5 is a review of active integrated antennas.

References:

[1] J. W. Mink, "Quasi-optical power combing of solid-state millimeter wave sources," *IEEE Trans. Micorwave Theory Techn.*, Vol. MTT-34, Feb. 1986, pp. 273–279.

[2] R. A. York, "Quasi-optical power combining techniques," in J. C. Wiltse (ed.), *Millimeter and Microwave Engineering for Communications and Radar*, CR54, SPIE Optical Engineering Press, Bellingham, WA, 1994, pp. 63–97.

Quasi-Optical Power Combining: A Perspective

JAMES W. MINK,* MICHAEL B. STEER,* AND JAMES C. WILTSE†
*North Carolina State University, Raleigh, NC 27695–7911
†Georgia Tech Research Institute, Atlanta, GA 30332

Abstract—**This section summarizes recent progess in power-combining of solid-state sources at microwave and millimeter wavelengths.**

Introduction

For many years, there has been a need to obtain more power from solid-state devices, both sources and amplifiers in the upper microwave, millimeter, and submillimeter wavelength regions of the electromagnetic spectrum. There exist many system applications in common use today and their range of application is expanding, It is safe to predict that these systems will be utilized in the future across the spectrum of endeavors from communications to radar, transportation, industrial, and scientific applications (such as radio astronomy and spectroscopy). Satisfying this expanding demand mandates the utilization of previously unused, or little used, millimeter and submillimeter wave bands. In accordance with a long-term trend, systems will migrate toward higher and higher frequencies; the necessary technology, however, is not very well developed at the present time. A fundamental limitation has been and continues to be the lack of convenient power sources and amplifiers. Component costs have been driven by the small size and tight tolerance associated for millimeter sources and in the case of waveguide components, by the need for hand assembly. This is more urgent at millimeter-wave frequencies than at microwave-wave frequencies because microwave sources generally give better performance in terms of parameters such as power output, efficiency, and/or spectral purity. Solid-state devices are highly reliable; however, their output power tends to be very low due to the small physical size of the active region, resulting in the well-known $1/f^2$ falloff of available power. Hence, a need exists to combine the outputs of many individual elements to satisfy the system power requirement.

Many of the problems stated above may be resolved through the use of quasi-optical techniques. The term "quasi-optical" is used to denote the utilization of a short-wavelength electromagnetic technique (approaching optical) in a relatively long wavelength (microwave) region. Quasi-optical devices typically have cross-sectional dimensions in the order of 10–100 wavelengths and are relatively easy to fabricate. Tolerance requirements are greatly relaxed since boundary surfaces along the propagating directions of the guiding structure are not critical for mode selection and maintenance of mode purity. Rather, easily manufactured lenses or reflectors, and the spacing between them, establish the mode parameters. In addition, the rather large transverse dimensions of quasi-optical structures allow one the freedom to include numerous solid state sources to achieve the desired output power.

Architectures

All quasi-optical systems have several features in common: at least one transverse dimension is large compared to the wavelength; the longitudinal dimension is also large and may be large compared to the transverse dimension; hence, many individual solid-state sources may be integrated into the structure. While dimensions are large compared to the wavelength, the mode supported by the structure is only a single mode, or at most a small number of modes may exist in the structure [1]. The concept employs a wavebeam resonator (Fabry-Perot resonator) as the power combining concept and is similar to an optical laser as shown in Figure 1. The resonator enforces the collective emission of otherwise independent oscillators with a resonator geometry practical for short-wavelength emission, which makes it possible for all oscillators to operate in a coherent manner. In the case of the laser, a very large number of oscillators, in the form of individually excited molecules, populate the volume of the resonator. Individual molecular oscillators are stimulated in a coherent fashion by the standing wave or by the mode that is characteristic of the quasi-optical geometry. This basic concept has been extended to the developing of coherent emission of a collection of individual solid-state devices in the millimeter and submillimeter wave combiners. The departure for analogy to the laser is due to the fact that individual oscillators are macroscopic devices which include coupling elements (antennas), rather than individual molecules.

In recent years, research emphasis has been placed upon three principal classes of quasi-optical systems. One of the first structures to be investigated was that of an open resonator, commonly referred to as the Fabry-Perot resonator, with solid-state sources located in a plane transverse to the direction of propa-

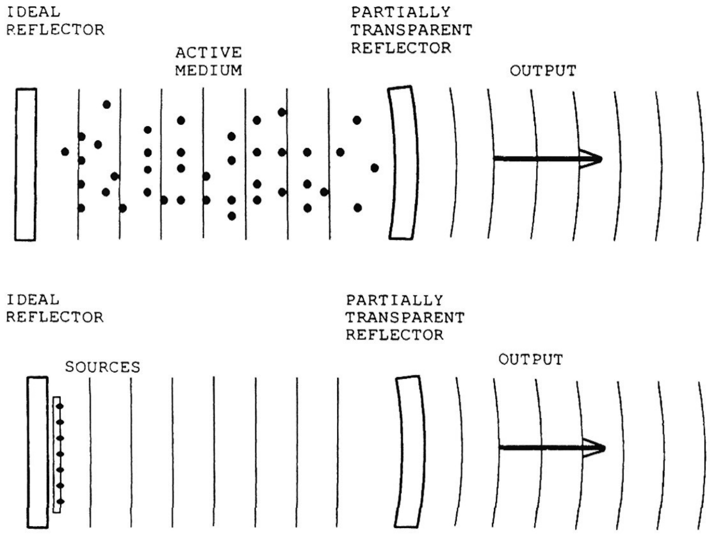

Fig. 1 Similarity between the gas laser and quasi-optical sources.

gation. The electromagnetic mode structure of open resonators is well known and characterized. [1] Since the physical size of each solid-state source is much smaller than the wavelength, a coupling device must be employed to extract energy from the active element and transfer it to the wavebeam. Many coupling devices have been investigated, including small dipoles [2], loop elements [3], microstrip elements [4], and one-dimensional waveguide structures [5]. In each case, the goal of such coupling elements is to impedance match between the active device and the electromagnetic wavebeam. An example of an open resonator structure is shown in Figure 2. Feedback required for oscillation is obtained primarily through the electromagnetic wavebeam, with a small but measurable contribution due to direct mutual interaction between the coupling devices [6].

The second structure is that of the grid oscillator and amplifier, which is the most highly developed quasi-optical structure at this point in time. The investigation of this structure is primarily due to the efforts of Professor Rutledge and his associates. In this case an array of active elements is placed in a uniform grid, which intercepts the electromagnetic wave, with each element connected to its nearest neighbors via a printed transmission line/antenna structure [7-9]. When one considers the grid structures, feedback to obtain oscillation is principally via the transmission line located between the active elements, also with significant coupling via the electromagnetic wave beam. Since the adequate feedback for oscillation requires both components of feedback, grid structures are well suited for both amplifiers as well as oscillators. In the oscillator case, the electromagnetic beam coupling is relatively small, and it becomes essential to ensure that all active elements oscillate coherently and in phase, as opposed to antiphase oscillation [10]. An example of the typical grid amplfier of the type pioneered by Professor Rutledge and his associates is shown in Figure 3a [7]. Also shown in Figure 3b is a detailed depiction of one active element cell [11]. Grid amplifiers have shown gain of about 5 dB operating at about 40 Ghz with maximum power output of 670 mW [12]. Grid oscillators are very similar to grid amplifiers, except that the feedback element, in this case a reflector, is added to the system. To date grid oscillators have produced the highest power level of about 10 W in the X-band [13].

The third class of quasi-optical systems are based upon the hybrid dielectric slab-beam waveguide [14, 15]. The hybrid slab-beam waveguide consists of a thin dielectric slab, usually grounded on one side, into which phase correcting elements are inserted. The phase correction element for an oscillator is usually a partially transparent curved reflector; energy is extracted through that reflector. The hybrid dielectric slab-beam wave-

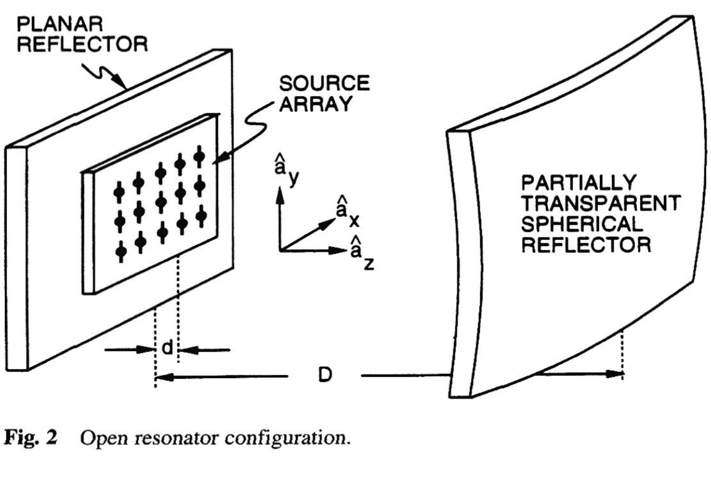

Fig. 2 Open resonator configuration.

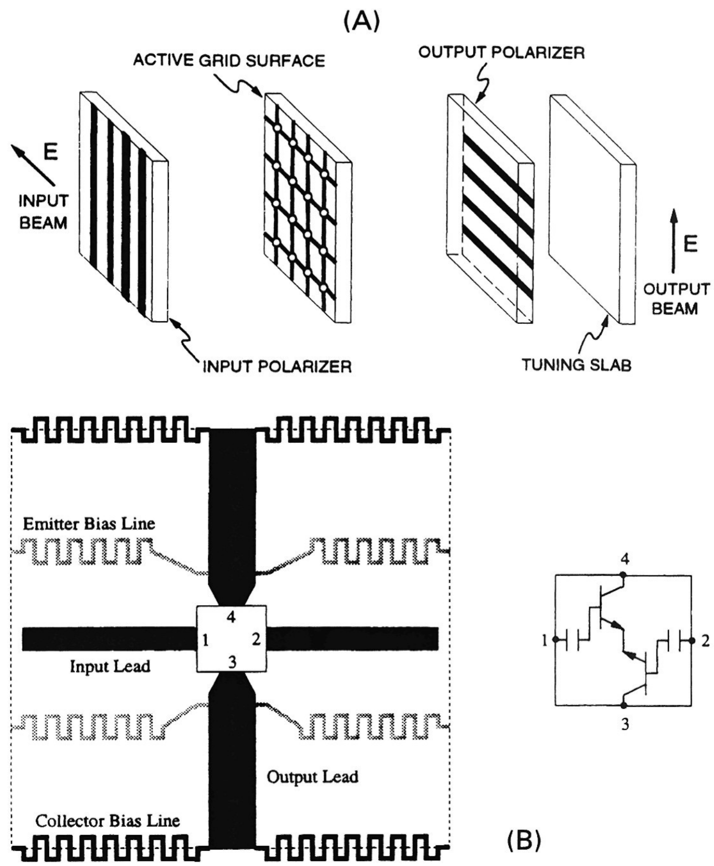

Fig. 3 Grid amplifier configuration. (a) Grid amplifier (b) Active surface unit cell.

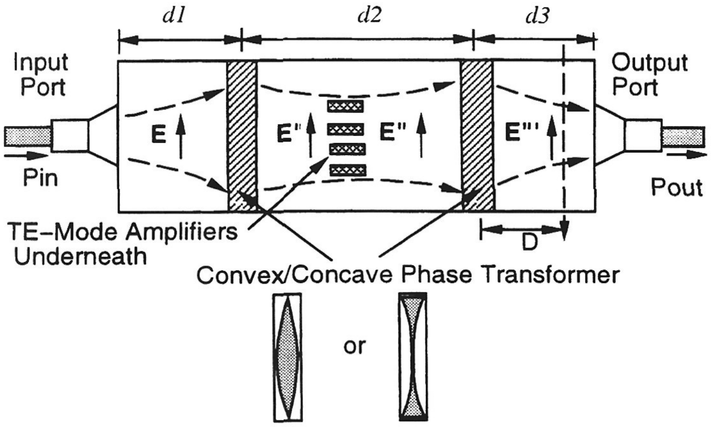

Fig. 4 Hybrid slab-beam configuration. Hybrid dielectric amplifier. (D = separation between the two reflectors; d = the distance between the array and the planar reflector; TE = transverse electric.)

guide confines the beam in one dimension through wavebeam techniques as discussed above and in the second transverse direction (normal to the dielectric slab surface) through the technique of total internal reflection as normally employed by slab dielectric waveguides. For this structure, one obtains a large area suitable for the integration of active elements along the direction of propagation and across the wavebeam. The advantage of this technique is that the active elements may be integrated as a component of the ground plane and coupled to the wavebeam through apertures in the ground plane. This technique provides adequate coupling to the wavebeam, while providing a mechanism for efficient cooling of the active elements. The hybrid dielectric slab-beam waveguide techniques continue to show promise; however, they are the least developed of the three techniques discussed here. An amplifier based upon these techniques has shown input to output gain of about 10 dB in the X-band [16]. An example of a hybrid dielectric slab / wave-beam amplifier system is shown in Figure 4. Also shown in Figure 4 are details of the active device to wavebeam coupling element and phase correcting elements.

Current Status and Recent Results

The early experiments with grid array power-combiners mainly employed two-terminal devices such as Gunn or impact avalanche transit time (IMPATT) diodes at X-band or below. Later, similar investigations were conducted at millimeter wavelengths. However, two-terminal devices have low efficiencies, as well as less flexibility than three-terminal devices. Thus, recent experiments have been conducted utilizing transistors such as field effect transistors (FETs), pseudo-morphic HEMT (PHEMT), or heterojunction bipolar transistors (HBTs) [4, 7, 11]. An excellent summary of this work through 1994 was given in a survey by R. A. York [17]. The three-terminal devices give an extra degree of control (albeit at the cost of added complexity), but, more important, offer higher efficiencies, particularly PHEMTs at $K_{[a]}$ - band. (This is important from the point of view of heat removal from the small grid array structure.) Monolithic grid structures have also been investigated [13].

TABLE 1. REPORTED QUASI-OPTICAL SOURCES

Frequency	Array Size	Device Type	Power (mW)	Reference
5.0	10 × 10	FET	550	[7]
7.3	3 × 3	FET	282	[9]
8.2	4 × 4	FET	184	[17]
9.8	10 × 10	FET	10,300	[13]
34.7	6 × 6	HBT	—	[11]
37	4 × 4	HEMT	—	[4]
60	2 × 4	IMPATT	2,200	[4]

Abbreviations: HEMT, high-electron-mobility transistor.

Conclusion

Table 1 lists the specification of selected results reported for quasi-optical spatial combiners. While the intention of quasi-optical techniques is to develop high-power sources at millimeter wavelengths, most research to date has been conducted in the microwave region of the spectrum. In addition to the references, a biblography of relevant, key papers which indicates the magnitude of research effort addressing quasi-optical power combining techniques is provided. It should be pointed out that the results shown in Table 1 have been primarily proof-of-concept demonstrations and additional development effort is required. However, several academic, government, and industrial institutions currently have programs focused upon the millimeter spectrum.

References

[1] G. Goubau and F. Schwering, "On the guided propagation of electromagnetic wavebeams," *IRE Trans. Antennas and Propagation,* Vol. AP-9, May 1961, pp. 248–259.

[2] J. W. Mink, "Quasi-optical power combining of solid-state millimeter wave sources," *IEEE Trans. Microwave Theory Tech.,* Vol. MTT-34, February 1986, pp. 273–279.

[3] K. J. Kogan, F. C. DeLucia, and J. W. Mink, "Design of a millimeter-wave quasi-optical power combiner for IMPATT diodes," *Proceedings of the SPIE,* Vol. 791, Nos. 21–22, May 1987, pp. 77–81.

[4] J. C. Wiltse, et al., "Quasi-optical power combing of solid state sources in K_a-band," 1993, pp. 159–162.

[5] Z. B. Popovic, R. M. Weikle, M. Kim, et al., "Bar-grid oscillators," *IEEE Trans. Microwave Theory Tech.,* Vol. MTT-38, March 1990, pp. 225–230.

[6] P. L. Heron, G. P. Monahan, J. W. Mink, et al., "Impedance matrix of an antenna array in a quasi-optical resonator," *IEEE Trans. Microwave Theory Tech.,* Special Issue on Quasi-Optical Techniques, Vol. MTT-41, October 1993, pp. 1816–1826.

[7] Z. B. Popovic, R. M. Weikle II, M. Kim, et al., "A 100–MESFET planar grid oscillator," *IEEE Trans. Microwave Theory Tech.,* MTT-39, February 1991, p. 193–200.

[8] J. Birkeland and T. Itoh, "Two-port FET oscillator with applications to active arrays," *IEEE Microwave Guided Wave Lett.,* Vol. 1, May 1991, pp. 112–113.

[9] A. Mortazawi and B. C. DeLoach, "A nine-MESFET two-dimensional power combining array with strongly coupled oscillators," *IEEE Microwave Guided Wave Lett.,* Vol. 3, July 1993, pp. 214–216.

[10] S. Nogi, J. Lin, and T. Itoh, "Mode analysis and stabilization of a spatial power-combining array with strongly coupled oscillators," *IEEE Trans. Microwave Theory Tech.,* Special Issue on Quasi-Optical Techniques, Vol. MTT-41, October 1993, pp. 1827–1837.

[11] M. Kim, E. A. Sovero, J. B. Hacker, et.al.. "A 100–element HBT grid amplifier," *IEEE Trans. Microwave Theory Tech.,* Special Issue on Quasi-Optical Techniques, Vol. MTT-41, October 1993, pp. 1762–1771.

[12] David B. Rutledge, Michael P. De Lisio, and Cheh-Ming Liu, "Progress in grid amplifiers," Twentieth International Conference on Infrared and Millimeter Waves, Orlando, FL, December 12, 1995.

[13] J. B. Hacker, M.P. DeLisio, M. Kim, et.al., "A 10-watt X-band grid oscillator," *IEEE MTT-S International Microwave Symposium,* 1994.

[14] J. W. Mink and F. K. Schwering, "A hybrid dielectric slab-beam waveguide for the sub-millimeter wave region," *IEEE Trans. Microwave Theory Tech.,* Vol. MTT-41, October 1993, pp. 1720–1729.

[15] F. Poegel, et. al., "Demonstration of an oscillating quasi-optical slab power combiner," *IEEE MTT-S International Microwave Symposium,* Orlando, FL, 1995.

[16] H. S. Hwang, T. W. Nuteson, M. B. Steer, et al., "A quasi-optical dielectric slab power combiner," *IEEE Microwave Guided Wave Lett.,* Vol. 6, No. 2, February 1996, pp. 73–75.

[17] R. A. York, "Quasi-Optical Power Combining Techniques," in J. C. Wiltse (ed.), *Millimeter and Microwave Engineering for Communication and Radar,* SPIE, Bellingham, WA, Vol. CR54, 1994, pp. 63–97.

Bibliography

(1) D. B. Rutledge and S.E. Schwarz, "Planar multimode detector arrays for infrared and millimeter-wave applications," *IEEE J. Quant. Elect.,* 1981, QE-17, p. 407.

(2) P. F. Goldsmith, "Quasi-optical techniques at millimeter and submillimeter wavelengths," in K. J. Button (ed.), *Infrared and Millimeter Waves,* vol. 6, Academic Press, New York, 1982, pp. 277–343.

(3) D. B. Rutledge, D. P. Neikirk, and D. P. Kasilingam, "Integrated circuit antennas," in K. J. Button (ed.), *Infrared and Millimeter Waves,* vol. 10, Academic Press, New York, 1982, pp. 1–90.

(4) K. Chang and C. Sun, "mm-wave power combining techniques," *IEEE Trans. Microwave Theory Tech.,* Vol. MTT-31, February, 1983, pp. 91–107.

(5) L. Wandinger and V. Nalbandian, "Millimeter-wave power combiner using quasi-optical techniques," *IEEE Trans. Microwave Theory Tech.,* Vol. MTT-31, February 1983, pp. 189–193.

(6) J. W. Mink, "Quasi-optical power combining of solid-state millimeter-wave sources," *IEEE Trans. Microwave Theory Tech.,* Vol MTT-34, February 1986, pp. 273–279.

(7) K. D. Stephan,"Inter-injection-locked oscillators for power combining and phased arrays," *IEEE Trans. Microwave Theory Tech.,* Vol. MTT-34, October 1986, pp. 1017–1025.

(8) K. J. Kogan, F. C. DeLucia, and J. W. Mink, "Design of a millimeter-wave quasi-optical power combiner for IMPATT diodes," *Proceedings of the SPIE,* Vol. 791, May 21–22, 1987, pp.77–81.

(9) R. Janaswamy and D. H. Schaubert, "Analysis of the tapered slot antenna," *IEEE Trans. Antennas Prop.,* Vol. 35, September 1987, pp. 1058–1065.

(10) C. Xue, S. Zhao, Q. Wang, et al., "6 mm solid-state source power combiner," *International Journal on Infrared and Millimeter-Waves,* Vol. 9, April 1988, pp. 385–393.

(11) S. Zhao, Q. Wang, and S. Zhang, "Millimeter-wave quasi-optical power combining techniques," *International Journal on Infrared and Millimeter-Waves,* Vol. 9, April 1988, pp. 395–403.

(12) W. W. Lam, C. F. Jou, H. Z. Chen, et al., "Millimeter wave diode-grid phase shifters," *IEEE Trans. Microwave Theory Tech.,* Vol. MTT-36, May 1988, pp. 902–907.

(13) K. D. Stephen and S.L. Young, "Mode stability of radiation-coupled interinjection-locked phased arrays," *IEEE Trans. Microwave Theory Tech.,* Vol. 36, May 1988, pp. 921–924.

(14) K. Mizuno, T. Ajikata, M. Hieda, et al., "Quasi-optical resonator for millimeter and submillimeter-wave solid-state sources," *Electronics Letters (UK),* Vol. 24, No. 13, June 1988, pp. 792–793.

(15) Z. B. Popovic, M. Kim, and D. B. Rutledge, "Grid oscillators," *International Journal on Infrared and Millimeter-Waves,* Vol. 9, July, 1988, pp. 647–654.

(16) K. Chang, K. A. Hummer, and J. L. Klein, "Experiments on injection-locking of active antenna elements for active phased and spatial power combiners," *IEEE Trans. Microwave Theory Tech.,* Vol. 37, July 1989, pp. 1078–1084.

(17) C. Xue, Q. Wang, and H. Li, "Optimization calculation of solid-state power combining source or waveguide cavity," *International Journal on Infrared and Millimeter-Waves,* Vol. 9, No. 8, August 1988, pp. 733–738.

(18) C. F. Jou, W. W. Lam, H. Z. Chen, et al., "Millimeter wave diode grid frequency doubler," *IEEE Trans. Microwave Theory Tech.,* Vol. MTT-36, November, 1988, pp. 1507–1514.

(19) Y. C. Shih and H. J. Kuno, "Solid-state sources from 1 to 100 GHz, state-of-the-art reference," *Microwave Journal,* September 1989, Suppl., pp.145–161.

(20) A. Mortazawi and T. Itoh, "A periodic planar gunn diode power combining oscillator," *IEEE Trans. Microwave Theory Tech.,* Vol. MTT-38, January 1990, pp. 86–89.

(21) Z. B. Popovic, R. M. Weikle II, M. Kim, et al., "Bar grid oscillator," *IEEE Trans. Microwave Theory Tech.,* Vol. 38, March 1990, pp. 225–230.

(22) D. B. Rutledge, Z. B. Popovic, R. M. Weikle II, et al., "Quasi-optical power-combining arrays," *IEEE MTT-S Int. Microwave Symp. Dig.,* 1990, pp. 1201–1204.

(23) J. Birkeland and T. Itoh, "Spatial power combining using push-pull FET oscillators with microstrip patch resonators," *IEEE Int. Microwave Symp. Dig.,* 1990, pp. 1217–1220.

(24) M. Nakayama, M. Hieda, T. Tanaka, et al., "Millimeter and sub-millimeter wave quasi-optical oscillator with multi- elements," *IEEE MTT-S Int. Microwave Symp. Dig.,* 1990, pp. 1209–1212.

(25) A. Mortazawi and T. Itoh, "A periodic second harmonic spatial power combining oscillator," *IEEE MTT-S Int. Microwave Symp. Dig.,* 1990, pp. 1213–1216.

(26) Q. Wang, C. Xue, H. Li, et al., " Optimized Design of quasi-optical source power combiner at frequence of 100 Ghz," *International Journal on Infrared and Millimeter-Waves,* Vol. 11, 1990, pp. 1269–1283.

(27) P. F. Goldsmith, "Quasi-optics in radar systems," *Microwave Journal,* January, 1991, pp. 79–100.

(28) M. Kim, J. Rosenberg, R. P. Smith, et al., "A grid amplifier," *IEEE Micro. Guided Wave Lett.,* 1991, 1, p. 322.

(29) Z. B. Popovic, R. M. Weikle II, M. Kim, and D. B. Rutledge, "A 100–MESFET planar grid oscillator," *IEEE Trans. Microwave Theory Tech.,* Vol. 39, No. 2, February 1991, pp. 193–200.

(30) N. Nakayama, M. Hieda, T. Tanka, et al., "Millimeter and submillimeter wave quasi-optical oscillator with multi elements," *Proceedings of the Second International Symposium on Space Terahertz Technology,* Pasadena, CA, February 26–28, 1991, pp. 187–190.

(31) R. A. York and R. C. Compton, "Teraherz power-combining with coupled oscillator arrays," *Proceedings of the Second International Symposium on Space Terahertz Technology,* February 26–28, 1991, pp. 179–186.

(32) K. D. Stephen, et al., "Resonant-tunneling diode oscillator using a slot-coupled quasi-optical open resonator," *Electronics Letters,* Vol. 27, April 11, 1991, pp. 647–649.

(33) J. Birkeland and T. Itoh, "Two-port FET oscillators with applications to active arrays," *IEEE Microwave and Guided Wave Letters,* Vol. 1, May 1991, pp. 112–113.

(34) R.A. York and R. C. Comption, "Quasi-optical power combining using mutually synchronized oscillator arrays," *IEEE Trans. Microwave Theory Tech.,* Vol. 39, June 1991, pp. 1000–1009.

(35) J.B. Hacker, R. M. Weikle, M. Kim, et al., "A 100-element Schkottky diode grid mixer," IEEE AP-S International Symposium, London, Ontario, June 1991.

(36) A. Balasubramaniyan and A. Mortazawi, "Two-dimensional MESFET-based spatial power combiners," *IEEE Microwave and Guided Wave Letters,* Vol. 1, August 1991, pp. 215–218.
(37) R. A. York and R. C. Compton, "Mode-locked oscillator arrays," *IEEE Microwave Guided Wave Letters,* Vol. 2, No. 8, August 1991, pp. 215–218.
(38) M. Kim, et al. "A grid amplifier," *IEEE Microwave and Guided Wave Letters,* Vol. 1, November 1991, pp. 322–324.
(39) R. M. Weikle II, *Quasi-optical planar grids for microwave and millimeter-wave power combining,* Phd. Dissertation, California Institute of Technology, Pasadena, November 1991.
(40) D. R. Gagnon, "Highly sensitive measurements with a lens-focused reflectometer," *IEEE Trans. Microwave Theory Tech.,* Vol. MTT-39, December 1991, pp. 2237–2240.
(41) M. Kim, et al., "A 35 GHz HBT monolithic grid oscillator," 17th Int. Conference on Infrared and Millimeter Waves, *Proc. SPIE* Vol. 1929, 1992, pp. 402–403.
(42) J. C. Wiltse and J. W. Mink, "Quasi-optical power combining of solid state sources," *Microwave Journal,* Vol. 35, No. 2, Feb. 1992, pp. 144–156.
(43) J. Birkland and T. Itoh, "A 16-element quasi-optical FET oscillator power combining array with external injection locking," *IEEE Trans. Microwave Theory Tech.,* Vol. MTT-40, March 1992
(44) H. Kondo, et. al., "Millimeter and submillimeter wave quasi-optical oscillator with multi-elements," *IEEE Trans. MTT,* MTT-40, May 1992, pp. 857–863.
(45) A. Mortazawi, H. D. Foltz, and T. Itoh, "A periodic second harmonic spacial power combining oscillator," *IEEE Trans. MTT,* Vol. 40, No. 5, May 1992, pp. 851–856.
(46) S. Bundy, T. B. Mader, and Z. B. Popovic, "Quasi-optical array VCO's," *IEEE MTT-S International Microwave Symposium Digest,* June 1992, pp. 1539–1542.
(47) J. Heinbockel, A. Mortazawi, and T. Itoh, "A periodic spatial power combining MESFET oscillator," *IEEE MTT-S International Microwave Symp. Digest,* June 1992, pp. 545–548.
(48) J. Birkeland and T. Itoh, "An FET oscillator element for spatially injection locked arrays," *1992 IEEE MTT-S Digest,* June 1992, pp. 1535–1538.
(49) S. Kawasaki and T. Itoh, "40 GHz quasi-optic second harmonic spatial power combiner using FETs and slots," *IEEE MTT-S International Microwave Symposium Digest,* June 1992, pp. 1543–1546.
(50) R. M. Weikle II, M. Kim, J.B. Hacker, et al., "Transistor oscillator and amplifier grids," *Proc. of the IEEE,* Vol. 80, Nov. 1992, pp. 1800–1809.
(51) M. Kim, et al., "A 35 Ghz HBT Monolithic Grid Oscillator," 17th Int. Conf. on Infrared and Millimeter Waves, *Proc. SPIE* 1929, 1992, pp. 402–403.
(52) A. Pance and M. J. Wengler, "Microwave modeling of 2-D active grid antenna arrays," *IEEE Trans. Microwave Theory Tech.,* Vol. MTT-41, January 1993, pp. 20–28.
(53) J. B. Hacker, et al., "A 100-element planar Schottky diode grid mixer," *IEEE Trans. Microwave Theory Tech.,* Vol. MTT-40, March 1993, pp. 557–562.
(54) F. K. Schwering and J. W. Mink, "Planar quasi-optical slab-beam waveguide for the sub-millimeter wave spectrum," *Proc. 1993 URSI Conference,* June 1993.
(55) A. Schuneman, S. Zeisberg, G. P. Monahan, et al., "Experimental investigation of a quasioptical slab resonator," *Proc. 1993 URSI Conference,* June 1993.
(56) C-Y Yu and G. M. Rebeiz, "A quasi-optical amplifier," *IEEE Microwave and Guided Wave Letters,* Vol. 3, June 1993, pp. 164–166.
(57) J. A. Benet, A. R. Perkons, and S. H. Wong, "Spatial power combining for millimeter-wave solid state amplifiers," *IEEE MTT-S International Symposium,* June 1993, pp. 619–622.
(58) H.-X. Liu, L. B. Sjorgren, C. W. Domier, et al., "Monolithic quasi-optical frequency tripler array with 5-W output power at 99 GHz," *IEEE Electron Device Letters,* Vol. 14, July 1993, pp. 329–331.
(59) A. Mortazawi and B. C. DeLoach, "A nine-MESFET two dimensional power combining array employing an extended resonance technique," *IEEE Microwave and Guided Wave Letters,* Vol. 3, July 1993, pp. 214–216.
(60) P. L. Heron, F. W. Schwering, G. P. Monahan, et al., "A dyadic Green's function for the plano-concave quasi-optical resonator," *IEEE Microwave and Guided Wave Letters,* Vol. 3, August 1993.
(61) S. Zeisberg, A. Schuneman, G. P. Monahan, et al., "Experimental investigation of a quasi-optical slab resonator," *IEEE Microwave and Guided Wave Letters,* Vol. 3, August 1993.
(62) P. L. Heron, F. W. Schwering, G. P. Monahan, et al., "A dyadic Green's function for the plano-concave quasi-optical resonator," *IEEE Microwave and Guided Wave Letters,* Vol. 3, August 1993, pp. 256–258.
(63) B. Toland, B. Houshmand, and T. Itoh, "Modelling of nonlinear active regions with the FDTD method," *IEEE Microwave Guided Wave Lett.,* Vol. 3, No. 9, September 1993, pp. 333–335.
(64) N. J. Kolias and R. C. Compton, "A microstrip-based unit cell for quasi-optical amplifier arrays," *IEEE Microwave and Guided Wave Letters,* Vol. 3, September 1993, pp. 330–332.
(65) T. Mader, J. Shoenberg, L. Harmon, et al., "Planar MESFET transmission wave amplifier," *Electronics Letters,* Vol 29, September 1993, pp. 1600–1603.
(66) P. L. Heron, J. W. Mink, G. P. Monahan, et al., "Impedance matrix of a dipole array in a quasi-optical resonator," *IEEE Trans. Microwave Theory Tech.,* October 1993.
(67) M. Kim, E. A. Sovero, J. B. Hacker, et al., "A 6.5 GHz-11.5 GHz source using a grid amplifier with a twist reflector," *IEEE Trans. Microwave Theory Tech.,* Vol. 41, October 1993, pp. 1772–1774.
(68) R. A. York, "Nonlinear analysis of phase relationships in quasi-optical oscillator arrays," *IEEE Trans. Microwave Theory Tech.,* Vol. 41, October 1993, pp. 1799–1809.
(69) P. Liao and R. A. York, "A new phase-shifterless beam scanning technique using arrays of coupled oscillators," *IEEE Trans. Microwave Theory Tech.,* Vol. 41, October 1993, pp. 1810–1815.
(70) J. B. Hacker, M. P. De Lisio, J.-C. Chiao, et al., "A 100-element HBT grid amplifier," *IEEE Trans. Microwave Theory Tech.,* Vol. 41, October 1993, pp. 1762–1771.
(71) T. Mader, S. Bundy, and Z. B. Popovic, "Quasi-optical VCO's," *IEEE Trans. Microwave Theory Tech.,* Vol. 41, October 1993, pp. 1775–1781.
(72) S. Nogi, J. Lin , and T. Itoh, "Mode analysis and stabilization of a spatial power combining array with strongly coupled oscillators," *IEEE Trans. Microwave Theory Tech.,* Vol. 41, October 1993, pp. 1827–1837.
(73) J. W. Mink and F. K. Schwering, "A hybrid dielectric slab-beam waveguide for the sub-millimeter wave region," *IEEE Trans. Microwave Theory Tech.,* October 1993.
(74) K. D. Stephan, P. H. Spooner, and P. F. Goldsmith, "Quasi-optical millimeter-wave hybrid and monolithic PIN diode switches," *IEEE Trans. Microwave Theory Tech.,* Vol. 41, October 1993, pp. 1791–1798.
(75) L. B. Sjogren, J. B. Hacker, and M. P. De Lisio, "A monolithic diode array millimeter-wave beam transmittance controller," *IEEE Trans. Microwave Theory Tech.,* Vol. 41, October 1993, pp. 1782–1790.
(76) J. McCleary, M.-K. Li, and K. Chang, "Slot-fed higher order mode Fabry-Perot filters," *IEEE Trans. Microwave Theory Tech.,* Vol. 41, October 1993, pp. 1703–1709.
(77) T. Matsui, K. Araki , and M. Kiyokawa, "Gaussian-beam open resonator with highly reflective circular-coupling regions," *IEEE Trans. Microwave Theory Tech.,* Vol. 41, October 1993, pp. 1710–1714.
(78) A. C. Davidson, F. W. Wise, and R. C. Compton, "A 60 GHz IMPATT oscillator array with pulse operation," *IEEE Trans. Microwave Theory Tech.,* Vol. 41, October 1993, pp. 1845–1850.
(79) J. Bae, H. Kondo, T. Tanaka, et al., "Millimeter and submillimeter wave quasi-optical oscillator with Gunn diodes," *IEEE Trans. Microwave Theory Tech.,* Vol. 41, October 1993, pp. 1851–1855.
(80) J. A. Navarro, L. Fan, and K. Chang, "Active inverted stripline circular patch antennas for spatial power combining," *IEEE Trans. Microwave Theory Tech.,* Vol. 41, October 1993, pp. 1856–1863.

(81) P. Liao and R.A. York, "A new phase-shifterless beam scanning technique using arrays of coupled oscillators," *IEEE Trans. Microwave Theory Tech.*, Vol. 41, October 1993, pp. 1810–1815.

(82) M. Kim, E. A. Sovero, J. B. Hacker, et al., "A 100-element HBT grid amplifier," *IEEE Trans. Microwave Theory Tech.*, Vol. 41, October 1993, pp. 1762–1771.

(83) P. L. Heron, G. P. Monahan, J. W. Mink, et al., "Impedance matrix of an antenna array in a quasi-optical resonator," *IEEE Trans. Microwave Theory Tech.*, Vol. 41, October 1993, pp. 1816–1826.

(84) S. Kawasaki, and T. Itoh, "Quasi-optical planar arrays with FET's and slots," *IEEE Trans. Microwave Theory Tech.*, Vol. MTT-41, October 1993, pp. 1838–1844.

(85) H. S. Tsai, M. J. W. Rodwell, and R. A. York, "Planar amplifier array with improved bandwidth using folded slots," *IEEE Microwave and Guided Wave Lett.*, Vol. 4, April 1994, pp. 112–114.

(86) J. Hacker, et al., "A 10–W X-band grid oscillator," *IEEE MTT International Symp. Digest*, pp. 823–826, 1994.

(87) N. Shith, T. Ivanaov, A. Balasubramaniyan, et al., "A nine HEMT spatial amplifier," *1994 IEEE MTT-S Microwave Symposium Dig.*, 1994.

(88) S. C. Bundy and Z. B. Popovic, "Analysis of planar grid oscillators," *IEEE MTT-S International Microwave Symposium Digest*, Vol. 2, May 1994, pp. 827–830.

(89) T. P. Budka, M. W. Trippe, S. Weinreb, et al., "A 75 Ghz to 115 Ghz quasi-optical amplifier," *IEEE Trans, Microwave Theory Tech.*, Vol. 42, May 1994.

(90) W. A. Shiroma, B. L. Shaw, and Z. B. Popovic, "A 100–transistor quadruple grid oscillator," *IEEE MTT Microwave and Guided Wave Letters*, Vol.4, No.10, pp. 350–352, October 1994.

(91) S. C. Bundy and Z. B. Popovic, "A generalized analysis for grid oscillator design," *IEEE Trans. Microwave Theory Tech.*, Vol. 42, No.12, pp. 2486–2491, December 1994.

(92) R. A. York, "Quasi-optical power combining techniques," in J. C. Wiltse (ed.), *Millimeter and Microwave Engineering for Communication and Radar*, SPIE, Bellingham, WA, Vol. CR54, 1994, pp. 63–97.

(93) J. S. H. Schoenberg, S. C. Bundy, and Z. B. Popovic, "Two-level power combining using a lens amplifier," *IEEE Trans. Microwave Theory Tech.*, Vol.42, No. 12, December 1994, pp. 2480–2485.

(94) M. P. DeLisio, S. W. Duncan, D.-W. Tu, et al., "Modelling and performance of a 100-element pHemt grid amplfiier," *IEEE Trans. Microwave Theory Tech.*, April 1995 (submitted).

(95) G. P. Monahan, P. L. Heron, M. B. Steer, et al., "Mode degeneracy in quasi-optical resonators," *Microwave and Optical Technology Letters*, Vol. 8, No. 5, April 5, 1995, pp. 230–232.

(96) G. P. Monahan, P. L. Heron, M. B. Steer, et al., "Mode degeneracy in quasi-optical resonators," *Microwave and Optical Technology Letters*, Vol. 8, No. 5, April 5, 1995, pp. 230–232.

(97) J. Schoenberg, T. Mader, B. Shaw, et al., "Quasi-optical antenna array amplifiers," *1995 IEEE MTT-S Int. Symp. Dig.* (Orlando, FL), May 1995, pp. 605–608.

(98) Hubert, J. Schoenberg, and Z. B. Popovic, "A Ka-band quasi-optical amplifier," *1995 IEEE MTT-S Int. Symp. Dig.* (Orlando, FL), May 1995, pp. 585–588.

(99) N. J. Kolias and R. C. Compton, "A microstrip based quasi-optical polarization rotator array," *IEEE MTT-Symposium Digest*, (Orlando, FL), May 1995, pp. 773–776.

(100) P. Liao and R. A. York, "A high power two-dimensional coupled oscillator array at X-band," 1995 *IEEE MTT-S International Microwave Symposium* (Orlando, FL), May 1995, pp. 909–912.

(101) M. P. DeLisio, C-M. Liu, A. Moussessian, et al., "A 100–element MODFET grid amplifier," *1995 IEEE AP-S Int. Symp. Dig.*, 1995.

(102) T. W. Nuteson, G. P. Monahan, M. B. Steer, et al., "Use of the moment method and dyadic green's functions in the analysis of quasi-optical structures," *1995 IEEE MTT-S International Microwave Symposium Digest*, May 1995, pp. 913–916.

(103) D. Griffin, "Monolithic active array limitations due to substrate modes," *IEEE Antennas and Propagation Society International Symposium*, Newport Beach, CA, June 1995, pp. 1300–1303.

(104) W. Shiroma, S. Bundy, S. Hollung, et al., "A quasi-optical isolator," *IEEE Microwave and Guided Wave Letters*, Vol. 6, No. 5, May 1996, pp. 205–206.

(105) T. Mader, M. Markovic, E. Bryerton, et al., "Analysis and design of class-E high-efficiency microwave power amplifiers," *IEEE Trans. Microwave Theory Tech.*, January 1996 (submitted).

(106) H. Hwang, T. W. Nuteson, M. B. Steer, et al., "A quasi-optical dielectric slab power combiner," *IEEE Microwave and Guided Wave Lett.*, Vol. 6, February 1996.

(107) A. Alexanian, N. J. Kolias, R. C. Compton, et al., "FDTD analysis of quasi-optical arrays using cyclic boundary conditions and berenger's PML," *IEEE Microwave Guided Wave Lett.*, March 1996.

(108) H. Hwang, T. W. Nuteson, M. B. Steer, et al., "A quasi-optical dielectric slab power combiner," *IEEE Microwave and Guided Wave Lett.*, Vol. 6, February 1996, pp. 73–75.

(109) L. W. Epp and R. P. Smith, "A generalized scattering matrix approach for analysis of quasi-optical grids and de-embedding of device parameters," *IEEE Trans. Microwave Theory Tech.*, Vol. 44, May, 1996, pp. 760–769.

(110) T. W. Nuteson, G. P. Monahan, M. B. Steer, et al., "Full-wave analysis of quasi-optical structures," *IEEE Trans. Microwave Theory Tech.*, Vol. 44, No. 5. May 1996, pp. 701–710.

(111) S. Hollung, W. Shiroma, M. Markovic, et al., "A quasi-optical isolator," *IEEE Microwave and Guided Wave Lett.*, May 1996 (submitted).

(112) C-M. Liu, E. A. Sovero, W. J. Ho, et al., "Monolithic 40–GHz 670 mW HBT grid amplifier," *1996 IEEE MTT-S Int. Microwave Symposium*, June 1996.

(113) M. P. DeLisio, S. W. Duncan, D.-W. Tu, et al., "A 44-60 GHz monolithic pHEMT grid amplifier," *1996 IEEE MTT-S Int. Microwave Symposium*, June 1996.

(114) W. Shiroma, E. Bryerton, S. Hollung, et al., "Quasi-optical receiver with angle diversity," to be presented at the IEEE MTT International Symposium, San Francisco, June 1996.

(115) A. Alexanian, H. S. Tsai, and R. A. York, "Quasi-optical traveling-wave amplifiers," IEEE MTT International Symposium, San Francisco, June 1996.

(116) A. R. Perkons and T. Itoh, "A 10-element active lens amplifier on a dielectric slab," IEEE MTT International Symposium, San Francisco, June 1996.

(117) M. P. DeLisio, C. M. Liu, D. B. Rutledge, et al., "A 44-60 Ghz monolithic pHEMT grid amplifier," IEEE MTT International Symposium, San Francisco, June 1996.

(118) T. W. Nuteson, M. B. Steer, J. W. Mink, et al., "Electromagnetic modeling of finite grid structures in quasi-optical systems," IEEE MTT International Symposium, San Francisco, June 1996.

(119) C. M. Sanagi, E. Yamamoto, and S. Nogi, "Axially symmetric Fabry-Perot power combiner with active devices mounted on both the mirrors," IEEE MTT International Symposium, San Francisco, June 1996.

(120) T. Fujii, H. Mazaki, F. Takei, et al., "Coherent power combining of millimeter wave resonator tunneling diodes in a quasi-optical resonator," IEEE MTT International Symposium, San Francisco, June 1996.

(121) H. S. Hwang, T. W. Nuteson, M. B. Steer, et al., "Two-dimensional quasi-optical power combining system performance and component design," IEEE MTT International Symposium, San Francisco, June 1996.

(122) M. P. DeLisio, S. W. Duncan, DW. Tu, et al., "Modeling and performance of a 100-element pHEMT grid amplifier," *IEEE Trans. Microwave Theory Tech.*, Vol. 44, No. 12, December 1996.

Quasi-Optical Power Combining of Solid-State Millimeter-Wave Sources

JAMES W. MINK, SENIOR MEMBER, IEEE

Abstract —Very efficient power combining of solid-state millimeter-wave sources may be obtained through the application of quasi-optical resonators and monolithic source arrays. Through the theory of reiterative wavebeams (beam modes) with application of the Lorentz reciprocity theorem, it is shown that planar source arrays containing 25 individual elements or more result in very efficient power transfer of energy from the source arrays to the fundamental wave-beam mode. It is further shown that for identical sources within a properly designed quasi-optical power combiner, the output power tends to increase much faster that number of source elements.

I. Introduction

CONVENTIONAL waveguide power combiners are limited in power output, efficiency, and number of sources that may be combined in the millimeter-wave region. This limitation is a consequence of the requirement that linear dimensions of conventional waveguide resonators be of the order of one wavelength to achieve acceptable mode separation and to avoid multimode operation. On the other hand, quasi-optical resonators have linear dimensions large compared to wavelength and they offer an attractive approach to overcome these limitations. Fundamental limitations of power combining utilizing quasi-optic resonator techniques is discussed in this paper, and it is shown that very high combining efficiency may be obtained. The approach utilizes an array of source elements placed within a transverse plane near one reflecting surface of the resonator. Energy is extracted from the system through one reflector which is partially transparent.

II. Combiner Configuration

To investigate the feasibility of quasi-optical power combining of millimeter-wave sources, an approach which combines a wavebeam resonator or Fabry–Perot resonator is used as the combining element and sources are modeled as an array of current elements within the resonant structure, as shown in Fig. 1. A wave-beam resonator of rectangular symmetry is utilized and power is extracted from the source array to the lowest order or "Gaussian" mode of the resonator. The resonator consists of two surfaces which are large in terms of the operating wavelength. One surface is a perfect, planar reflector and is located in the plane $z = 0$; the other reflector, located at $z = D$, is partially transparent and curved. Useful energy will "leak" through this reflector with a well-defined spatial distribution. The reflector curvature may be expressed by a pair of focal lengths which define the curvature in two perpendicular axial planes, usually the $x-z$ and the $y-z$ planes. The sources are placed in a transverse plane between the reflectors and slightly displaced from the plane reflector. It is assumed that each source, which may be an IMPATT or GUNN diode, is attached to a short dipole which also lies in a transverse plane. A planar array of source diodes with connecting dipoles lends itself to integrated-circuit fabrication techniques [1]. Feedback coupling or signal interaction occurs between the resonant mode and the individual sources leading to injection locking and single-frequency operation. The coupling coefficient of the source array for each mode is calculated through application of the Lorentz reciprocity theorem. Also, the driving point resistance of each dipole in the presence of all other excited dipoles is calculated.

For this configuration, one must consider the electromagnetic fields within two regions of space. Between the reflectors, $0 < z < D$, a resonant field exists which consists of two traveling waves, one propagating in the $+z$ or "forward" direction and a second equal amplitude wave traveling in the $-z$ or "backward" direction. The sum of the traveling waves may be expressed as a standing wave whose transverse distribution is described as a sum of the "wavebeam modes." In the region $z > D$, only waves traveling in the $+z$ direction exist, and contain the same spectrum of modes as the fields within the resonator.

III. Theory

A. Electromagnetic Wavebeams and Resonators

Quasi-optic resonators are based upon reiterative wave beams or beam modes. These modes were first described by Goubau and Schwering [2] and they satisfy orthogonality relations like the wave modes in conventional tubular waveguides. In directions transverse to the direction of propagation, characteristic dimensions of fields contained within wave-beam resonators are much larger than those in conventional waveguides. They range from about 20 to many thousand wavelengths depending on the frequency and structures used. In the millimeter/sub-millimeter range, the transverse dimensions are typically from 20 to 100 wavelengths.

Modes of rectangular symmetry are utilized for this investigation since the beam modes, as well as source

Manuscript received April 30, 1985; revised September 12, 1985.
The author is with the U.S. Army Research Office, P.O. Box 12211, Research Triangle Park, NC 27709.
IEEE Log Number 8406473.

Reprinted from *IEEE Transactions on Microwave Theory and Techniques,* Vol. MTT-34, No. 2, pp. 273-279, February 1986.

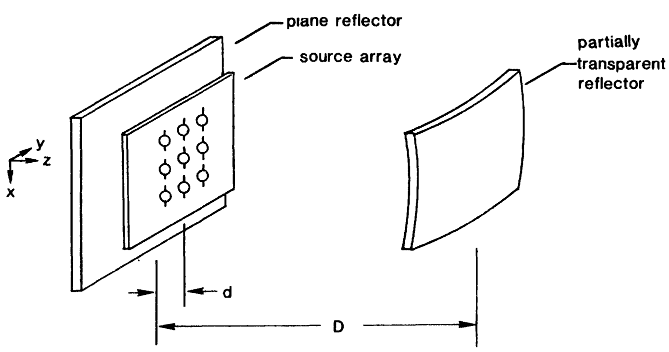

Fig. 1. Resonator–source array configuration.

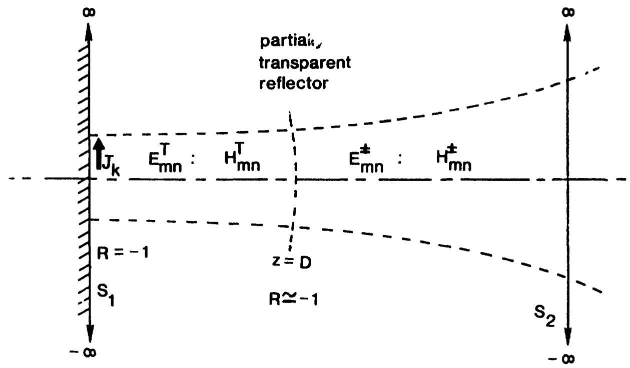

Fig. 2. Cross section showing spatial regions.

coordinates of a regular rectangular array, may be expressed in Cartesian coordinates. Wave beams expressed in Cartesian coordinates are satisfied by Hermite–Gaussian functions [3], [4]. Since the definition of the Hermite polynomials is not uniform in the literature, the following definition is used [3], [5]:

$$H_{en}(X) = (-1)^n (X^2/2) \frac{d^n}{dX^n} (\exp(-X^2/2)). \quad (1)$$

The following recurrence relation is also useful:

$$H_{e(n+1)}(X) = XH_{e(n)}(X) - nH_{e(n-1)}(X). \quad (2)$$

The Hermite polynomials form a complete system of orthogonal functions within the range $-\infty \leqslant X \leqslant \infty$ with the weight function $\exp(-X^2/2)$. An ortho-normal spectrum of wave-beam modes may be obtained from this definition, and is shown below for each linearly polarized component of the wave beam [4]*:

$$\begin{aligned} E^{\pm}_{mn}&(x, y, z) \\ &= \frac{(\mu/\epsilon)^{1/4}}{\sqrt{\pi \overline{X}\overline{Y} m! n!}} (1+u^2)^{-1/4} (1+v^2)^{-1/4} \\ &\cdot H_{em}(\sqrt{2}\, x/x_z) H_{en}(\sqrt{2}\, y/y_z) \\ &\cdot \exp\Bigg\{ -\frac{1}{2}\left[(x/x_z)^2 + (y/y_z)^2 \right] \\ &\mp j \Bigg[kz + \frac{1}{2}\left(u(x/x_z)^2 + v(y/y_z)^2 \right. \\ &- \left(m+\frac{1}{2}\right)\tan^{-1}(u) - \left(n + \frac{1}{2}\right)\tan^{-1}(v) \Bigg]\Bigg\} \quad (3) \end{aligned}$$

where

$$u = z/k\overline{X}^2, \quad v = z/k\overline{Y}^2$$

$$x_z = \overline{X}^2\left(1 + \frac{z^2}{k^2\overline{X}^4}\right), \quad y_z = \overline{Y}^2\left(1 + \frac{z^2}{k^2\overline{Y}^4}\right)$$

and the relationship between field components is

$$E^{\pm}_{xmn} = \pm\sqrt{\frac{\mu}{\epsilon}}\, H^{\pm}_{ymn}, \quad E^{\pm}_y = \mp\sqrt{\frac{\mu}{\epsilon}}\, H^{\pm}_{xmn}. \quad (4)$$

*The argument (x, y, z) of beam modes will be suppressed throughout this paper except when it is necessary to refer to a specific point, such as the location of a current source.

The $E^{\pm}_{mn}$ fields represent the desired wave-beam modes and the + sign refers to traveling waves progressing in the positive z direction, and the − sign refers to waves traveling in the negative z direction. The subscript x or y refers to the polarization. Quantities $\overline{X}$ and $\overline{Y}$ which determine the decay of the field in the x and y directions are called mode parameters. Mode parameters are parameters which are adjusted so that the wavebeam satisfies an imposed condition. When one considers a resonator structure, the condition that must be satisfied is that for each round trip of a wave within the resonator, the field repeats itself in both phase and amplitude distribution. It has been shown that the mode parameter is a function of resonator configuration and wavelength. For the resonator described above, the mode parameters are [4]

$$k\overline{X}^2 = \sqrt{(2 - D/F_x)F_x D} \quad (5)$$

$$k\overline{Y}^2 = \sqrt{(2 - D/F_y)F_y D} \quad (6)$$

where

$k = 2\pi/\lambda$
D = distance between the reflecting surfaces,
F_x = focal length of the curved reflector referenced to the x axis,
F_y = focal length of the curved reflector referenced to the y axis.

The modes satisfy, in any plane z = constant, the orthogonality relations

$$\sqrt{\frac{\epsilon}{\mu}} \iint_{-\infty}^{\infty} E_{mn} \cdot E^{*}_{m'n'}\, dx\, dy = \delta_{mm'}\delta_{nn'}. \quad (7)$$

Since the Hermite–Gaussian functions form a complete system of orthogonal functions, any beam whose transverse electric field is known in a plane z = constant can be expanded into a series of wave-beam modes, providing the beam satisfies a paraxial propagation condition. Experience, however, has shown that this requirement is satisfied in practical systems and that the error tends to occur in higher order modes which usually are not of interest.

The modes described by (3) represent waves traveling freely in space. With reference to Fig. 2, they describe the fields outside of the resonator, or in the region $z > D$. In order to satisfy the boundary conditions within the resonator region, $0 \leqslant z \leqslant D$, one must take for each mode a sum of "forward" and "backward" traveling waves. Under resonant conditions, the fields within the resonator may build up due to multiple reflections, and the amplitude will be limited by the reflection coefficient of the partially transparent reflector. For application of the Lorentz reciprocity theorem that will follow, it is required to determine the resonator fields when excited by a properly adjusted wave beam consisting of a single mode or spectrum of modes incident from $z = \infty$ upon the resonator. These fields become the test fields. In order to compute the worst-case fractional power coefficient, it is assumed that all modes resonate simultaneously. Because the total phase shift of a wave traveling from one reflector to the other depends upon the mode numbers m and n [4], all modes will not resonate simultaneously in an actual wave-beam resonator. The condition of simultaneous resonance is necessary to determine the best location of source elements. This formulation results in the worst-case fractional power-coupling coefficient. The fractional power-coupling coefficient is defined as the power in the desired mode, usually the fundamental Gaussian mode, divided by the power in all modes excited by the given current distribution.

The partially transparent reflector must be characterized in order to determine the electromagnetic field within the resonator. This reflector may be considered as a lossless two-port junction. The scattering matrix of such a junction has certain well-defined properties listed below [6]:

$$S_{11} = S_{22} = Re^{j\theta} \tag{8}$$

$$S_{12} = S_{21} = \sqrt{1 - R^2}\, e^{j(\theta + \pi/2)}. \tag{9}$$

Now, it is postulated that for a wave beam incident upon the resonator from $z = \infty$, the wave beams within the resonator have both amplitude and phase differences from the incident wave beam. Since a perfect reflector is located at $z = 0$, there is no net power flow through any plane $z > 0$. Using the condition of zero net power flow through any transverse plane along with the properties of the lossless partially transparent reflector, the field within the resonator becomes

$$E_{mn}^{T} = A\,\mathrm{Re}\left(E_{mn}^{+}\right)\sin(kz) \tag{10}$$

where

$$A = \frac{2R\sin(\psi) + \sqrt{1 - R^2\cos^2(\psi)}}{\sqrt{1 - R^2}}\, e^{j(\psi + \pi/2)}. \tag{11}$$

As seen by (11), the field strength is at its maximum when $\psi = \pi/2$. For this value of ψ, the fields within the resonator are real; thus, the system is considered to be resonant.

B. Coupling to an Array of Current Sources

One can now determine the coupling coefficient to a current element or to an arbitrary array of current elements through application of the Lorentz reciprocity theorem [7] with the further requirement that all current sources are located within the resonator. There is no loss in generality by considering only modes where $E_{ymn} = H_{xmn} = 0$, and the impressed currents are x-directed

$$\oint_S \left(E_{mn}^{\pm} \times H_1 - E_1 \times H_{mn}^{\pm}\right) \cdot n\, da = \iiint_{V_R} J \cdot E_{mn}^{T}\, dv \tag{12}$$

where

$E_{mn}^{\pm}$ and $H_{mn}^{\pm}$ = modal fields in space,
E_{mn}^{T} and H_{mn}^{T} = fields within the resonator expressed in terms of the modal fields,
E_1 and H_1 = fields in space due to the current elements,
V_R = volume bounded by the resonator.

The method used to find the field radiated by an arbitrary array of filamentary currents within a quasi-optical resonator is to expand the radiated field in terms of normal beam waveguide modes (Hermite–Gaussian functions) and to determine the amplitude coefficients in this expansion. With reference to Fig. 2, let J_k represent an arbitrary infinitely thin current element. Such a current must be maintained by some external source (e.g., an IMPATT or GUNN diode), but in the evaluation of the coupling to beam modes, only radiated fields are of interest, and, consequently, the source which maintains the specified current does not enter the picture here.

The field radiated in the positive z direction by the array of x-directed current elements may be represented by

$$E_1 = \sum_{kq} a_{kq} E_{kq}^{+} \hat{x} \qquad \text{for } z > D \tag{13}$$

$$H_1 = \sqrt{\frac{\epsilon}{\mu}} \sum_{kq} a_{kq} E_{kq}^{+} \hat{y} \qquad \text{for } z > D. \tag{14}$$

Since there is a perfectly conducting plane located at $z = 0$ as shown in Fig. 2

$$E_{mn}^{T}(x, y, \phi) = 0. \tag{15}$$

The volume chosen over which it is required to evaluate the Lorentz reciprocity relation is bounded by a surface S which extends to infinity in the transverse directions and consists of an infinite, perfectly conducting plane S_1, located at $z = 0$ and a second infinite plane S_2, located in some plane $z > D$. When one then performs the integration over this "closed surface", there is only a contribution by the integrals evaluated on S_2. There is no contribution to the integral over S_1 since the $n \times E = 0$ along that surface.

$$\oiint_{S_2} \left[E_{mn}^{\pm} \hat{x} \times \sqrt{\frac{\epsilon}{\mu}} \sum_{kq} a_{kq} E_{kq}^{+} \hat{y} - \sum_{kq} a_{kq} E_{kq}^{+} \hat{x} \times \sqrt{\frac{\epsilon}{\mu}} E_{mn}^{\pm} \hat{y} \right] \cdot \hat{n}\, da = \iiint_{V_R} J \cdot E_{mn}^{T}\, dv. \tag{16}$$

Since $E_{mn}^{-} = E_{mn}^{+*}$, one can utilize the orthogonality relation (eq. (7)) for wave beams and perform the integration term by term. Therefore

$$\oiint_{S_2}\left(E_{mn}^{\pm}\times H_1 - E_1\times H_{mn}^{\pm}\right)\cdot n\,da = 2a_{mn}. \tag{17}$$

Hence

$$a_{mn} = \frac{1}{2}\iiint_{V_R} J\cdot E_{mn}^{T}\,dv. \tag{18}$$

Again, if one considers the case where the array consists of an array of filamentary currents, that the currents are all aligned with the electric field, and that the length of each current elements is small compared to the mode parameter, this equation can be written as follows:

$$a_{mn} \simeq \frac{1}{2}\sum_{p} I_p\,\Delta X_p\,E_{mn}^{T}(x_p, x_p, z_p) \tag{19}$$

where

I_p = the current into the "terminals" of the pth current element,

$E_{mn}^{T}(x_p, y_p, z_p)$ = the electric field strength of the m, n mode at the location of the pth current element,

ΔX_p = effective length of the pth current element.

Hence

$$\Delta X_p = \frac{1}{I_p}\int I_p(l)\cdot dl_p. \tag{20}$$

Now with the knowledge of the expansion coefficients a_{mn} given by (19) and (10), which relates fields internal to the resonator to the external fields, one can determine the total electric and magnetic fields E_1, H_1 due to an array of current elements.

C. Driving Point Resistance of Each Element

Since the goal is to obtain a technique for efficient power transfer from an array of sources, one must know the driving point resistance to each element and then to match the source to that resistance. It is assumed that the resonator is adjusted for resonance; hence, the reactive component is zero or at least very small. Since the dipole elements will be surrounded by a strong electric field due to resonator, the self impedance of the dipole is neglected. The input impedance of a dipole element in the presence of an electric field (created by all sources) may be expressed as [8]

$$Z_p^T = \frac{1}{I_p^2}\iiint_{V_R} J_p\cdot E^T\,dv \tag{21}$$

where Z_p^T is the driving point impedance for the pth current element.

A more useful result is the driving-point impedance for a given mode. It has been shown theoretically and verified experimentally that a wave-beam resonator may be adjusted so that only one mode may exist for a given frequency (for example, the mode patterns of lasers [9]). One can, therefore, express the driving-point resistance for each mode as follows:

$$Z_{pmn} = \frac{1}{I_p^2}\iiint_{V_R} J_p\cdot E_{mn}^{T}\,dv. \tag{22}$$

Again, considering the case of small dipoles of equal equivalent length, the following expression is obtained:

$$Z_{pmn} = 2A(\Delta X)^2\sin^2(kz_p)\cdot\mathrm{Re}\left[E_{mn}^{+}(x_p, y_p)\right]\sum_q \frac{I_q}{I_p}\mathrm{Re}\left[E_{mn}^{+}(x_q, y_q)\right]. \tag{23}$$

This result also may be obtained through considerations of energy conservation. The power flowing into a dipole element may be represented as the square of its terminal current, multiplied by its driving-point resistance. Now, total power into the system is the sum of the power flowing into all individual elements. When this total power is equated to the power flux of the forward-traveling wave beam, one obtains the same result as shown by (23).

IV. Computed Results

The theory developed above enables one to determine the number of current elements required to obtain efficient transfer of power to any wave-beam mode. Of primary interest is the current source locations within the resonator, their amplitudes, and the driving-point resistance for each element when the lowest order "Gaussian wave beam" is efficiently excited. In this section, two specific cases will be considered. First, the case where all current elements are assumed to have equal current moment, and second, where the current moment amplitude is adjusted such that it is proportional to the field strength of the fundamental mode at its location.

To obtain efficient coupling, the current elements must be distributed in a transverse plane in such a way that power is efficiently transferred to the lowest order mode and very little power is transferred to any of the other modes. The efficiency of coupling may be calculated for a given distribution of currents by computing the power radiated by the lowest order mode and comparing it to the total power radiated. From (13), it is seen that the amplitude of each mode is represented by the coefficient a_{qk}; thus, using (4), the power of each mode may be calculated as follows:

$$\begin{aligned} P_{qk} &= a_{qk}a_{qk}^{*}\sqrt{\frac{\epsilon}{\mu}}\iint_{-\infty}^{\infty} E_{qk}\cdot E_{qk}^{*}\,dx\,dy \\ &= a_{qk}a_{qk}^{*}. \end{aligned} \tag{24}$$

Since the modes are orthogonal for a given array of current elements, the fractional power of the fundamental mode ($m = 0$, $n = 0$) compared to the total power of all modes becomes

$$FP_{00} = \frac{a_{00}a_{00}^{*}}{\sum_{qk} a_{qk}a_{qk}^{*}}. \tag{25}$$

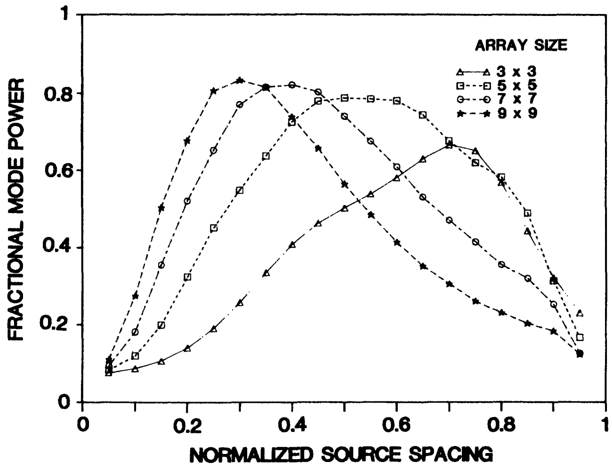

Fig. 3. Fractional power into fundamental mode by equal weight sources.

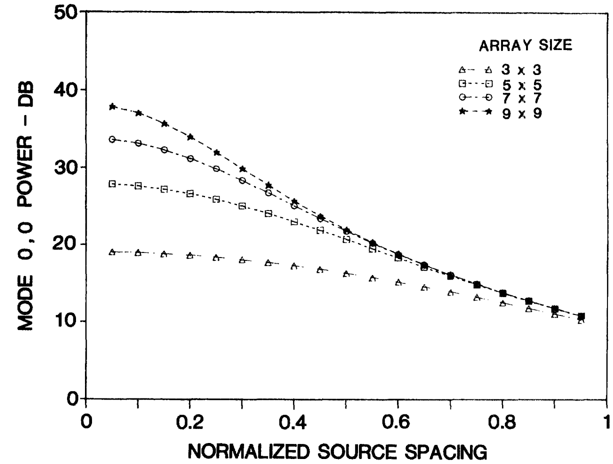

Fig. 4. Power into fundamental mode by equal weight sources.

It should be noted that the excitation coefficient for any mode is determined only by the current distribution and the modal spectrum as if it were freely propagating in space. This restriction is required to obtain the optimum current distribution for the excitation of any given mode. If it were not applied, the mode spectrum would not be complete from the mathematical point of view. From an engineering view point, it represents the worst case since it assumes that all modes are at resonance. Thus, each mode could extract energy from the current elements and is included in the denominator of (25). This assumption clearly aids in determining the optimum source array configuration.

Fig. 3 illustrates the fractional power coupled into the fundamental mode for four different array configurations containing 9, 25, 49, and 81 elements in regular rectangular arrays of equal moment sources with their individual phases adjusted such that each term of (19) is real. All figures that follow have been normalized such that the results presented are independent of the details of the wave-beam resonator; a total of 441 modes are utilized for the computation of the denominator in equation (25). Of course, the normalization must be removed when a particular case is to be considered. To achieve meaningful normalization, the spacing between source elements in each direction is expressed in terms of the wave-beam mode parameter (the $1/e^2$ distance). The source array is considered to lie in a plane transverse to the wave beam and is symmetrical about the wave-beam axis. A practical location for the source array is very close to the reflecting surface located at $z = 0$. For this location, all elements will have uniform phase and the reflecting surface can also become the heat sink for active elements. In terms of coupling energy into the fundamental mode, Fig. 3 shows that for each array configuration there is an optimum source element spacing. It also shows that the maximum source array length for optimum coupling is approximately independent of the number of array elements. The array will extend in each direction from the wave-beam axis about 1.2 mode parameters. Since the ultimate goal is to combine many individual sources to obtain a high power source, the total power

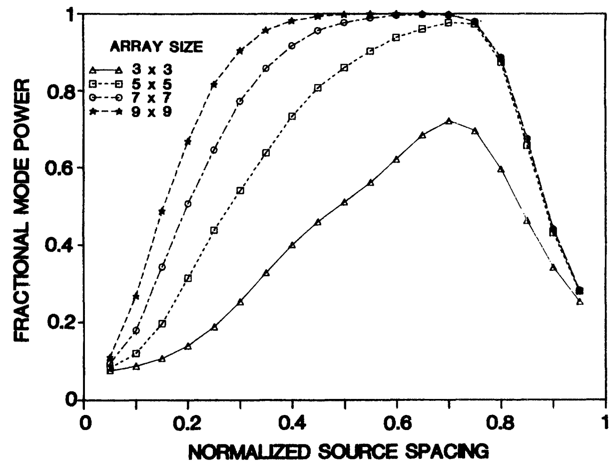

Fig. 5. Fractional power into fundamental mode by Gaussian weight sources.

delivered to the fundamental mode must be determined. Fig. 4 shows the increase of power as the number of sources increases. Zero decibels is the power delivered to the fundamental mode by a single source located on axis. The trend of these curves shows that one should make a tradeoff between array element spacing for optimum fractional power and fundamental mode power. It appears that the source spacing should be reduced so that the optimum fractional power reduces by about 1 dB.

Fig. 5 illustrates the fractional power into the fundamental mode for four different array configurations consisting of regular rectangular source arrays of 9, 25, 49, and 81 elements, and the current moment of each element is adjusted to have a value proportional to the field strength of the fundamental mode at the location of the element (the source array current moments have a Gaussian taper). In this case, very efficient coupling may be obtained since the source array has been matched to the fundamental mode. However, Fig. 6 shows that the fundamental mode power decreases much faster as the source spacing is increased than for the previous case. The net conclusion is that for a power combiner, significant output power reduction will occur if the source spacing is allowed to increase.

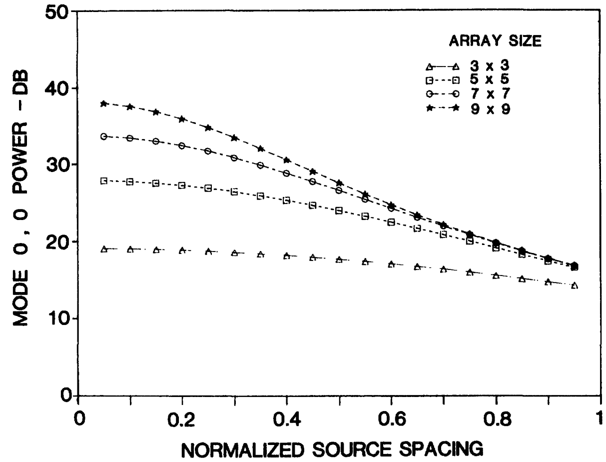

Fig. 6. Power into fundamental mode by Gaussian weight sources.

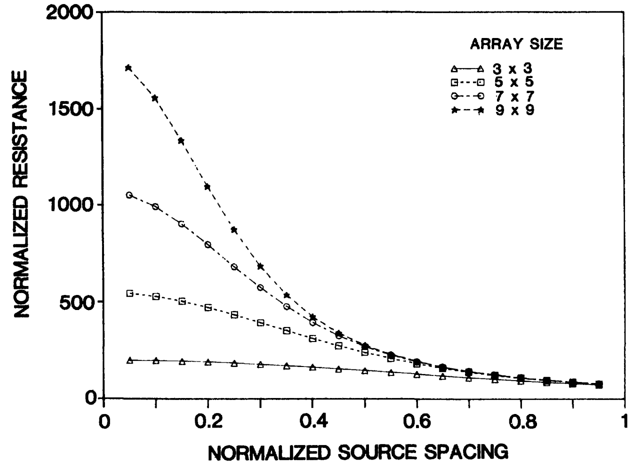

Fig. 8. Driving-point resistances for Gaussian weight sources.

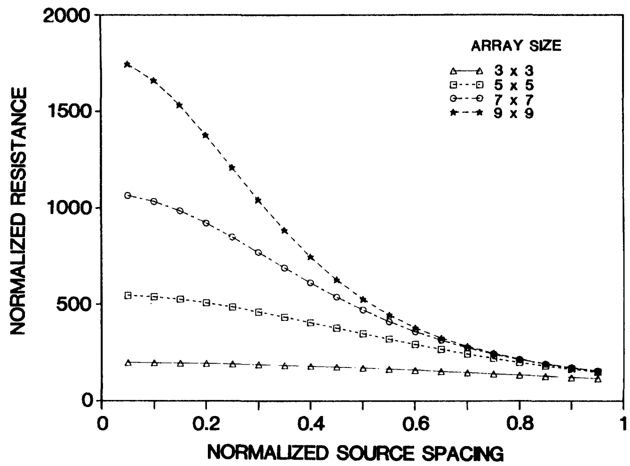

Fig. 7. Driving-point resistances for equal weight sources.

This is especially true for source arrays containing a large number of elements.

Utilizing (23), a family of curves for the driving-point resistance of each element of the source array is obtained. However, this family of curves can be reduced to a single curve for each array configuration. Equation (23) may be written as

$$R_{pmn} = \frac{(\Delta X)^2}{\overline{XY}} \sin^2(kz_p)\sqrt{\frac{1+R}{1-R}} \cdot \left[\mathrm{Re}\left[\sqrt{\overline{XY}}\, E^+_{mn}(x_p, y_p)\right]\overline{R}\right. \quad (26)$$

where

$$\overline{R} = 2\sum_q \frac{I_q}{I_p} \mathrm{Re}\left[\sqrt{\overline{XY}}\, E^+_{mn}(x_q, y_q)\right]. \quad (27)$$

Now (27) represents a normalized resistance factor and depends only upon normalized source spacing, while (26) is the actual driving-point resistance and requires detailed knowledge of the resonator configuration. Fig. 7 is the normalized driving-point resistances for the four array configurations described above, where each element has the same effective length and driving-point current. Fig. 8 is the normalized driving-point resistances for the four array configurations when each element has the same effective length and the terminal current is proportional to the field strength of the fundamental mode at the current element location.

V. Examples

Quasi-optical millimeter-wave power combining was experimentally investigated by Wandinger and Nalbandian [10]. They utilized a wave-beam resonator with two waveguide ports loaded with dielectric rods to couple energy into the system and reported power-combining efficiency of 52 percent. This value is in general agreement with the theory presented here. Each waveguide aperture loaded with a dielectric rod was modeled as four small current elements in a rectangular array separated by 0.1 mode parameters. The location of these "patches" of currents was estimated from the photograph in the paper by Wandinger and Nalbandian to be 0.45 mode parameters from the beam axis. Due to the mode-dependent phase shift of wave-beam modes, only one fourth of the total mode spectrum would simultaneously be resonant in a confocal resonator for a given frequency. All of the above conditions were applied and a coupling efficiency of 40 percent was calculated. Since this theory does not take into account direct, near-field coupling between closely spaced dielectric rod antennas, the agreement is considered good.

Figs. 3 and 5 show that efficient transfer of energy between the array and the wave beam may be obtained for source arrays of a 5×5 and larger if the proper spacing between elements is chosen, while Figs. 4 and 6 show that with the same spacing between array elements there is a diminishing return of power transferred to the fundamental mode as source arrays become larger. The following example is representative. It is assumed that active elements are arranged in the configuration of a uniform 5×5 array and are fabricated as a monolithic structure in GaAs [1]. The transverse dimension of the plane reflector is taken to be 5 cm, which is about the size of available GaAs wafers. The resonator will be "semi-confocal", therefore, $F_x = F_y = D$. The following conditions are also chosen: the

TABLE I
DRIVING-POINT RESISTANCES FOR 5×5 SOURCE ARRAY LOCATED d MILLIMETERS FROM PLANE REFLECTOR

R-ohms \ d-mm	0.05	0.1	0.15
R_{00}	2.11	8.43	18.9
R_{10}	1.95	7.78	17.5
R_{11}	1.79	7.78	16.2
R_{20}	1.53	6.12	13.7
R_{21}	1.41	5.65	12.7
R_{22}	1.11	4.44	10.0

mode parameters $\bar{X}$ and $\bar{Y}$ are 1 cm; the operating frequency is 100 GHz; the normalized current element length $\Delta X/\bar{X}$ is 1/50; the normalized spacing between source elements is 0.4; and the reflection coefficient R of the partially transparent reflector is 0.98. From (5) and (6), one obtains $D = 20.9$ cm. The driving-point resistance for each element of the source array is shown in Table I. It should be noted that, because of symmetry, there are only six different driving-point resistances. The array elements all are numbered in matrix notation with the 0,0 element located on the wave-beam axis. For the example shown in Table I, the driving-point resistances were computed by (26) are shown for a 5×5 source array located 0.05, 0.1 and 0.16 mm from and parallel to the plane reflector. In addition, the region of space between the source array and the plane reflector is filled with GaAs. Since IMPATT devices are designed to operate with low driving-point resistances [11], a distance d of 0.1 mm may be chosen as a compromise between the desired low driving-point resistances and the minimum practical thickness of GaAs.

If each active source element is able to maintain the same driving current independent of other nearby sources, and if a single source provides an output power of 1 mw when combined in the quasi-optical power combiner, 25 such sources in a 5×5 array would provide an output power of about 300 mw, 49 such sources in a 7×7 array would provide about 630 mw, and 81 such sources in a 9×9 array would provide less than 800 mw. The above example assumes the separation between source elements remains constant at 0.4 mode parameters and indicates that there may be a diminishing return upon increasing the number of source elements to very large numbers. However, with proper design, one may conclude from this study that it is practical to combine large numbers of millimeter-wave sources using quasi-optical techniques and that substantial power may be obtained.

ACKNOWLEDGMENT

The author is particularly grateful for the support and encouragement of Dr. J. R. Suttle, of the Army Research Office, during this investigation and to Dr. F. Schwering of CENCOMS, Fort Monmouth, NJ, on assignment to the Army Research Office, for many valuable discussions and for his very careful critique of the theory.

REFERENCES

[1] D. B. Rutledge, D. P. Neikirk, and D. P. Kasilingam, "Integrated-circuit antennas," in *Infrared and Millimeter Waves*, vol. 10, K. J. Button, Ed. New York: Academic Press, 1983, pp. 1–87.

[2] G. Goubau and F. Schwering, "On the guided propagation of electromagnetic wave beams," *IRE Trans. Antennas Propagat.*, vol. AP-9, pp. 248–256, 1961.

[3] F. Schwering, "Reiterative wavebeams of rectangular symmetry," *Arch. Elek. Übertragung.*, vol. 15, pp. 555–564, 1961.

[4] G. Goubau, "Beam waveguides," in *Advances in Microwaves*, vol. 3. New York: Academic Press 1968, pp. 67–126.

[5] W. Magnus and F. Oberhettinger, *Functions of Mathematical Physics*, Toronto: Chelsea Publishing, 1965, pp. 80–82.

[6] R. E. Collin, *Foundations for Microwave Engineering.* New York: McGraw-Hill, 1966, pp. 176–177.

[7] R. E. Collin, *Field Theory of Guided Waves.* New York: McGraw-Hill, 1960, pp. 200–202.

[8] C. A. Balanis, *Antenna Theory.* New York: Harper & Row, 1982, pp. 292–295.

[9] H. Kogelnik and W. W. Rigrod, "Visual display of isolated optical modes," *Proc. IRE*, vol. 50. p. 220, 1962.

[10] L. Wandinger and V. Nalbandian, "Quasioptical millimeter-wave power combiner," in *Proc. 6th Int. Conf. Infrared and Millimeter Waves.*

[11] R. K. Mains and G. I. Haddad, "Properties and capabilities of millimeter-wave IMPATT diodes," in *Infrared and Millimeter Waves*, vol. 10, K. J. Button, Ed. New York: Academic Press 1983, pp. 111–233.

Errata to Quasi-Optical Power Combining of Solid-State Millimeter-Wave Sources

SINCE publication of my paper entitled "Quasi-optical power combining of solid-state millimeter-wave sources," the following corrections have been found and pointed out by various individuals. Since the paper has been widely referenced and now reprinted as a contribution to this book, the following should be noted.

Equation 1 should read

$$H_{en}(X) = (-1)^n \exp\left(\frac{X^2}{2}\right)\frac{d^n}{dX^n}\left[\exp\left(\frac{-X^2}{2}\right)\right]$$

In Equation 3 the $(\mu / \epsilon)^{1/4}$ should be replaced by a_{mn}. Equation 7 should then read

$$\int\int_{-\infty}^{\infty} E_{mn} E^*_{m'n'}\, dxdy = \delta_{mm'}\, \delta_{nn'}\, a_{mn}\, a^*_{mn}$$

And in final form, Equation 24 should read

$$P_{qk} = \sqrt{\frac{\varepsilon}{\mu}}\, a_{qk}\, a_{qk}$$

In Equation 4 replace $E^{\pm}_{y}$ with $E^{\pm}_{ymn}$

Below Equation 3 the following changes should be made: replace x_z with $x^2{}_z$ and replace y_z with $y^2{}_z$

Equation 15 should read $E^{\pm}_{ymn}\,(x, y, 0) = 0$

The argument of Equation 19 should read (x_p, y_p, z_p)

The ordinate title of Figures 7 and 8 should be replaced by Normalized Resistance $x\,(\mu / \epsilon)^{1/4}$

In Table 1 the entry in the third column ($d = 0.1$) for R_{11} should read 7.16 and the first column should be titled R-ohms $x\,(\mu / \epsilon)^{1/2}$

I wish to take this opportunity to thank those who have brought these corrections to my attention, in particular to the graduate students of Professor Steer, to Dr. Nuteson, and to Chris Hicks, all of North Carolina State University.

Transistor Oscillator and Amplifier Grids

ROBERT M. WEIKLE II, MEMBER, IEEE, MOONIL KIM, STUDENT MEMBER, IEEE, JONATHAN B. HACKER, STUDENT MEMBER, IEEE, MICHAEL P. DE LISIO, STUDENT MEMBER, IEEE, ZOYA B. POPOVIĆ, MEMBER, IEEE, AND DAVID B. RUTLEDGE, SENIOR MEMBER, IEEE

Invited Paper

In this paper, we review recent developments in quasi-optical power combining. In particular, we examine planar periodic grids and their use as quasi-optical active components. A variety of grids used for the generation and amplification of electromagnetic radiation have been investigated. Although quasi-optical techniques are applicable to a large variety of solid-state devices, special attention is given to transistors. Transistors are attractive because they can be used as either amplifiers or oscillators. Experimental results for MESFET bar-grid and planar grid oscillators are presented. In addition, we discuss a MESFET grid amplifier that receives only vertically polarized waves at the input and radiates horizontally polarized waves at the output. An advantage of these planar grids is they can be scaled for operation at millimeter- and submillimeter-wave frequencies. By using modern IC fabrication technology, planar grid oscillators and amplifiers containing thousands of devices can be built, thereby realizing an efficient means for large-scale power combining.

I. Introduction

Millimeter- and submillimeter-wave systems continue to be a subject of growing interest. The applications involving this portion of the electromagnetic spectrum cover a broad range of scientific disciplines, varying from the measurement of electron densities in tokamak plasmas [1] to studying emission spectra of distant celestial bodies [2]. Millimeter waves correspond to the frequencies between 30 GHz and 300 GHz and the submillimeter-wave range is regarded as the region between 300 GHz and 3 THz. The shorter wavelengths at these frequencies allow the use of smaller and lighter components than for microwave systems. This is important in military and space-borne applications where size and weight are a prime concern. In addition, the atmospheric attenuation of millimeter and submillimeter waves is relatively low compared with infrared and optical wavelengths [3], particularly in the transmission windows that lie between water vapor and oxygen absorption peaks. This property can be exploited to build radars and cameras that penetrate clouds, smoke, and haze. Other commonly cited advantages of millimeter- and submillimeter-wave components over their microwave counterparts include broader bandwidths and higher resolution for radars and imaging systems.

The lack of reliable, inexpensive high-power sources, however, has been a persistent obstacle in the development of millimeter- and submillimeter-wave systems. The first devices to produce radiation in this part of the spectrum were electron tubes. Today, electron tube devices such as klystrons and crossed-field amplifiers (CFA's) are widely available and can produce several kilowatts of power in the microwave and lower millimeter-wave range [4], [5]. Traveling-wave tubes are capable of better than 100 W at 100 GHz [6]. In the far infrared and submillimeter-wave range, optically pumped FIR lasers have achieved several megawatts of pulsed power [7]. Nevertheless, in many circumstances, the size, weight, and required high-voltage power supplies of these devices often limit their usefulness.

For most low and medium power applications, electron tube sources have been replaced by solid-state devices. Compared with tube sources, solid-state devices are small, lightweight, inexpensive, and require small to moderate voltages. At present, IMPATT's — the most powerful millimeter-wave solid-state sources — can produce several watts of power at 100 GHz. Silicon IMPATT's have produced useful power up to 300 GHz [8]. A major drawback of IMPATT's, however, is the high noise level arising from the avalanche multiplication process. Gunn diodes have better noise performance but only generate a few hundred milliwatts at 100 GHz [9]. Other two-terminal solid-state devices used to produce millimeter- and submillimeter-

Manuscript received October 4, 1991; revised February 26, 1992. This research was supported by the Army Research Office, the Northrop Corporation, and a fellowship from the Rockwell International Trust. J. Hacker holds an NSERC Fellowship from Canada and M. De Lisio holds an NSF Fellowship.

R. M. Weikle II was with the Division of Engineering and Applied Science, California Institute of Technology, Pasadena, CA 91125. He is now with the Department of Applied Electron Physics, Chalmers University of Technology, Göteborg, Sweden.

M. Kim, J. B. Hacker, M. P. De Lisio, and D. B. Rutledge are with the Division of Engineering and Applied Science, California Institute of Technology, Pasadena, CA 91125.

Z. B. Popović is with the Department of Electrical and Computer Engineering, University of Colorado, Boulder, CO 80309.

IEEE Log Number 9205761.

Reprinted from *Proceedings of IEEE*, Vol. 80, No. 11, pp. 1800-1809, November 1992.

wave radiation include quantum well oscillators [10] and Josephson junctions [11], although the power levels are extremely small. An additional drawback of two-terminal solid-state sources is low dc-to-RF conversion efficiency. Better efficiencies can be realized with transistors. Pseudomorphic HEMT's have demonstrated output powers near 60 mW at 94 GHz [12]. HEMT's with 0.15 μm gate lengths have shown cutoff frequencies of over 170 GHz with $f_{\max}$ near 350 GHz [13]. Heterojunction bipolar transistors (HBT's) also have the potential to provide reasonable power levels at millimeter-wave frequencies without the need for submicron lithography. An HBT with emitter area of 80 $\mu\mathrm{m}^2$ has shown 15 dB of gain with output power of 16 dBm at 35 GHz [14].

In an attempt to overcome the limited power output of solid-state devices, a variety of power-combining methods have been developed. A good review of these methods has been given by Chang and Sun for millimeter-wave frequencies [15]. Many of these techniques are based on scaled-down microwave circuits and involve resonant cavities [16] or hybrids. Resonant cavity combiners allow good isolation between the active devices and have been used up to 300 GHz. Hybrid power combiners, which often rely on external injection locking to synchronize the sources, have been used up to 140 GHz. These approaches have a number of disadvantages. To prevent moding problems, the size of the waveguide cavities must be scaled down at higher frequencies. This makes circuit fabrication more difficult. Resistive losses in the waveguide walls, which reduce power-combining efficiency, become more severe at millimeter and submillimeter frequencies. In addition, combiners based on resonant cavities and hybrids can accommodate a limited number of devices, making large-scale power combining impractical.

II. Quasi-Optical Power Combining

An approach which overcomes the limitations of power combiners based on scaled-down microwave systems involves combining the output powers of many devices in free space. Mink suggested using an array of millimeter-wave devices placed in an optical resonator as a means of large-scale power combining [17]. While it is unlikely that solid-state power combiners will replace high-power electron tube sources, there is great potential for improvement in output power and combining efficiency by using quasi-optical techniques. Because the power is combined in free space, losses associated with waveguide walls and feed networks are eliminated. The power can be distributed over a larger number of devices than in a waveguide cavity because the quasi-optical resonator can be many wavelengths across. An external injection-locking signal is unnecessary because synchronization of the sources is accomplished by mutual coupling through the modes of the resonator.

Several types of quasi-optical power combiners have been demonstrated over the past few years. Wandinger and Nalbandian combined the outputs of two Gunn diodes at 60 GHz using tapered dielectric rod antennas coupled to a Gaussian resonator [18]. Many designs have used microstrip radiators which are synchronized with feedback or an external signal. Stephan *et al.* investigated the coupling between open resonators and microstrip circuits at 10 GHz [19]. The microstrip ground plane and a spherical reflector formed the Gaussian cavity. Using this configuration, the output powers of two Gunn diodes were combined in free space [20]. A different approach involves an array of weakly coupled patch antenna elements [21]. This method is similar to classic antenna arrays; each patch antenna is a free-running oscillator containing an active device [22]. The patch elements, which may contain either Gunn diodes or MESFET's, are synchronized using separate dc bias to each device. A dielectric slab placed above the array also facilitates locking. With this scheme, a 16-element MESFET array operating at 8 GHz produced 184 mW of power with a dc-to-RF efficiency of 25%. Linear arrays of patch antennas have also been used to combine the outputs of Gunn diodes at the second harmonic (18 GHz) [23]. More recently, a two-sided microstrip configuration has been developed that permits isolation between an external locking signal and the array output [24].

A different approach to quasi-optical power combining is based on integrating solid-state devices directly into a periodic grid. Grid arrays have long been important components for infrared and millimeter-wave applications. Conductive meshes can be used as quasi-optical filters, beam splitters, and output couplers for lasers [25]–[27]. By integrating microbolometers and Schottky diodes into these grids, various investigators have demonstrated their use as multimode detectors, grid phase shifters, and quasi-optical multipliers [28]–[30].

III. Grid Oscillators

Grid oscillators are periodic arrays embedded with active solid-state devices. The grid is placed in a Fabry–Perot resonator to provide the feedback necessary for oscillation. This is illustrated in Fig. 1. Two important features distinguish grid oscillators from most quasi-optical power combiners built from microstrip circuits. First, grid oscillators do not necessarily have a ground plane and, as a result, do not rely on the interaction of microstrip modes with free-space radiation. Second, microstrip-based power combiners tend to be a collection of individual free-running oscillators that are weakly coupled. Thus, the operating frequency depends primarily on the behavior of the individual oscillators. In contrast, the elements making up an oscillator grid are not themselves free-running oscillators. Mutual interaction of all the devices in the grid is necessary for oscillation to occur. Consequently, the oscillation frequency and the output power are strongly affected by the device spacing and the grid configuration. Each device in the array is presented with an embedding impedance which is a function of the grid structure. This embedding impedance, together with the device impedance, determines the grid's overall behavior as an oscillator.

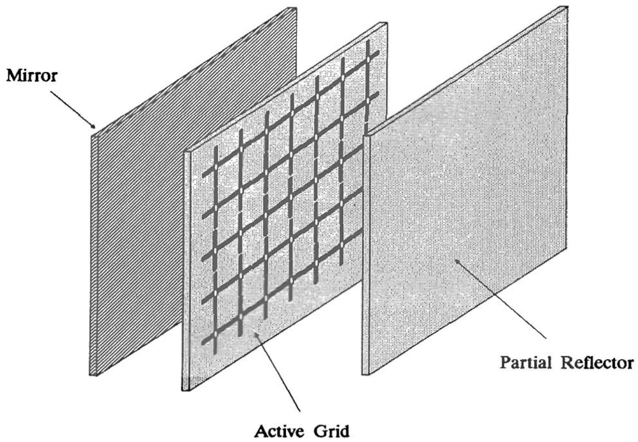

Fig. 1. Schematic of a grid oscillator. Active devices are embedded in a two-dimensional periodic array supported by a dielectric substrate. The grid array is placed in a Fabry–Perot cavity that couples the devices together.

In principle, any solid-state device can be used in an oscillator grid. Although readily amenable to planar integration, two-terminal devices generally have poor dc-to-RF efficiencies and can prove difficult to synchronize. Transistors, on the other hand, have respectable dc-to-RF conversion efficiencies and a separate control terminal. This allows the devices to be more easily stabilized, permitting oscillation to be controlled through an appropriately designed feedback circuit.

A variety of transistor grid configurations have been investigated. The first transistor oscillator grid, demonstrated by Popović *et al.* [31] in 1988, is shown in Fig. 2(a). The array is fabricated on a dielectric substrate (Duroid, Rogers Corporation) with $\epsilon_r = 10.5$ and a thickness of 2.35 mm. Packaged MESFET's (Fujitsu FSC11LF) are soldered into the grid. The vertical metal lines, which are connected to the transistor drain and gate terminals, are parallel to the radiated electric field. Horizontal metal leads running across the grid are used for dc biasing. The back side of the substrate is metallized and serves as both a mirror and ground for the MESFET source leads. Figure 2(b) shows details of the grid configuration. The device spacing is 13 mm. The gate, which is connected to a 5 mm long inductive strip, is not dc biased. When 4 V is applied to the drain, the grid oscillates at 9.7 GHz. Figure 3 shows the spectrum. The metallized back side of the substrate and a planar dielectric slab ($\epsilon_r = 10.5$ and thickness of 2.5 mm) placed in front of the grid form a Fabry–Perot resonator. Varying the distance of the front dielectric slab tunes the frequency about 1% and the output power by nearly 10%. The total radiated power, calculated by measuring the far-field radiation pattern, is 464 mW. This corresponds to an effective radiated power (ERP) of 20.7 W and a dc-to-RF conversion efficiency of about 15%. The maximum ERP obtained from the grid was 37 watts.

An attractive feature of planar grid arrays is they can be modeled with relatively simple transmission-line circuits. Fig. 4 shows an example. Energy radiated from the grid is modeled as a wave propagating along a transmission line. The characteristic impedance of the transmission line corresponds to the TEM impedance for a wave traveling

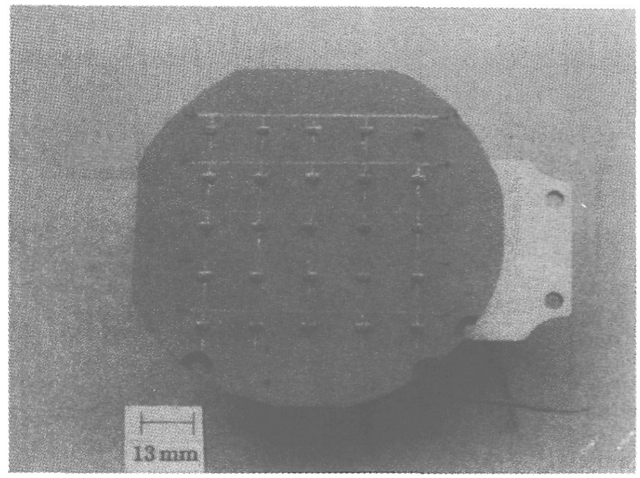

(a)

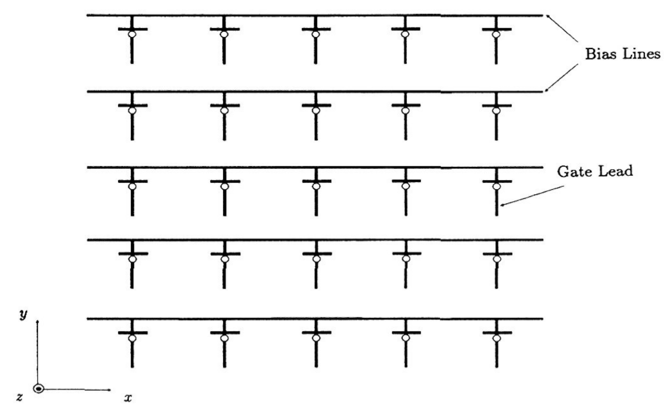

(b)

Fig. 2. (a) Photograph of a 25-element MESFET grid oscillator. The back side of the substrate is metallized and a dielectric slab is placed in front of the grid to form a Fabry–Perot cavity. (b) Schematic of the grid configuration. The MESFET drain and gate are connected to the vertical leads.The source leads run through the substrate and are soldered to the ground plane [31].

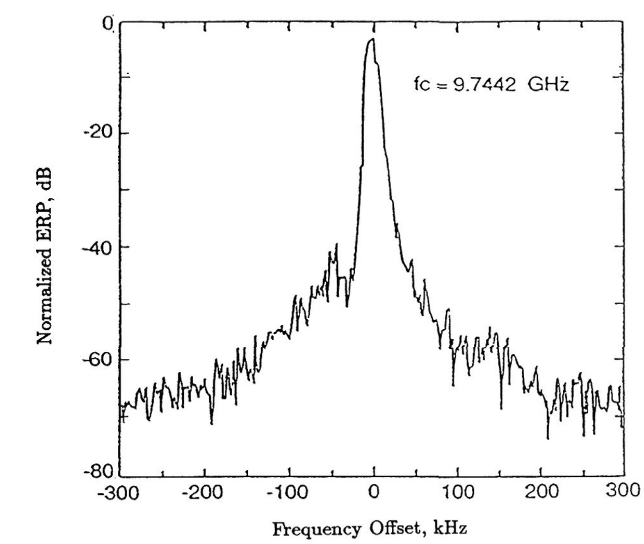

Fig. 3. Spectrum of the 25-element MESFET grid [31].

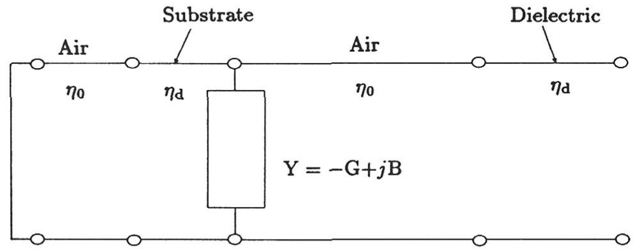

Fig. 4. Transmission-line model for a planar grid. Radiated power isrepresented as a wave traveling along a transmission line.

in that particular dielectric medium. Thus, for the grid of Fig. 2(a), free space is represented with a 377 Ω transmission line and the dielectric slabs are modeled with 116 Ω lines. A short circuit models the mirror behind the grid. A shunt admittance, Y, represents the devices and the embedding impedance. This admittance is a function of the grid configuration as well as the impedance of the embedded devices. For a grid containing active solid-state devices, the real part of the admittance is negative.

IV. Bar-Grid Oscillators

An alternative quasi-optical grid configuration is shown in Fig. 5. The grid consists of an array of metal bars on which packaged devices are mounted. This structure has been used to combine the output powers of both transistors [32] and Gunn diodes [33]. A mirror placed behind the grid couples the devices together and is also used for reactive tuning. The metal bars, which are used to provide dc bias to the devices, make an excellent heat sink. For convenience, the devices in adjacent rows share dc biasing. This arrangement minimizes the number of biasing connections. It also gives the grid a symmetric structure that can be exploited to determine the grid's embedding impedance.

A transmission-line model similar to that shown in Fig. 4 is used to describe the bar grid. Each device in the grid is viewed as occupying a unit cell which is defined by symmetry. If the devices in the grid are identical and all are oscillating in phase, the electric and magnetic fields must satisfy symmetry-imposed boundary conditions along the edges of the unit cell. In effect, the entire grid is reduced to an equivalent waveguide representation as illustrated in Fig. 5(b). The equivalent waveguide has electric walls on the top and bottom and magnetic walls (where the tangential magnetic field vanishes) on the sides. A device placed in the grid is viewed as a source which excites the equivalent waveguide. By finding the impedances present at the terminals of a device in the unit cell, the behavior of the grid can be predicted. Details of the analysis have already been presented and it is unnecessary to repeat them here [32]. A transmission-line model representing the MESFET bar-grid oscillator is shown in Fig. 6. The drain and gate leads excite different waveguides which are formed by the metal bars. These waveguides are modeled with two sections of transmission line with characteristic impedance

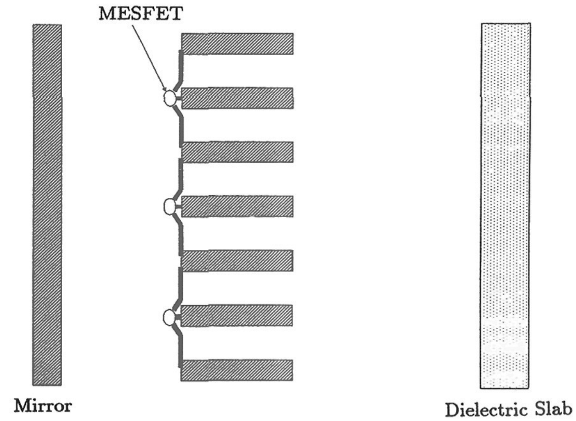

(a)

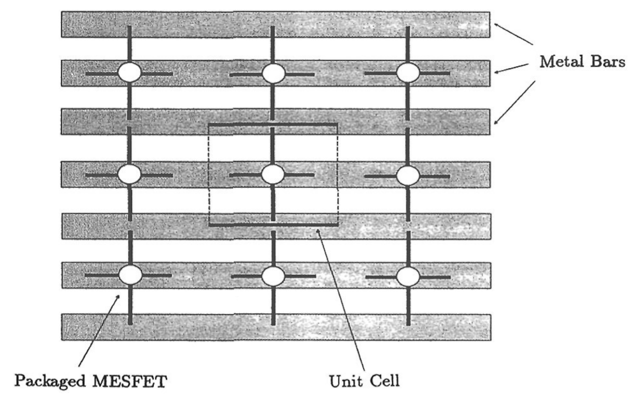

(b)

Fig. 5. (a) Side view of the MESFET bar-grid oscillator. (b) Front view of the bar grid. Adjacent rows of devices share bias. The unit cell is shown with solid lines to indicate electric walls and dashed lines to represent magnetic walls.

Z_{TEM}. The discontinuity at the edges of the metal bars produce evanescent capacitive modes and is represented with lumped capacitors, C and C_m. C_m is the mutual capacitance arising from fields of one waveguide coupling to the fields of the other waveguide. Currents on the drain and gate leads generate evanescent inductive modes which we model with lumped inductors. There is also a mutual inductance, M, describing the coupling of the magnetic fields between the metal-bar waveguides.

A grid containing 36 MESFET's mounted on metal bars produced 220 mW of power at 3 GHz. The grid period is 10 mm ($0.1\lambda_0$). The measured dc-to-RF conversion efficiency was 22%. Grid directivity, measured from the far-field radiation pattern, was 11.3 dB. Moving the position of the back-short tunes the operating frequency of the grid over a 300 MHz bandwidth. In addition, the frequency can be varied by changing the bias to the gate leads (250 MHz/V). Gate bias, however, has little effect on the amplitude of the radiated signal, indicating that this property can be used to frequency modulate the grid output. Fig. 7 shows the output spectrum of the bar grid when a 5 MHz ac signal is superimposed over the gate bias. The FM Bessel function coefficients [35] are shown for comparison.

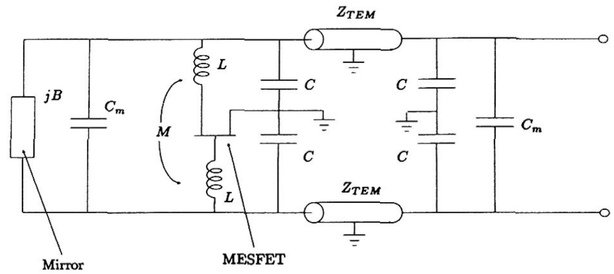

Fig. 6. Transmission-line model of the MESFET bar-grid oscillator. The MESFET is added to the model using its small-signal equivalent circuit.

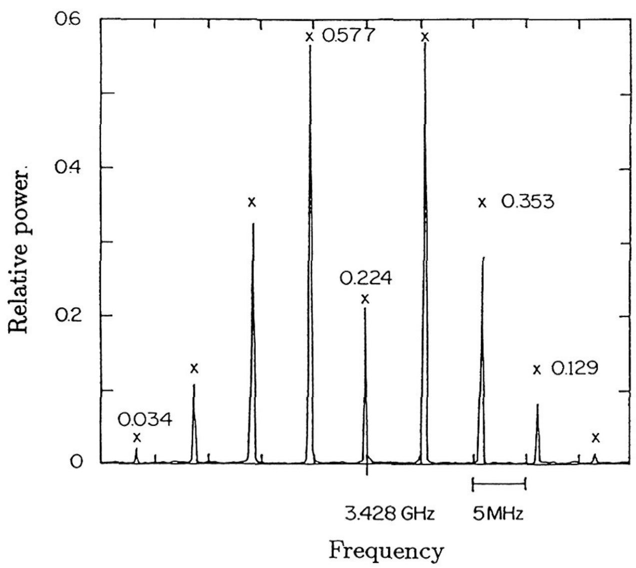

Fig. 7. Measured bar-grid oscillator FM spectrum. The scale is linear in power and the Bessel function coefficients are shown with ×'s [32].

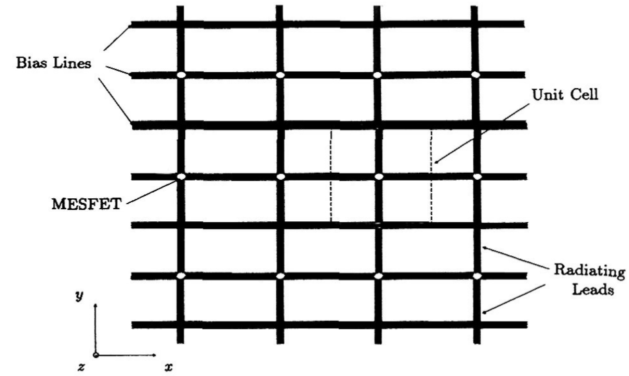

Fig. 8. Physical layout of the planar MESFET grid oscillator. Adjacent rows of devices share bias lines. The unit cell equivalent waveguide is shown with solid lines for electric walls and dashed lines for magnetic walls.

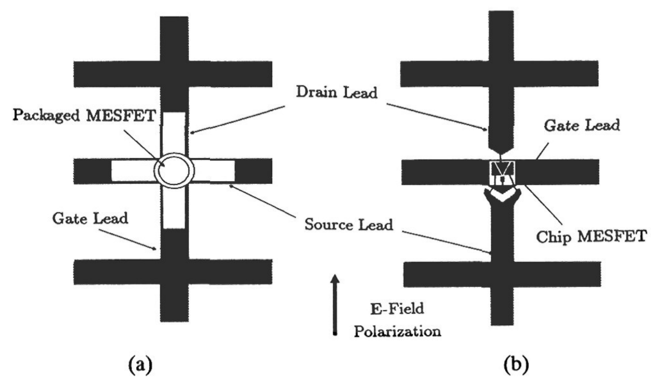

Fig. 9. (a) Unit cell for a vertical drain–gate grid which uses packaged devices. (b) Unit cell for a gate-feedback grid oscillator with chip MESFET's. The gate lead, which runs horizontally, is capacitively coupled to the incident electric field [37].

V. Planar-Grid Oscillators

The transistor grids discussed thus far operate at microwave frequencies. To extend the operating frequencies to the millimeter- and submillimeter-wave region, high-frequency devices need to be integrated into the grid. Packaged devices are unsuitable because of the associated parasitics. In addition, the devices in the grid need to be placed closer together at higher frequencies. Thus, millimeter- and submillimeter-wave grids are only feasible if monolithic fabrication techniques are used. For this reason, planar grid configurations are particularly important.

Two types of planar grids have been investigated to date [36], [37]. The grids, which have the same basic structure, differ by the manner in which the MESFET's are connected. A schematic of the planar grid is shown in Fig. 8. Like the bar grid, vertical leads couple to the radiated field and horizontal leads are used for dc biasing. Two transistor terminals are connected to the vertical leads while the third is connected to the horizontal bias line. Initial work with the planar grid structure utilized packaged MESFET's (Fujitsu FSC11LF). Because of the physical layout of the device package, the grid was restricted to the vertical drain–gate configuration illustrated in Fig. 9(a). Subsequent investigations involved chip MESFET's (Fujitsu FSC11X) which were connected in a vertical drain–source configuration (Fig. 9(b)).

To find a grid equivalent circuit model, symmetry is exploited to define a unit cell equivalent waveguide. An EMF analysis of the unit cell (similar to that used by Eisenhart and Khan for a post in a waveguide [34]) leads to the transmission-line model of Fig. 10. The terminals labeled 1 and 2 represent connections to the vertical leads of the grid. The center terminal labeled 3 represents the horizontal lead. Free space is modeled with a 377 Ω transmission line which is scaled by the aspect ratio (b/a) of the unit cell. A lumped inductor, L, accounts for the inductance of the vertical leads. Currents in the horizontal leads are orthogonal to the radiated field and thus generate nonpropagating (evanescent) modes. These modes are represented with the lumped reactive elements, C_m and L_m. Coupling between the radiated field and currents in the various transistor leads is described by a center-tapped transformer.

Strictly speaking, a transmission-line model derived using an equivalent waveguide is only valid for infinite grids. As a result, the applicability of the model is questionable with small grids because the equivalent waveguide boundary

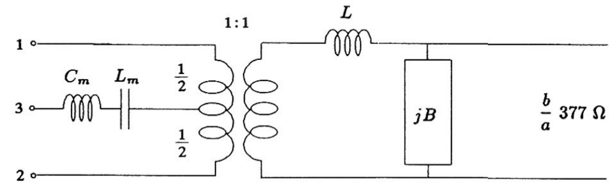

Fig. 10. Transmission-line model for the planar MESFET grid. The mirror behind the grid is represented with a shunt susceptance jB [37].

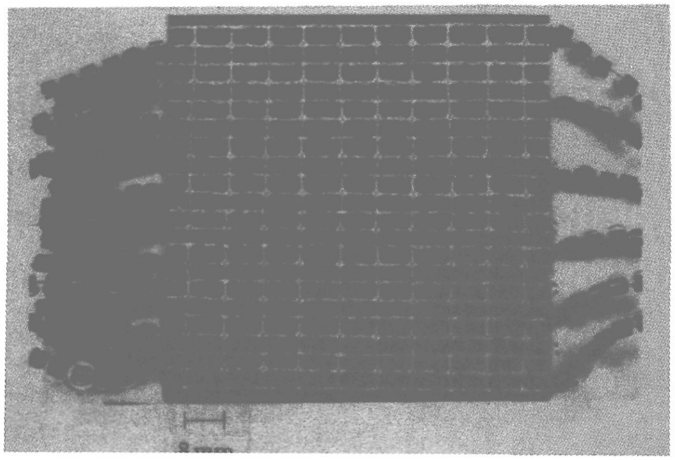

Fig. 11. Photograph of the 100-element MESFET grid. Ferrite beads placed in the bias lines suppress low-frequency oscillation. The vertical leads are parallel to the radiated electric field [36].

conditions do not hold at the grid edges. It may be possible, however, to terminate the grid edges in a way that simulates the equivalent waveguide boundary conditions. Electric walls at the top and bottom of the grid can be approximated with vertical $\lambda/4$ open-circuited stubs. This should prevent currents there from abruptly dropping to zero. In addition, RF chokes or inductive leads can be used at the sides of the grid to create large impedances, thus simulating magnetic walls. Using edge terminations such as these, we have found the EMF models to be in reasonably good agreement with measurement for grids containing as few as 16 elements.

MESFET arrays based on the vertical drain–gate configuration of Fig. 9(a) are called source-feedback grids. This terminology arises because the vertical leads (drain and gate) couple directly to the radiated field, and part of this radiated field is capacitively coupled to the horizontal transistor lead (the source) through the grid embedding circuit. A 100-element grid based on the unit cell of Fig. 9(a) is shown in Fig. 11 [36]. The grid is built on a 0.5 mm thick substrate ($\epsilon_r = 2.2$) which lies on top of a second substrate (2.5 mm thick and $\epsilon_r = 10.5$). Devices in the grid are spaced 8 mm apart. The grid, which oscillates at 5 GHz, produces 600 mW of power with a dc-to-RF efficiency of 20%. A planar mirror behind the grid is used to tune the frequency and output power (Fig. 12).

A disadvantage of the common-source grid is the radiating gate lead. Because the gate strongly couples to the radiated field, the grid tends to oscillate at lower frequencies where the devices have high gain. The common-gate grid

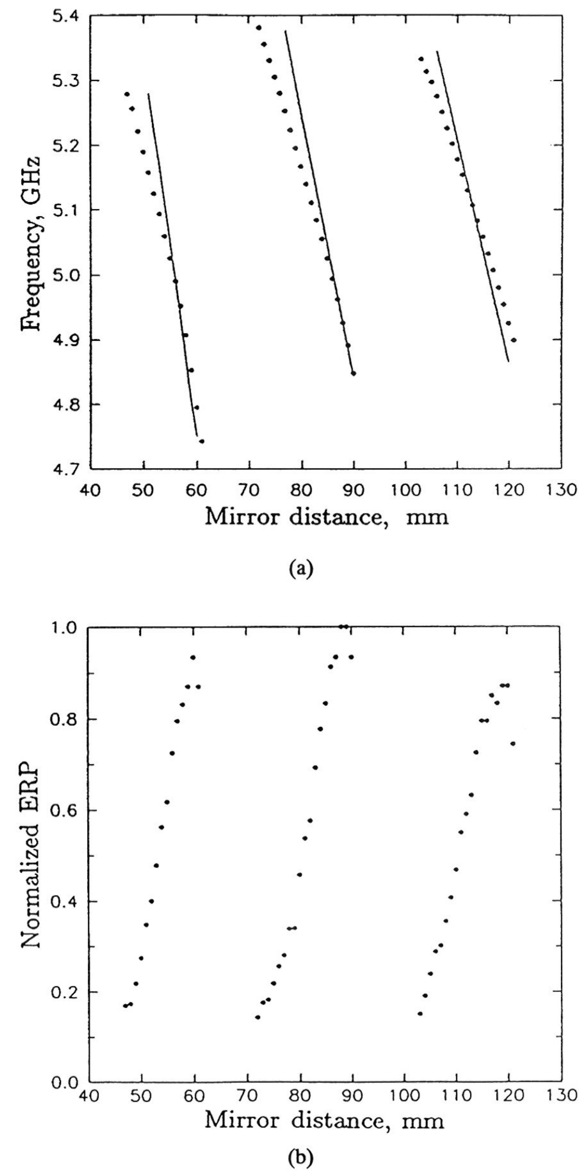

Fig. 12. (a) Theoretical (—) and measured (···) frequency tuning with mirror position. (b) Normalized ERP as a function of mirror position. The theoretical curve is obtained using the manufacturer's MESFET model with the grid embedding circuit. The mirror position is defined as the distance from the mirror to the back of the grid substrate [36].

of Fig. 9(b) overcomes this problem [37]. Bond wire is used to connect the gate to the horizontal lead. This allows the feedback between the radiated field and the gate to occur through the grid embedding circuit. Figure 13 shows a 16-element gate-feedback grid designed for operation in X-band. The substrate is Rogers Duroid with $\epsilon_r = 2.2$ and thickness of 2.5 mm. Chip MESFET's, spaced 9 mm apart, are soldered and wire-bonded to the grid. The width of the device leads are 1 mm. Figure 14 shows the far-field radiation pattern of the grid when a drain bias of 4 V is applied. The grid oscillates at 11.6 GHz (within 2% of the design frequency) and produces 335 mW of output power, corresponding to a dc-to-RF efficiency of 20%.

Illustrating that planar grids can be scaled for use at higher frequencies, the X-band gate-feedback grid was

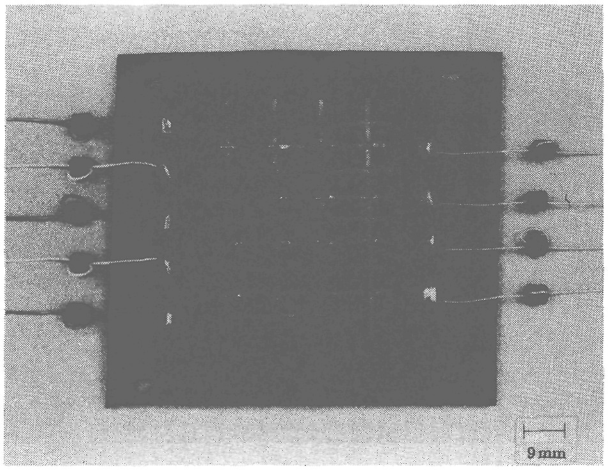

Fig. 13. Photograph of the X-band gate-feedback grid. The substrate is 2.5 mm thick Rogers Duroid with $\epsilon_r = 2.2$. The grid is placed between a planar mirror and dielectric slab which form the Fabry–Perot cavity [37].

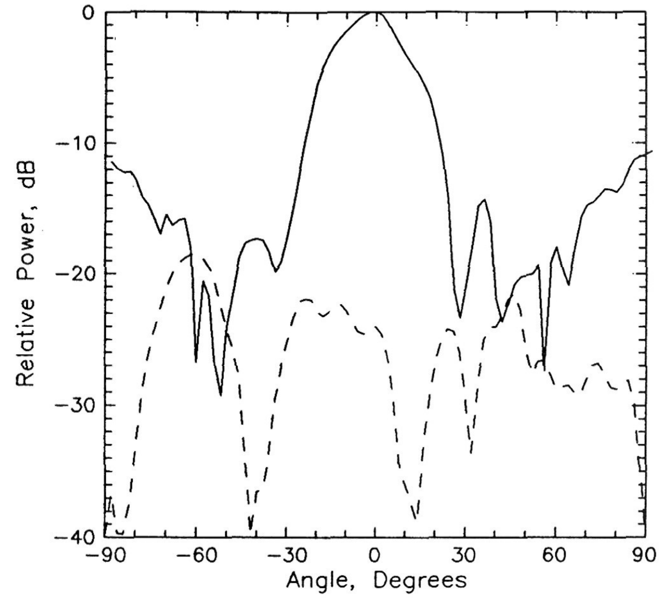

(a)

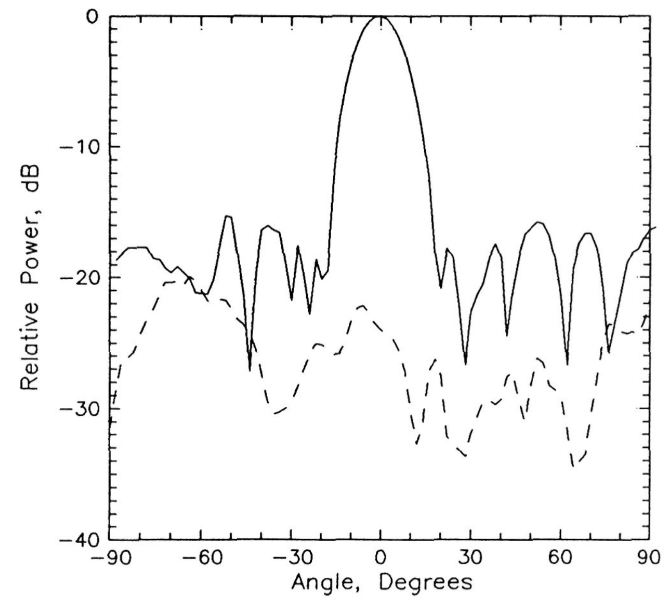

(b)

Fig. 14. Measured far-field radiation patterns for the X-band grid in (a) the H plane (a) and (b) the E plane. The cross-polarized patterns are shown with dashed lines [37].

redesigned for operation in the Ku-band. The scaled grid has 0.5 mm wide lines and the devices are placed 5 mm apart. Using an identical substrate and the same devices (FSC11X), a 36-element grid produced 235 mW at 17 GHz [37]. This oscillation frequency is near the f_T of the transistors (19 GHz), suggesting that suitably designed HEMT grids may oscillate well over 100 GHz. The dc-to-RF conversion efficiency of the Ku-band grid is about 7%. This observed reduction in output power and efficiency, compared with the X-band grid, is expected from the higher operating frequency.

VI. Amplifier Grids

Although they are important for many millimeter- and submillimeter-wave systems, oscillators represent only one possible use for MESFET grids. Amplifiers — which are difficult to build at millimeter- and submillimeter-wave frequencies — are necessary in most applications. Grid amplifiers offer the same advantages as grid oscillators: increased power-handling capability and elimination of the losses associated with waveguides and feed networks. In essence, a grid amplifier is a planar structure that radiates an amplified version of a wave incident on its surface. As a result, the grid design must accommodate an array of transistors and suppress potential spurious oscillations. In addition, there needs to be a means of isolating the output wave from the input wave.

Figure 15 shows a unit cell of the grid amplifier. The grid receives radiation polarized in the y direction and radiates a horizontally polarized wave [38]. Polarizing plates are placed on either side of the grid to provide isolation between the amplifier input and output. The unit cell of the grid contains a pair of MESFET's with joined sources. Vertical metal leads are attached to the MESFET gates and horizontal leads connect to the drains. A Duroid substrate with $\epsilon_r = 10.5$ supports the array. A dc bias, which is applied to lines running horizontally across the back of the substrate, is fed to the MESFET's through via holes. To eliminate spurious oscillations, 1-kΩ carbon resistors are placed between the bias lines and the MESFET gates. Additional 120-Ω resistors connect the source leads to dc ground.

Amplifier gain is measured by illuminating the grid with vertically polarized radiation and measuring the power radiated in the orthogonal polarization. We can write an expression for the amplifier gain as

$$G = \frac{P_r}{P_c}\left(\frac{\lambda r}{2A}\right)^2, \tag{1}$$

where P_r is the received power with the amplifier grid

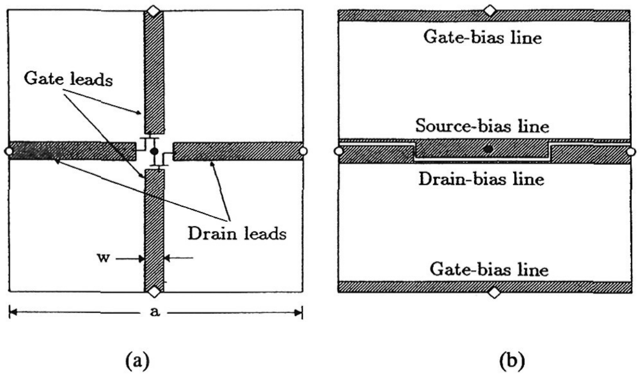

Fig. 15. A unit cell of the grid amplifier: (a) front view and (b) back view. The symbols indicate different connections between the front and back of the grid amplifier. •: 120-Ω source-bias resistor; ◇: 1-kΩ gate-bias resistor; o: drain-bias pin [38].

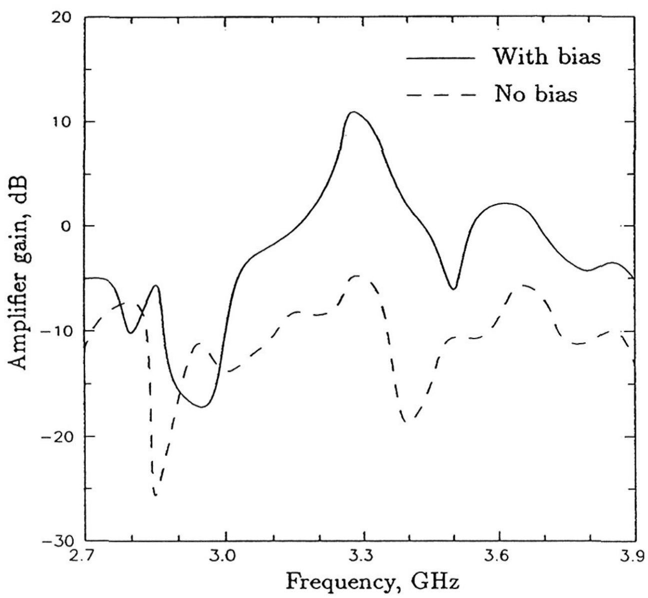

Fig. 16. Measured amplifier gain (—) and grid response with no bias(- - -) [38].

in place, P_c is the received power with the amplifier grid removed, A is the geometrical area of the grid, and r is the distance between the grid and each horn [38]. This simple formula allows us to calculate the gain from a relative power measurement and three well-known parameters.

Figure 16 shows the measured gain of a 50-element MESFET amplifier grid. A maximum gain of 11 dB occurs at 3.3 GHz. The input and output polarizers, which are probably responsible for the narrow (90 MHz) bandwidth, are important; gain is not observed without them. For comparison, the grid response when dc bias is removed is also shown in Fig. 16.

VII. Quasi-Optical Systems

Amplifiers and oscillators are just two of the components used in millimeter- and submillimeter-wave systems. Many other important system components, such as mixers, multipliers, filters, and phase shifters, can also be realized with quasi-optical grids. A common property of these grids is that their dynamic range increases in proportion to the number of devices in the array, yet noise performance is no worse than for circuits containing a single device.

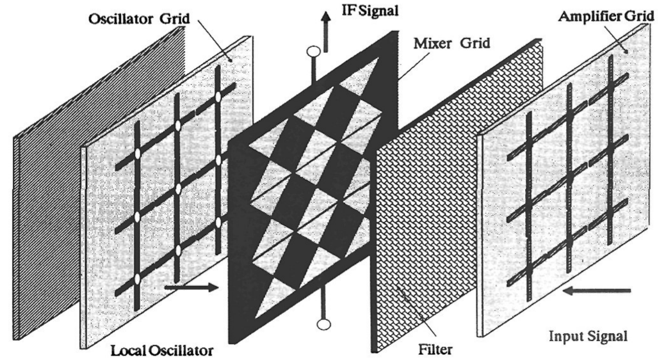

Fig. 17. Schematic of a quasi-optical heterodyne receiver. A grid oscillator provides the LO and a grid amplifier constitutes the receiver's front end. The IF signal is removed from the mixer with a coaxial cable.

Lam *et al.* built a monolithic Schottky-diode grid phase shifter which exhibited 70° of phase shift at 93 GHz [29]. The same grid, used as a millimeter-wave diode-grid frequency doubler, generated 0.5 W with 9.5% efficiency at the second harmonic (66 GHz) [30]. More recently, Hacker *et al.* demonstrated a Schottky diode grid mixer at 10 GHz [39]. The local oscillator (LO) and RF signals illuminate the mixer grid, and the IF signal is removed from the bias lines with a coaxial cable. The grid, which consists of 100 beam-lead Schottky diodes in a bow-tie antenna array, has shown a 20 dB increase in dynamic range over a single diode mixer. The conversion loss and noise figure are comparable to those of a conventional single-diode mixer.

To form a complete quasi-optical system, individual grid components need to be integrated. A heterodyne receiver, for example, consists of a mixer, a local oscillator, an amplifier, and filters. Fig. 17 illustrates how a quasi-optical heterodyne receiver may be realized by cascading grids. An oscillator grid illuminates the mixer to provide an LO. A grid amplifier, followed by a quasi-optical filter, is placed at the receiver input. Dielectric slabs can be included to provide input and output matching. Such a system is straightforward to build and does not require separate antennas that feed waveguide or transmission-line circuits; all signal propagation occurs in free space.

VIII. Conclusions

This paper has reviewed a variety of MESFET grids used for the generation and amplification of microwave power. The approach, which involves a periodic grid of transistors, is relatively simple to implement and suitable for wafer-scale integration. Bar grids, which have excellent heat-sinking capacity, offer an attractive means of combining the output power of low-efficiency devices such as Gunn diodes. Planar grids, although less efficient at removing heat, are compatible with modern IC fabrication techniques. This is a real advantage for large-scale power combining at millimeter- and submillimeter-wave frequencies. Experimental results have shown that the power-handling capacity of quasi-optical grids increases in proportion to the number of devices. Other important figures of merit such as conversion loss and noise figure are no worse than for circuits containing one device.

Much work, however, remains to be done on quasi-optical arrays. Questions involving grid robustness and tolerance to device failure need to be addressed. The thermal properties of planar transistor grids require investigation as well as other aspects pertaining to monolithic integration. The operating frequency and output power of oscillator grids must be increased. Better understanding of the nonlinear dynamics of and interaction between devices in the grid may lead to higher dc-to-RF efficiencies. Grid amplifiers are still in their infancy; new grid configurations allowing broader bandwidths and higher-frequency operation need to be studied. In addition, the various issues involved in integrating grid components to form quasi-optical systems will need to be examined.

Nevertheless, with the recent advances in IC fabrication technology and the continuing development of new millimeter- and submillimeter-wave devices, quasi-optical power combining remains a most promising method for realizing high output power from solid-state sources.

References

[1] N. C. Luhmann, Jr., "Intrumentation and techniques for plasma diagnostics: An overview," in *Infrared and Millimeter Waves*, vol. 2, K. J. Button, Ed. New York: Academic Press,1979, ch. 1.

[2] T. G. Phillips and D. B. Rutledge, "Superconducting tunnel detectors in radio astronomy," *Scientific American* vol. 254, pp. 96–102, 1986.

[3] J. C. Wiltse, "Introduction and overview of millimeter waves," *Infrared and Millimeter Waves*, vol. 4, K. J. Button, Ed. New York: Academic Press, 1981, ch. 1.

[4] G. Kantorowicz and P. Palluel, "Backward wave oscillators," in *Infrared and Millimeter Waves*, vol. 1, K. J. Button, Ed. New York: Academic Press, 1979, ch. 4.

[5] H. Bierman, "Microwave tube design efforts yield steady performance improvements," *Microwave J.*, pp. 52–73, June 1988.

[6] J. W. Hansen, "US TWT's from 1 to 100 GHz," *Microwave J.*, pp. 179–193, 1989 (State of the Art Reference).

[7] T. A. DeTemple. "Pulsed optically pumped far infrared lasers," in *Infrared and Millimeter Waves,* vol. 1, K. J. Button, Ed. New York: Academic Press, 1979, ch. 3.

[8] Y. C. Shih and H. J. Kuno, "Solid-state sources from 1 to 100 GHz," *Microwave J.*, pp. 145–161, 1989 (State of the Art Reference).

[9] T. B. Ramachandran, "Gallium arsenide power sources," *Microwave J.*, pp. 91–107, 1990 (State of the Art Reference).

[10] E. R. Brown, T. C. L. G. Sollner, C. D. Parker, W. D. Goodhue, and C. L. Chen, " Oscillations up to 420 GHz in GaAs/AlAs resonant-tunneling diodes," *Appl. Phys. Lett.*, vol. 49, pp. 1777–1779, Oct. 1989.

[11] S.P Benz and C. J. Burroughs, "Coherent emission from two-dimensional Josephson junction arrays," *Appl. Phys. Lett.*, vol. 58, pp. 2162–2164, May 1991.

[12] M. Y. Kao *et al.*, "Very high power-added efficiency and low-noise 0.15-μm gate-length pseudomorphic HEMT's," *IEEE Electron Device Lett.*, vol. 10, pp. 580–582, Dec. 1989.

[13] C. A. Liechti, "High-speed transistors: Directions for the 1990's," *Microwave J.* pp. 165–177, 1989 (State of the Art Reference).

[14] J. A. Higgins, "GaAs heterojunction bipolar transistors: A second generation microwave power amplifier transistor," *Microwave J.*, pp. 176–194, May 1991.

[15] K. Chang and C. Sun, "Millimeter-wave power combining techniques," *IEEE Trans. Microwave Theory Tech.*, vol. 31, pp. 91–107, Feb. 1983.

[16] K. Kurokawa, "The single-cavity multiple-device oscillator," *IEEE Trans. Microwave Theory Tech.*, vol. 19, pp. 793–801, Oct. 1971.

[17] J. W. Mink, "Quasi-optical power combining of solid-state millimeter-wave sources," *IEEE Trans. Microwave Theory Tech.*, vol. 34, pp. 273–279, Feb. 1986.

[18] L. Wandinger and V. Nalbandian, "Millimeter-wave power combiner using quasi-optical techniques," *IEEE Trans. Microwave Theory Tech.*, vol. 31, pp. 189–193, Feb. 1983.

[19] K. D. Stephan, S. L. Young, and S. C. Wong, "Microstrip circuit applications of high *Q* open microwave resonators," *IEEE Trans. Microwave Theory Tech.*, vol. 36, pp. 1319–1327, Sept. 1988.

[20] S. L. Young and K. D. Stephan, "Stabilization and power combining of planar microwave oscillators with an open resonator," in *1987 IEEE MTT-S Int. Symp. Dig.* (Las Vegas, NV) vol. 1, pp. 185–188.

[21] R. A. York and R. C. Compton, "Quasi-optical power combining using mutually synchronized oscillator arrays," *IEEE Trans. Microwave Theory Tech.*, vol. 39, pp. 1000–1009, June 1991.

[22] K. Chang, K. A. Hummer, and J. L. Klein, "Experiments on injection locking of active antenna elements for active phased arrays and spatial power combiners," *IEEE Trans. Microwave Theory Tech.*, vol. 37, pp. 1078–1084, July 1989.

[23] A. Mortazawi and T. Itoh, "A periodic second harmonic spatial power combining oscillator," in *1990 IEEE MTT-S Int. Symp. Dig.* (Dallas, TX), vol. 3, pp. 1213–1216.

[24] J. Birkeland and T. Itoh, "A 16-element quasi-optical fet oscillator power-combining array with external injection locking," *IEEE Trans. Microwave Theory Tech.*, vol. 40, pp. 475–481, Mar. 1992.

[25] J. A. Arnaud and A. Pelow, "Resonant-grid quasi-optical diplexers," *Bell Syst. Tech. J.,* vol 54, pp. 263–283, 1975.

[26] R. Watanabe, "A novel polarization independent beam splitter," *IEEE Trans. Microwave Theory Tech.*, vol. 8, pp. 685–689, 1980.

[27] R. Ulrich, T. J. Bridges, and M. A. Pollack, "Variable metal mesh coupler for far infrared lasers," *Appl. Opt.*, vol. 11, pp. 2511–2516, 1970.

[28] D. B. Rutledge and S. E. Schwarz, "Planar-multimode detector arrays for infrared and millimeter-wave applications," *IEEE J. Quantum Electron.*, vol. 17, pp. 407–414, Mar. 1981.

[29] W. W. Lam *et al.*, "Millimeter-wave diode-grid phase shifters," *IEEE Trans. Microwave Theory Tech.*, vol. 36, pp. 902–907, May 1988.

[30] C. F. Jou *et al.*, "Millimeter-wave diode-grid frequency doubler," *IEEE Trans. Microwave Theory Tech.*, vol. 36, pp. 1507–1514, Nov. 1988.

[31] Z. B. Popović, M. Kim, and D. B. Rutledge, "Grid oscillators," *Int. J. Infrared and Millimeter Waves,* vol. 9, no. 7, pp. 647–654, 1988.

[32] Z. B. Popović, R. M. Weikle, II, M. Kim, K. A. Potter, and D. B. Rutledge, "Bar-grid oscillators," *IEEE Trans. Microwave Theory Tech.*, vol. 38, pp. 225–230, Mar. 1990.

[33] M. Nakayama. M. Hieda, T. Tanaka, and K. Mizuno, "Millimeter and submillimeter wave quasi-optical oscillator with multi-elements," in *1990 IEEE MTT-S Int. Symp. Dig.* (Dallas, TX), vol. 3, pp. 1209–1212.

[34] R. L. Eisenhart and P. J. Khan, "Theoretical and experimental analysis of a waveguide mounting structure," *IEEE Trans. Microwave Theory Tech.*, vol. 19, pp. 706–719, Aug. 1971.

[35] R. E. Ziemer and W. H. Tranter, *Principles of Communications,* 2nd ed. Boston: Houghton Mifflin, 1985, pp. 146–148.

[36] Z. B. Popović, R. M. Weikle II, M. Kim, and D. B. Rutledge, "A 100-MESFET planar grid oscillator," *IEEE Trans. Microwave Theory Tech.*, vol. 39, pp. 193–200, Feb. 1991.

[37] R. M. Weikle, II, M. Kim, J. B. Hacker, M. P. De Lisio, and D. B. Rutledge, "Planar MESFET grid oscillators using gate feedback," *IEEE Trans. Microwave Theory Tech.,*, vol. 40, Nov. 1992.

[38] M. Kim *et al.*, "A grid amplifier," *IEEE Microwave and Guided Wave Letters*, vol. 1, pp. 322–324, Nov. 1991.

[39] J. B. Hacker, R. M. Weikle II, M. Kim, M. P. De Lisio, and D. B. Rutledge, "A 100-element planar Schottky diode grid mixer," *IEEE Trans. Microwave Theory Tech.*, vol. 40, Mar. 1992.

Recent Progress of Quasi-Optical Integrated Microwave and Millimeter-Wave Circuits and Components

T. ITOH
ELECTRICAL ENGINEERING RESEARCH LABORATORY
THE UNIVERSITY OF TEXAS AT AUSTIN
AUSTIN, TX 78712 USA

Abstract. This paper reviews recent developments of quasi-optical integrated components for microwave and millimeter-wave applications. Historical and more recent developments of quasi-optical mixers are first presented. In addition, recent efforts by a number of research groups on expanding the range of available quasi-optical circuits and components are addressed. The latter include amplifiers, frequency multipliers, oscillators and power combiners, and receiver and transceiver modules.

1. INTRODUCTION

As microwave systems progress to higher frequencies and complexities, the engineer may be forced to simplify components and to combine functions whenever possible. At millimeter-wave frequencies and beyond, combinations of individual components become increasingly more costly and difficult. Rather than scaling low frequency techniques to shorter wavelengths, a completely new approach is needed.

Quasi-optical components provide a solution to this problem by combining the function of an antenna and a functional component such as a mixer into a single entity. As the microwave integrated circuit (MIC) technique has advanced, it has been attempted to make use of the planar and printed circuit technology for MIC in these quasi-optical components by implementing printed antennas with MICs and making use of special properties of these antennas whenever possible. This technique has been extensively used in the area of mixers. A quasi-optical mixer combines the function of a receiving antenna and a mixer into one compact entity. This type od circuit can be simple enough to be mass produced by MIC technology. To date, the development of most of the quasi-optical mixers is in the laboratory phase, however, a wide range of working designs have evolved in the past several years which may have a wider appeal to practical systems. Advances in the technology of monolithic microwave and millimeter-wave integrated circuits (MIMIC) have accelerated the development.

The recent resurgence of interest in millimeter-wave systems increases the already broad range of potential applications that quasi-optical mixers can fill. These applications include phased arrays, radars and satellite communication and imaging systems. In addition, as described later, an essentially simple construction of quasi-optical mixer can be used not only at millimeter-wave frequencies but also at microwave frequencies where cost reduction is important as in the case of industrial applications.

The quasi-optical technique itself is not limited to mixer structures. However, until very recently, the development of functional components other than mixers has essentially been nonexisting. The present article also reviews the emergence of these functional components that include power combiners, multipliers amplifiers and oscillators as well as complete receiver front ends. Compared to quasi-optical mixers, development of these components are even less mature. However, advancement of technology on these components is essential for eventual implementation of quasi-optical components for the entire millimeter-wave and even microwave systems which are cost effective and still retain high performance. In what follows, we first present the basic properties and a review of recent developments of quasi-optical mixers. Subsequently, we present a number of attempts in the development of quasi-optical functional components including complete receiver front ends and transceivers.

2. QUASI-OPTICAL MIXER PRINCIPLES

Fig. 1 shows the basic diagram of the quasi-optical mixer. It should be recognized that the antenna is an integral part of the mixer and the «RF port» of the mixer is not accessible. The RF signal is captured by the antenna which is integrated into the mixer circuit. The local oscillator (LO) signal can also be captured by the same antenna although this is not an absolute requirement. The LO-to-RF isolation is more difficult than the conventional mixer. However a number of techniques such as polarization duplexing can be used for

Reprinted with permission from *Alta Frequenza*, T. Itoh, "Recent progress of quasi-optical integrated microwave and millimeter-wave circuits and components," Vol. LVIII, No. 5-6, pp. 507-515, September-December 1989.

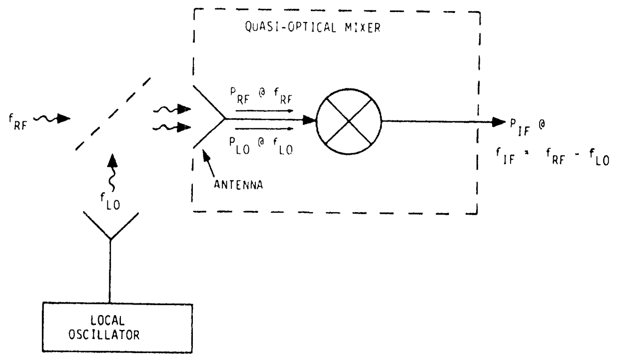

Fig. 1 - Basic quasi-optical mixer.

improvement of this characteristic.

Mixers are usually characterized by two quantities; conversion loss and noise figure. The conversion loss is the ratio of the input RF power delivered to the mixer P_{RF} to the IF frequency power available P_{IF}.

$$L_c = P_{RF}/P_{IF} \tag{1}$$

The problem in the quasi-optical mixer is the difficulty in finding the P_{RF} since the RF port is not accessible. One way to rectify this problem is to introduce the concept of isotropic conversion loss L_{iso}. This quantity is related to the conversion loss via

$$L_{iso} = L_c/G \tag{2}$$

where G is the antenna gain [1]. This quantity can be obtained if the RF wave's power density is measured, and the antenna is assumed to be isotropic. The mixer conversion loss L_c can be obtained if G is found from a scale model measurement or by some other means.

Noise figure is another important parameter for mixer design. This quantity is a function of diode parameters, diode mounting parasitics, and interfaces. If the mixer circuit noise figure is F_{mix} and its conversion loss is L_c, then the overall noise figure of the system F_{sys} is determined not only by F_{mix} but also by the noise figure F_{IF} of the IF system and the losses in the antenna and RF path, L_a, and is given by

$$F_{sys} = L_a F_{mix} + L_a L_c (F_{IF} - 1) \tag{3}$$

This equation clearly indicates that loss in the antenna or RF path contributes directly to the system noise figure. Since the RF path between the antenna and the mixer is eliminated in the quasi-optical mixer, the noise figure of the latter is expected to be superior to a system employing a conventional mixer.

3. DESIGN CONSIDERATIONS

Since a quasi-optical mixer is a combination of an antenna and a mixer circuit into a single entity, its design requires consideration of an antenna in addition to the usual consideration of noise figure, conversion loss and frequency response. The antenna is required not only to couple the free space wave to the mixer devices but also to provide a suitable impedance, called the embedding impedance, to the mixer devices. The importance of this impedance over a wide frequency range was pointed out by Held and Kerr on the performance of the mixer in terms of conversion loss and noise, since various frequency components exist the mixer circuits [2].

The antennas used in a quasi-optical mixer depend on the nature of the incoming wave front. If the mixer is used without an external focusing systems such as a lens or a reflector, an antenna with a reasonable gain in the direction of the RF signal source is desirable. Simple printed antennas such as slots or dipoles do not meet such a goal. Kollberg, et al., investigated and endfire tapered slot antenna as a candidate for a high gain antenna for a quasi-optical mixer [3].

In a typical application, a quasi-optical mixer is placed at the focal plane of a focusing imaging system which converts the incoming plane wave into a converging spherical wave. In such an application, the radiation pattern of the mixer antenna should match the converging cone of the imaging system. If the former is wider than the cone, background noise is captured by the quasi-optical mixer while if the beam is narrower than the cone the desired incoming signal energy cannot be captured completely.

Another important characteristic of the antenna is its impedance. Wideband antennas have a constant impedance over a broad frequency range. This is suitable for many mixer designs, especially for subharmonically pumped mixers where the RF frequency is approximately twice that of the LO signal. The disadvantage of a wideband antenna is its poor spurious rejection. Narrowband antennas are designed to resonate at a frequency that allow efficient coupling of the RF and LO signals. However, the reactive impedance of these antennas to the mixer outside the bandwidth can lead to lower conversion loss.

4. REVIEW OF QUASI-OPTICAL MIXER DEVELOPMENTS

Only some representative examples of quasi-optical mixers are presented in this chapter. Clifton [4] has developed an 600 GHz quasi-optical mixer consisting of a plastic lens which focused both RF and LO signals through free space inside the conical housing onto a mixer element. The latter is made of a Schottky-barrier diode in a stripline filter structure. A waveguide short behind the diode was used for tuning. The element lead acted as an antenna. This concept of using the element lead as antenna is also used in a corner cube mixer developed by Fetterman, et al. [5]. In this structure which is not planar, the diode wisker contact is elongated to several wavelengths and the diode and the wisker are placed in an open three-sided corner reflector, called the corner cube. RF and LO power can be coupled efficiently to the diode via this long wire antenna over one octave of frequency range.

Kerr, et al., [6] developed a planar coupled slot quasi-optical mixer shown in Fig. 2. Two slot antennas are fabricated on a 7-mil quartz substrate and are coupled to a Schottkybarrier chip diode via a quartz microstrip and a wisker contact wire that was mounted parallel to the substrate. The resonant slot antenna and wisker caused the design to have a relatively narrow bandwidth. However, the higher coupling efficiency within the antenna's frequency range is believed to have led to a lower conversion loss. The single sideband con-

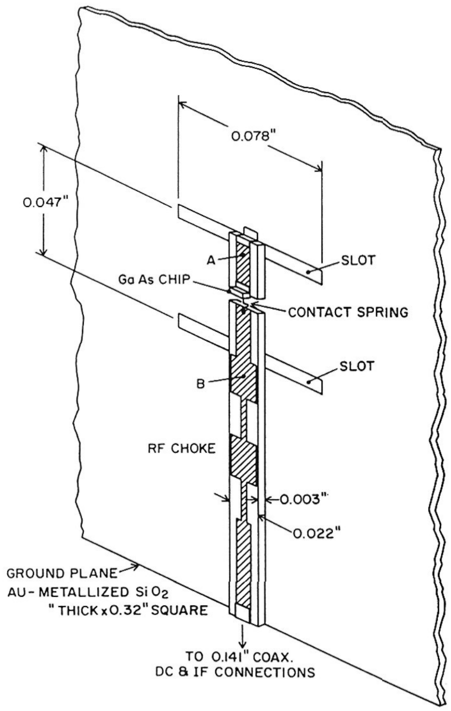

Fig. 2 - 100-120 GHz slot-antenna quasi-optical mixer (© 1977 IEEE Reprinted with permission from Fig. 3, A.R. Kerr, P.H. Siegel and R.J. Mattauch, «A simple quasi-optical mixer for 100-120 GHz», 1977 IEEE MTT-S International Microwave Symposium, June 1977, San Diego, CA, p. 96-98).

version loss of 8.6 dB and the noise temperature of 1000 K were obtained at 112 GHz.

The quasi-optical mixer made monolithically with GaAs materials was reported by Clifton, et al. [7]. As shown in Fig. 3, the circuit consists of a wide slot an-

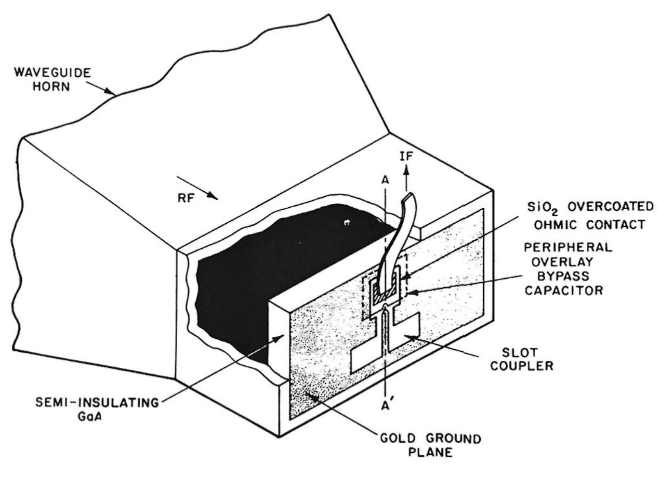

Fig. 3 - 110 GHz monolithic quasi-optical mixer on a GaAs substrate (© 1981 IEEE Reprinted with permission from Fig. 5, B.J. Clifton, G.D. Alley, R.A. Murphy and I.H. Mrockowski, «High-performance quasi-optical GaAs monolithic mixer at 110 GHz», IEEE Trans. Electron Devices, vol. 337: Millimeter Wave Technology, May 1982, Arlington, VA, Paper n. 30).

tenna with a coupling probe which is connected to the Schottky-barrier diode fabricated with the antenna. The circuit was mounted at the narrow end of a horn as shown in the figure. The mixer was designed for 110 GHz and produced a double sideband noise figure of 3.4 dB.

Since quasi-optical mixers can be made compact and are potentially low cost, they may be an excellent candidate for imaging array. The basic configuration of an imaging array is shown in Fig. 4. The field of view

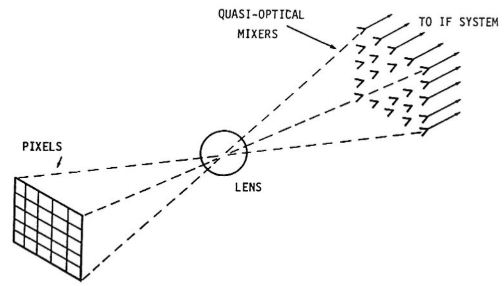

Fig. 4 - Basic configuration of a quasi-optical mixer imaging array.

is represented by a grid of boxes, each containing one picture element called the pixel. The scene may either be illuminated by a radar signal or may merely emit the black-body radiation. The energy received from the scene is focused through an object lens onto an array of receivers. Each receiver generates an output proportional to the energy emitted by its respective pixel. An appropriate processing circuit can display a visual image of the microwave scene of the far field. Since many identically built receivers are required for this application, quasi-optical design has an advantage. First, quasi-optical mixer can be made small and can be cost effective. In addition, one local oscillator can be used for all mixers if they are illuminated by the LO signal in a quasi-optical manner. One earlier example of an imaging array with quasi-optical mixers is the 2×2 printed dipole array by Parish, et al., [8] designed for 140 GHz. Since the printed dipoles are formed on a substrate backed by a ground plane, the radiation is directed only in one side of the substrate while the mixers with slot type antennas interface with free spaces on both sides of the substrate.

One of the most important applications of imaging arrays is plasma diagnostics in nuclear fusion at frequencies above 100 GHz. For this purpose, the group headed by D. Rutledge developed quasi-optical one-dimensional bowtie mixer arrays. The initial design was based on bolometer detectors instead of Schottky diodes (Fig. 5) [9]. A later design is based on a monolithic

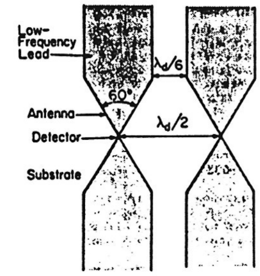

Fig. 5 - Bowtie antenna array quasi-optical delector (© 1981 IEEE Reprinted with permission from Fig. 2, D.P. Neikirki, D.B. Rutledge, M.S. Muha, H. Park and C.-X. Yu, «Imaging antenna arrays», Sixth International Conference on Infrared and Millimeter Waves, December 1981, Miami Beach, FL., Paper Th-4-1).

structure using a bowtie antenna feeding a Schottky-barrier diode, both integrated on a GaAs substrate. The mixer-detector is placed on a flat side of a hemispherical dielectric lens so that excitation of surface waves has been alleviated (Fig. 6). The single sideband conversion loss at 94 GHz was 13.5 dB including about 6 dB of coupling loss to the mixer [10].

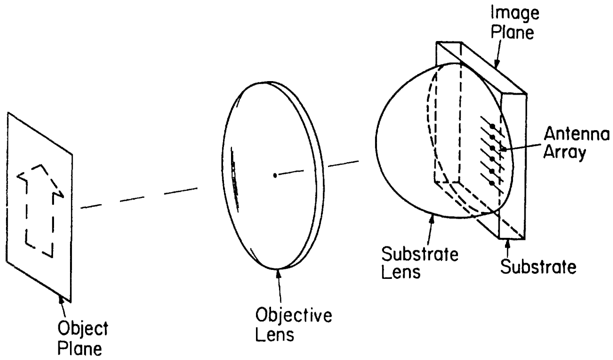

Fig. 6 - «Reverse microscope» optical system (© 1981 IEEE Reprinted with permission from Fig. 1, D.P. Neikirki, D.B. Rutledge, M.S. Muha, H. Park and C.-X. Yu, «Imaging antenna arrays», Sixth International Conference on Infrared and Millimeter Waves, December 1981, Miami Beach, FL., Paper Th-4-1).

In many mixer applications, a balanced mixer is desirable as the AM noise contained in the LO signal does not in principle appear in the IF output if the diode pair used is ideally matched to each other. Yuan, et al., reported a 125 GHz balanced mixer made of two slot antennas. The LO signal was fed through a waveguide rather than quasi-optically as shown in Fig. 7. A conversion loss of 7 dB was achieved [11]. Stephan,

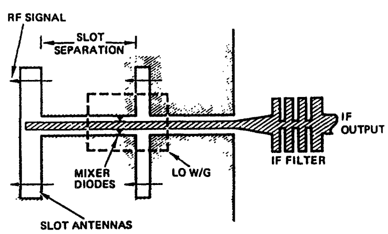

Fig. 7 - Quasi-optical crossbar mixer (© IEEE Reprinted with permission from Fig. 1, L. Yuan, J. Paul and P. Yen, «140 GHz quasi-optical planar mixers», 1982 IEEE MTT-S International Microwave Symposium, June 1982, Dallas, TX, p. 374-375).

et al., have developed a quasi-optical balanced mixer by taking advantage of orthogonally polarized RF and LO signals [12]. As shown in Fig. 8, the structure consists of a slot ring antenna in the metal covering one side of the substrate. This antenna is capable of receiving incoming radiation perpendicular to the substrate on either side. Two balanced mixer diodes at right angles to each other bridge the slot. A vertically polarized local oscillator signal drives the diodes so that a horizontally polarized RF signal is down converted at each diode. The resulting IF signals are combined and extracted through a low pass filter built in a coplanar waveguide. Versions of this mixer have performed at frequencies as high as 35 GHz. An X band model produced a conversion loss as low as 5.5 dB and a mixer single sideband noise figure of about 6.5 dB.

Since the RF and LO signals are polarized orthogonally, they enjoy a built-in isolation which is often difficult in a quasi-optical design. In addition, certain quasi-optical techniques can be used for enhancing the utility of this mixer. As shown in Fig. 9, a vertically oriented wire grid can be placed in front of the mixer

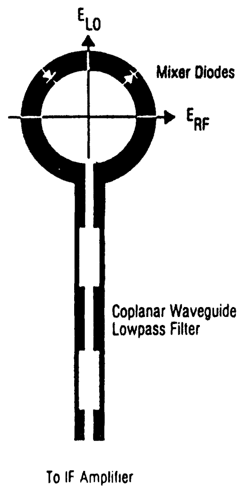

Fig. 8 - Slot ring mixer show in LO and RF field polarizations. Slot in one-sided metal cladding on a dielectric substrate is indicated with black.

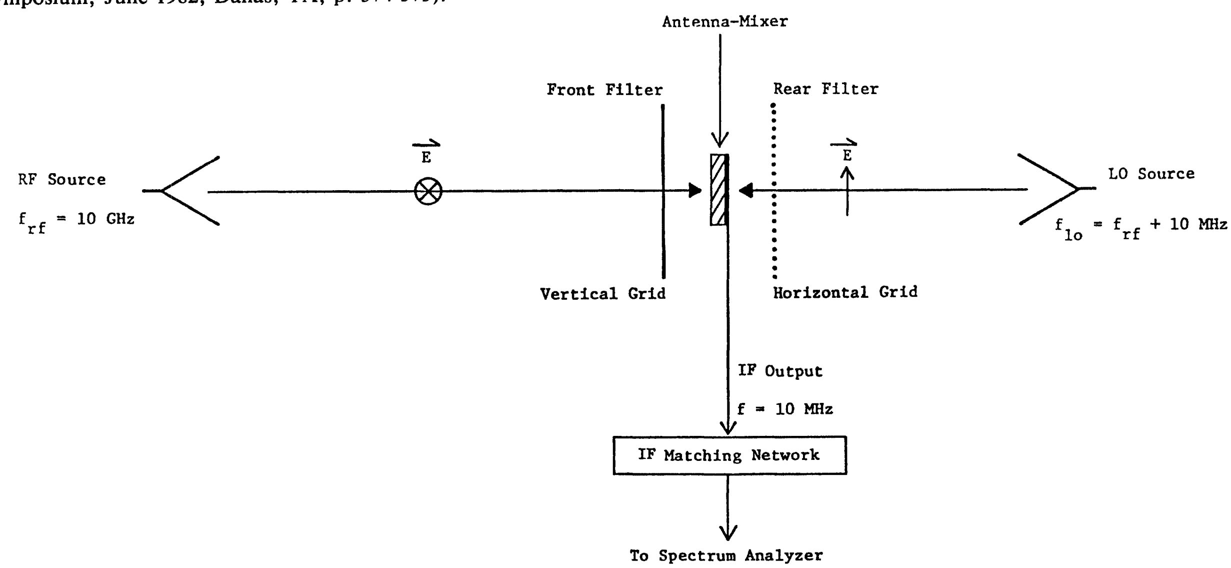

Fig. 9 - Quasi-optical slot-ring mixer setup for polarization duplexing (© 1983 IEEE Reprinted with permission from Fig. 5, K.D. Camilleri and T. Itoh, «A quasi-optical polarization-duplexed balanced mixer for millimeter-wave applications», IEEE Trans. Microwave Theory and Techniques, vol. MTT-31, n. 2, p. 164-170, February 1983; Erratum, vol. MTT-31, n. 6, p. 504, June 1983).

which can be made transparent to the incoming horizontally polarized RF while the vertically polarized LO uncaptured by the mixer is reflected back to the mixer so that the mixer is quiet as seen from the RF source direction. At the same time, a horizontal grid can be placed behind the mixer so that the RF signal uncaptured by the mixer is reflected back to the mixer.

All the circuits described above are fundamental mixers in that the fundamental of the RF is mixed with the fundamental of the LO. As the frequency of operation is increased, direct supply of fundamental LO becomes increasing more difficult and more costly. A subharmonically pumped mixer provides a possible solution. Such a mixer usually shows a poorer conversion loss than its fundamental counterpart. However, certain circuits can enhance their efficiency. Schneider and Snell found that a back-to-back pair of diodes can be made to conduct twice per LO cycle, and thus can function nearly as well as a conventional mixer with twice the LO frequency [13]. Stephan and Itoh used this principle in developing a quasi-optical subharmonically pumped mixer by making use of the broadband nature of the bowtie antenna as shown in Fig. 10 [1]. The con-

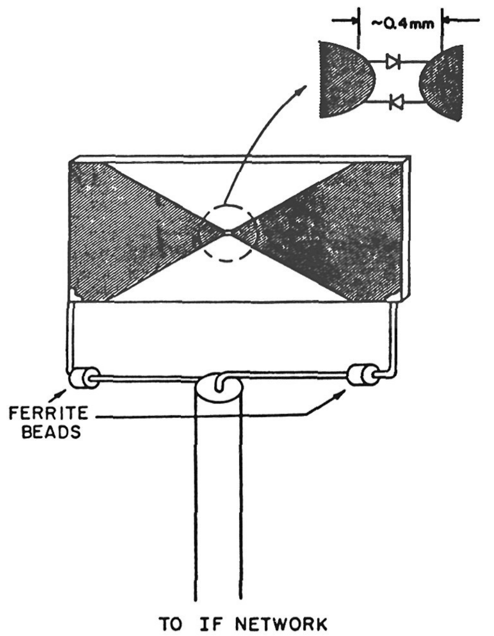

Fig. 10 - Subharmonic mixer using antiparallel diodes and bowtie antenna (©1984 IEEE Reprinted with permission from Fig. 10, K.D. Stephan and T. Itoh, «A planar quasi-optical subharmonically pumped mixer characterized by isotropic conversion loss», IEEE Trans. Microwave Theory and Techniques, vol. MTT-32, n. 1, p. 97-102, January 1984).

version loss obtained at X band was as good as 8.6 dB. The model shown in the figure was usable over a 2.5:1 frequency range (14-35 GHz) because of the inherently broad band nature of the bowtie antenna.

Excellent review articles on planar integrated antennas and millimeter wave imaging have been written by Rutlege, et al., [14]and Yngvesson [15].

5. EMERGING EFFORTS FOR OTHER QUASI-OPTICAL ACTIVE COMPONENTS

In the past several years, a number of attempts have been initiated for developing planar integrated quasi-optical components other than a mixer. They range from amplifiers, oscillators, frequency multipliers and power combiners. In addition, integrated receiver front ends have also been developed.

Amplifier

The concept of polarization-duplexing similar to the one used in the slot ring mixer [12] was exploited in developing a quasi-optical transistor amplifier and an amplifier array [16]. As shown in Fig. 11, a slot antenna is used for pick up of the input power. After the input power is delivered to the transistor amplifier and amplified, the output is coupled out from the circuit via the output slot antenna which is oriented at 90 degrees with respect to the input slot. Hence, the input and the output are isolated by means of polarization duplexing. A 5 GHz single amplifier was built on a Duroid substrate with relative dielectric constant of 10.2. The measurement of the power in the two polarizations indicated that the circuit has a gain of about 10 dB from one polarization to another. The isolation between two polarizations were found to be greater than 20 dB.

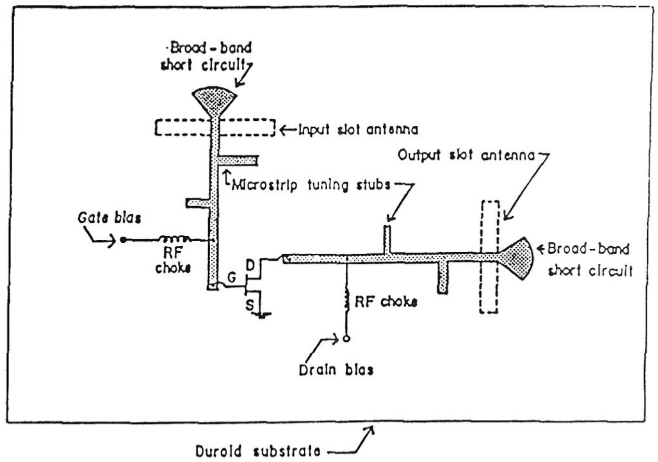

Fig 11 - A polarization-duplexed quasi-optical transistor amplifier (© 1985 IEEE Reprinted with permission from Fig. 2, W.L. Williams, D.P. Kasilingam and D.B. Rutledge, «Progress in quasi-optical transistor power amplifiers», Tenth International Conference on Infrared and Millimeter Waves, December 1985, Lake Buena Vista, FL, p. 50-51).

Frequency Multiplier

The frequency multiplier becomes increasingly important as the frequency of operation becomes higher, since coherent direct signal generators become more difficult to realize. In the quasi-optical design, there are two schemes possible. One is the use of a plane wave input at the fundamental frequency onto a planar multiplier with the output emerging as a plane wave. Another is to use a fundamental input from other signal generators or on the same substrate and only the output emerges as a plane wave. One example for the former design is illustrated in Fig. 12. This diode grid is a square mesh of metal strips on a GaAS substrate. The diodes are located on the vertical strips which add inductance to cancel the diode capacitance. The horizontal strips permit applications of dc bias. This

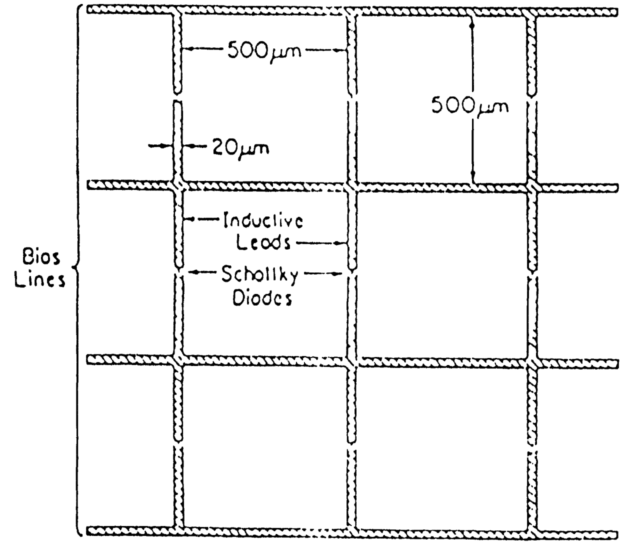

Fig. 12 - Double grid dimensions (© 1985 IEEE Reprinted with permission from Fig. 2, C.F. Jou, W.W. Lam, D.B. Rutledge and N.C. Luhman, Jr., «Watt-level monolithic quasi-optical diode frequency multiplier grid», Tenth International Conference on Infrared and Millimeter Waves, December 1985, Lake Buena Vista, FL, p. 56-57).

structure is sandwiched between combinations of wire grid filters and a half-wave plate and other quasi-optical components so that the fundamental and the harmonic are separated. For a grid with 40 diodes per square centimeter, the output power is 0.56 W/cm^2 [17].

An example of the second design is shown in Fig. 13. An array of slots with a nonlinear device is fed by

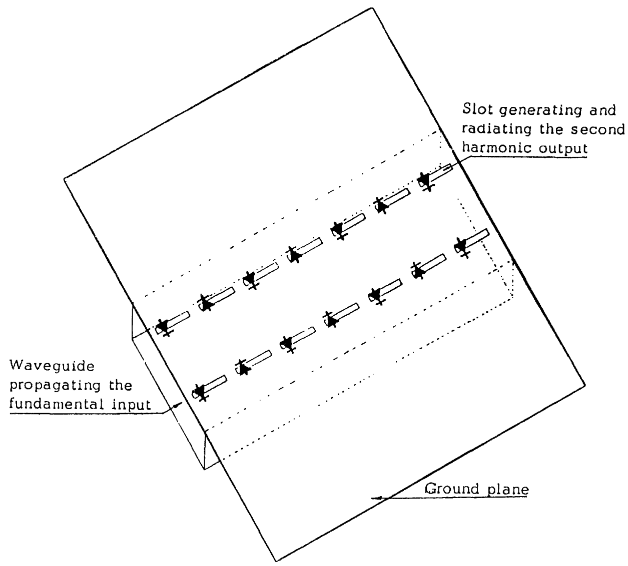

Fig. 13 - A two-by-seven multiplying slot array fed by a waveguide (© 1985 IEEE Reprinted with permission from Fig. 1, N. Camilleri and T. Itoh, «A quasi-optical multiplying slot array», IEEE Trans. Microwave Theory and Techniques, vol. MTT-33, n. 11, p. 1189-95, November 1985).

a reduced height waveguide. Since the slots are approximately 1/4 wavelength at the fundamental frequency, they do not radiate at this frequency. However, once the frequency is doubled by the nonlinear devices, the slots become efficient radiators as the length is 1/2 wavelength. The radiation pattern can be adjusted by a proper design. A version for 35 GHz-to-70 GHz array of 1 × 8 elements exhibited a sidelobe level less than 12 dB in the E plane [18]. A structure more compatible with a planar technology was reported by Nam, et al. [19]. In this structure, an array of slots in the ground plane is fed by a microstrip line on the opposite side of the substrate.

Oscillator and power combiner

Development of oscillators are closely related to the spatial power combining technique. Essentially, a major problem of quasi-optical power generation is the lack of a high Q resonator needed for a stable oscillator. One remedy of this problem is the use of a Fabry-Perot cavity in conjunction with a planar quasi-optical structure. Such a cavity provides not only a high Q environment for the oscillating device but also an opportunity for power combining of multiple oscillator. A milestone work on this subject is the paper by Mink [20]. The schematic is shown in Fig. 14. By placing the

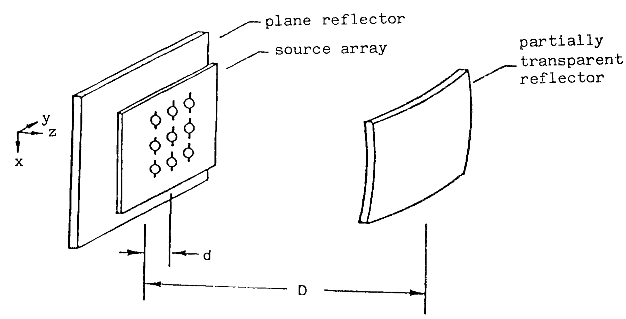

Fig. 14 - Resonator - source array (© 1985 IEEE Reprinted with permission from Fig. 1, J.W. Mink, «Power combining of solid state millimeter wave sources», Tenth International Conference on Infrared and Millimeter Waves, December 1985, Lake Buena Vista, FL, p. 52-53).

millimeter wave planar sources within the high Q Fabry-Perot cavity, the sources are injection locked and the coherently combined output power can be extracted through a partially transparent reflector. Up to 21 diodes have been combined in this manner. A similar idea was carried out by using 25 transistors at a frequency in the X band [21]. The result obtained was about 464 mW with the DC to RF conversion efficiency of 14.5%.

Detailed investigations of an open resonator used for a filter as well as a coupled oscillator have been reported by Stephan, et al. [22, 23, 24]. A planar Gunn oscillator has been stabilized if it is coupled to the open reso-

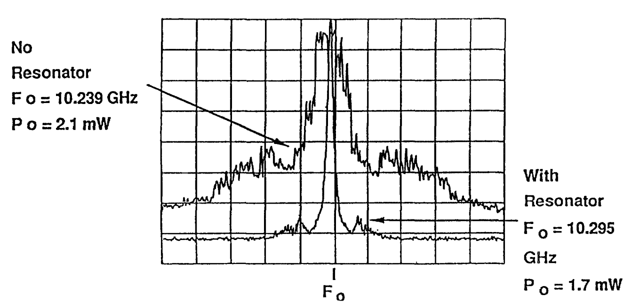

Fig. 15 - Output spectra of planar oscillator with or without an open resonator (© 1987 IEEE Reprinted with permission from Fig. 6, S.-L. Young and K.D. Stephan, «Stabilization and power combining of planar microwave oscillators with an open resonator», 1987 IEEE MMT-S International Microwave Symposium, June 1987, Las Vegas, NV, p. 185-188).

nator by placing the spherical reflector at a distance D = 11.6 cm above the planar oscillator ground plane. A dramatic improvement of the output spectrum is shown in Fig. 15. Power combining of two planar oscillators was tested with the scheme shown in Fig. 16.

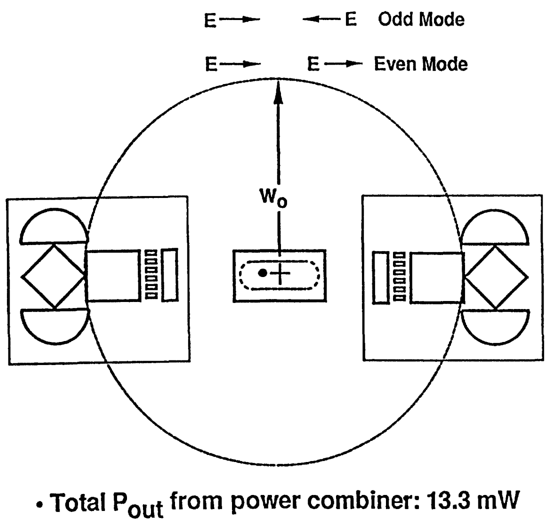

Fig. 16 - Power combining of two planar oscillators and output patch antenna (© 1987 IEEE Reprinted with permission from Fig. 7, S.-L. Young and K.D. Stephan, «Stabilization and power combining of planar microwave oscillators with an open resonator», 1987 IEEE MTT-S International Microwave Symposium, June 1987, Las Vegas, NV, p. 185-188).

This figure is a view looking down on the circuits from the spherical reflector. The distance separating the oscillators was chosen in such a way that the quarter-wave resonators of the oscillators were within the beam waist W_0 as shown. An additional microstrip patch antenna was placed between the oscillators. By changing the distance of the reflector from the oscillator plane, various frequencies of oscillation were detected. Adjustment of the reflector position and output probe coupling led to output of several milliwatts from the central patch antenna. Without the open resonator, only several microwatts were available. The maximum output was 13.3 mW when the reflector distance was D = 29 mm.

In the meantime, GaAs IMPATT diodes were monolithically integrated with a microstrip resonator and a loop antenna as shown in Fig. 17. An output of 27 mW CW was obtained at 43.3 GHz. This chip were mounted on a waveguide wall to form a power combining array [25].

A completely different approach to obtain a stable oscillation makes use of a leaky wave antenna. When a periodic structure is operated with the frequency at which one period of the structure is one guide wavelength, the input VSWR of the leaky wave antenna becomes extremely high. This mechanism is used for frequency selective feedback to an active device which then oscillates at this frequency. At the same time, the output signal of this oscillator is radiated in the broadside direction. This concept was tested at a scale model with an MESFET at X band [26]. Fig. 18 presents a basic configuration of the leaky wave FET oscillator. The low pass or band pass filter is designed to heavily load the device so that the device does not oscillate at the surface wave stopband of the periodic structure

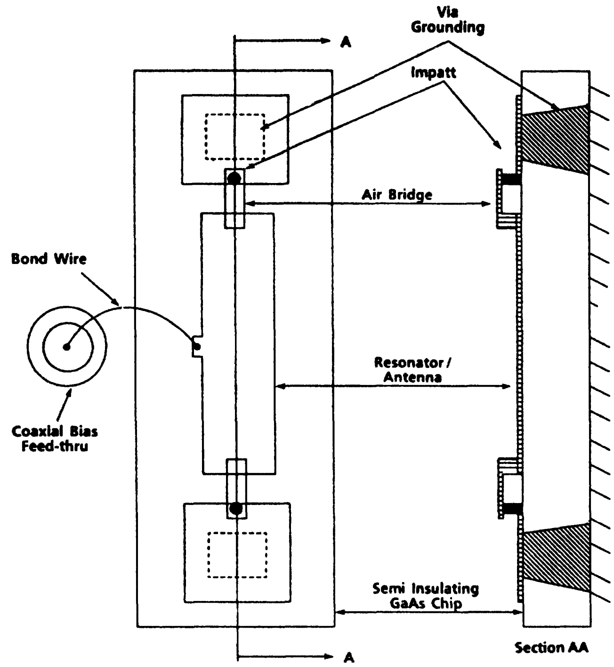

Fig. 17 - Monolithic IMPATT resonator/antenna (© 1988 IEEE Reprinted with permission from Fig. 2, N. Camilleri and B. Bayraktaroglu, «Monolithic millimeter-wave IMPATT oscillator and active antenna», IEEE Trans. Microwave Theory and Techniques, vol. 36, n. 12, p. 1670-1676, December 1988).

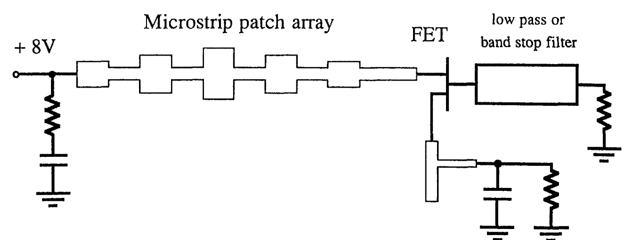

Fig. 18 - Schematic view of oscillator using a leaky-wave stopband.

which is about one half of the design frequency. The isotropic conversion gain was measured at 9 dB in the broadside direction with a 17 element antenna.

The concept of leaky wave antennas have been extended to coupled oscillator structures. For this purpose, a coupled periodic antenna called rampert antenna was used to develop a balanced oscillator in push-pull mode or a frequency doubling oscillator in a push-push mode [27]. The basic configuration is shown in Fig. 19. If we choose the widths and spacing of the cou-

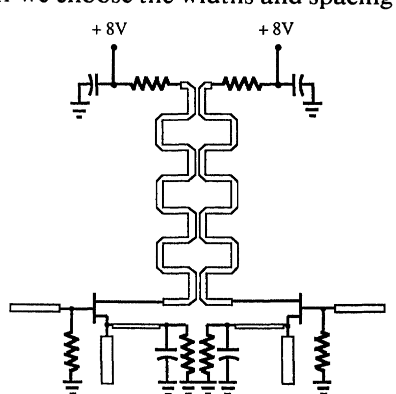

Fig. 19 - Schematic view of coupled oscillator using a leaky-wave stopband.

pled sections so that $Z_{0o} < Z_0$ and $Z_{0e} = Z_0$, then reflective stopbands will exist in the odd mode due to the periodic impedance variation, but will not occur in the even mode. On the other hand, if we have $Z_{0o} = Z_0$ and $Z_{0e} > Z_0$, then the stopbands will occur in the even mode. The measured conversion gain of the balanced oscillator was 6.1 dB. When the balanced oscillator was operated in the push-push mode, a frequency doubling planar source was created with the radiated second harmonic at 19.7 GHz.

Planar integrated receiver and transceiver

The planar oscillator using a periodic leaky wave antenna can be used as a transceiver. This can be attained by slight modifications of the single and coupled oscillators described above. In such cases, the FETs perform a dual function, serving as the source for the transmitted signal and as self-oscillating mixers for down conversion of the received signal [27].

Much more compact integrated receivers than those in [27] were designed and tested by an ingeneous use of a coupled slot antenna [28, 29]. The core of these circuits is the coupled slot. It is well known that the coupled slot supports two orthogonal fundamental modes; coupled slot line (CSL) mode and coplanar wave guide (CPW) mode. In the CSL mode, the electric field in the two slots are oriented in the same direction across each slot and this mode can be radiated easily. Therefore, the RF incoming signal is captured with the coupled slot antenna operating in this mode. On the other hand, in the CPW mode the electric fields in the two slots are opposite. Since this mode does not radiate easily, the coupled slot operated in this mode can be used as a part of the local oscillator circuit which is required to be of high Q. As shown in Fig. 20, two mixer diodes are implemented in the slots. These diodes see the same RF polarizations while the LO signal is fed out of phase so that a balanced mixer operation takes place. The local oscillator shown in the figure is a MESFET version although a Gunn diode version was also tried. The isotropic conversion loss measured at X band was about 3 dB [28].

The self-oscillating mixer circuit shown in Fig. 21 is once again based on the diplexing function of the coupled slot. In this structure, no mixer diodes are involved. Instead, either MESFETs or HEMTs are used in the balanced oscillation mode so that the two devices are gate-coupled to produce the LO power in the odd (CPW) mode while the RF signal is coupled to the CSL mode. The circuit exhibited isotropic conversion gain of 3.0 dB for the MESFET version and as high as 4.5 dB for the HEMT version [29].

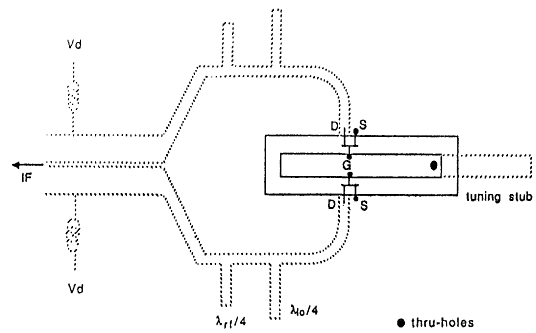

Fig. 21 - Circuit diagram of the self-oscillating mixer (© 1988 IEEE Reprinted with permission from Fig. 1, V.D. Hwang and T. Itoh, «Quasi-optical HEMT and MESFET self-oscillating mixers», IEEE Trans. Microwave Theory and Techniques, vol. 36, n. 12, p. 1701-1705, December 1988).

6. CONCLUSIONS

In this paper, recent efforts in the development of planar quasi-optical microwave and millimeter-wave circuits were reviewed, In addition to the quasi-optical mixers for which the state-of-the-art is more advanced, recent attempts to increase availability of other active circuits are also included. Although many developments are still in the laboratory stages, these efforts are believed beneficial in exploring the enhanced capability of millimeter-wave applications. Most efforts have been directed to high millimeter-wave frequency applications such as imaging arrays. However, due to the inherent simplicity of the structure, many quasi-optical components that include several functions can find useful applications in the area of industrial and commercial applications in addition to more traditional ones in radars and communications even at low frequencies.

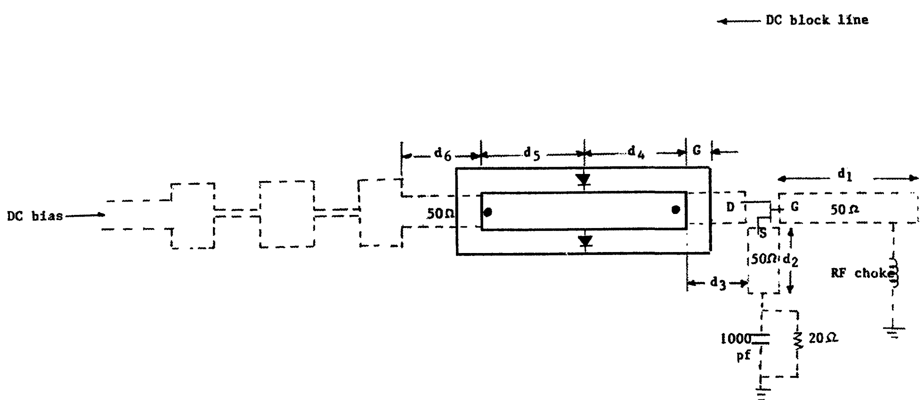

Fig. 20 - Receiver circuit using the MESFET oscillator (© 1988 IEEE Reprinted with permission from Fig. 2, V.D. Hwang, T. Uwano and T. Itoh, «Quasi-optical integrated antenna and receiver front end», IEEE Trans. Microwave Theory and Techniques, vol. 36, n. 1, p. 80-85, January 1988).

Acknowledgment

This work was supported by the U.S. Army Research Office under Contract DAAL03-88-K-0005, the Joint Services Electronics Program through the Air Force Office of Scientific Research Contract F49620-89-C-0044 and the Texas Advanced Technology Program.

Manuscript received on June 13, 1989

REFERENCES

[1] K.D. Stephan, T. Itoh: *A planar quasi-optical subharmonically pumped mixer characterized by isotropic conversion loss.* «IEEE Trans. Microwave Theory and Techniques», vol. MTT-32, n. 1, January 1984, p. 97-102.

[2] D.N. Held, A.R. Kerr: *Conversion loss and noise of microwave and millimeter-wave mixers: Part I - Theory.* «IEEE Trans. Microwave Theory and Techniques», vol. MTT-26, n. 2, February 1978, p. 49-54.

[3] E.L. Kollberg, J. Johansson, T. Thungren, T.L. Lozeniowski, K.S. Yngvesson: New results on tapered slot endfire antennas on dielectric substrates. IEEE International Conference on Infrared and Millimeter Waves, Paper F3.6, Miami Beach, FL, December 1983.

[4] B. Clifton: *Schottky-barrier diodes for submillimeter heterodyne detection.* «IEEE Trans. Microwave Theory and Techniques», vol. MTT-25, n. 6, June 1977, p. 457-463.

[5] H.R. Fetterman, et al.: *Far-ir heterodyne radiometric measurements with quasi-optical Schotkly diode mixers.* «Appl. Phys. Lett.», vol. 33, n. 2, 15 July 1978, p. 151-154.

[6] A.R. Kerr, P.H. Siegel, R.J. Mattauch: *A simple quasi-optical mixer for 100-120 GHz.* 1977 IEEE MTT-S International Microwave Symposium, June 1977, San Diego, CA, p. 96-98.

[7] B.J. Clifton, G.D. Alley, R.A. Murphy, I.H. Mrockowski: *High-performance quasi-optical GaAs monolithic mixer at 100 GHz.* «IEEE Trans. Electron Devices», vol. ED-28, n. 2, February 1981, p. 151-157.

[8] P. Parish, et al.: *Printed dipole-Schottky diode millimeter wave antenna array.* SPIE Proceedings, vol. 337: Millimeter Wave Technology, May 1982, Arlington, VA, Paper n. 30.

[9] D.P. Neikirk, D.B. Rutledge, M.S. Muha, H. Park, C.-X. Yu: *Imaging antenna arrays.* Sixth International Conference on Infrared and Millimeter Waves, December 1981, Miami Beach, FL., Paper Th-4-1.

[10] D.B. Rutlege: Private Communication.

[11] L. Yuan, J. Paul, P. Yen: *140 GHz quasi-optical planar mixers.* 1982 IEEE MTT-S International Microwave Symposium, June 1982, Dallas, TX, p. 374-375.

[12] K.D. Stephan, N. Camilleri, T.Itoh: *A quasi-optical polarization-duplexed balanced mixer for millimeter-wave applications.* «IEEE Trans. Microwave Theory and Techniques», vol. MTT-31, n. 2, February 1983, p. 164-170; Erratum, vol. MTT-31, n. 6, June 1983, p. 504.

[13] M.V. Schneider, W.N. Snell, Jr: *Stripline downconverter with subharmonic pump.* «Bell System Tech. Journal», vol. 53, n. 7, July-Aug. 1974, p. 1179-1183.

[14] D.B. Rutledge, D.P. Neikirk, D.P. Kasilingam. *Integrated-circuit antennas.* Infrared and Millimeter Waves, vol. 10 (ed. K. Button), Chapter 1, p. 1-90. 1983, Academic Press, New York, N.Y.

[15] K.S. Yngvesson: *Near-millimeter imaging with integrated planar receptors: General requirements and constraints.* Infrared and Millimeter Waves, vol. 10 (ed. K. Button), Chapter 2, p. 91-110, 1983, Academic Press, New York, NY.

[16] W.L. Williams, D.P. Kasilingam, D.B. Rutledge: *Progress in quasi-optical transistor power amplifiers.* Tenth International Conference on Infrared and Millimeter Waves, December 1985, Lake Buena Vista, FL, p. 50-51.

[17] C.F. Jou, W.W. Lam, D.B. Rutledge, N.C. Luhman, Jr: *Watt-level monolithic quasi-optical diode frequency multiplier grid.* Tenth International Conference on Infrared and Millimeter Waves, December 1985, Lake Buena Vista, FL, p. 56-57.

[18] Camilleri, T. Itoh: *A quasi-optical multiplying slot array.* «IEEE Trans. Microwave Theory and Techniques», vol. MTT-33, n. 11, November 1985, p. 1189-1195.

[19] S. Nam, T. Uwano, T. Itoh: *Microstrip-fed planar frequency-multiplying space combiner.* «IEEE Trans. Microwave Theory and Techniques», vol. MTT-35, n. 12, December 1987, p. 1271-1276.

[20] J.W. Mink: *Power combining of solid state millimeter wave sources.* Tenth International Conference on Infrared and Millimeter Waves, December 1985, Lake Buena Vista, FL, p. 52-53.

[21] D.B. Rutledge, Z.B. Popovic, M. Kim: *Millimeter wave grid oscillators.* Thirteenth International Conference on Infrared and Millimeter Waves, December 1988, Honolulu, Hawai, p. 1-2.

[22] K.D. Stephan, S.-L, Young, S.-C. Wong: *Microstrip circuit application of high-Q open microwave resonators.* «IEEE Trans. Microwave Theory and Techniques», vol. 36, n. 9, September 1988, p. 1319-1327.

[23] K.D. Stephan, S.-L. Young: *Mode stability of radiation-coupled interinjection-locked oscillators for integrated phased array.* «IEEE Trans. Microwave Theory and Techniques», vol. 36, n. 5, May 1988, p. 921-924.

[24] S.-L. Young, K.D. Stephan: *Stabilization and power combining of planar microwave oscillators with an open resonator.* 1987 IEEE MTT-S International Microwave Symposium, June 1987, Las Vegas, NV, p. 185-188.

[25] N. Camilleri, B. Bayraktaroglu: *Monolithic millimeter-wave IMPATT oscillator and active antenna.* «IEEE Trans. Microwave Theory and Techniques», vol. 36, n. 12, December 1988, p. 1670-1676.

[26] J. Birkeland, T. Itoh: *Planar FET oscillators using periodic microstrip patch.* «IEEE Trans. Microwave Theory and Techniques», vol. 37, n. 8, August 1989.

[27] J. Birkeland, T. Itoh: *FET-based planar circuits of quasi-optical sources and transceivers.* To appear in IEEE Trans. Microwave Theory and Techniques, Special Issue on FET Structures and Their Circuit Applications, vol. 37, n. 9, September 1989.

[28] V.D. Hwang, T. Uwano, T. Itoh: *Quasi-optical integrated antenna and receiver front end.* «IEEE Trans. Microwave Theory and Techniques», vol. 36, n. 1, January 1988, p. 80-85.

[29] V.D. Hwang, T. Itoh: *Quasi-optical HEMT and MESFET self-oscillating mixers.* «IEEE Trans. Microwave Theory and Techniques», vol. 36, n. 12, December 1988, p. 1701-1705.

Active Integrated Antennas

J. LIN, STUDENT MEMBER, IEEE, AND T. ITOH, FELLOW, IEEE

Abstract— **The development of active integrated antennas is reviewed in this paper. The circuit structures of different types of active integrated antennas are discussed. Various circuits integrating solid state devices and low-profile passive antenna elements are demonstrated. The applications in quasi-optical power combining arrays and beam-scanning phased arrays are reviewed. By using the modern MIC and MMIC fabrication technology, compact, light-weight, and low-cost active integrated antennas are realized. In addition, nonlinear electromagnetic simulations of active integrated antennas are discussed.**

I. Introduction

WHILE the terminology of "active antenna" means that the active devices are employed in the passive antenna elements to improve antenna performance, the terminology of "active integrated antenna" indicates more specifically that the passive antenna elements and the active circuitry are integrated on the same substrate. Due to the mature technology of microwave integrated circuit (MIC) and monolithic microwave integrated circuit (MMIC), the active integrated antenna became an area of growing interest in recent years.

The idea of using active antennas can be traced back to as early as 1928 [1]. A small antenna with electron tube was commonly used in radio broadcast receivers around 1 MHz at that time. In 1960's and 1970's, due to the invention of high frequency transistors, the study of active antennas received much attention and several pioneering works were reported [2]–[11]. The implementation of active devices [12] in passive radiating elements showed several advantages, e.g., increasing the effective length of short antenna, increasing the bandwidth, decreasing the mutual coupling between array elements, and improving the noise factor. These advantages helped improve the antenna performance and made the research of active antennas popular at that time.

Quasi-optical techniques spurred the development of active integrated antennas in 1980's and 1990's. As the operating frequency increases, the available power from solid state devices decreases. Therefore, power combining of solid state devices using quasi-optical techniques in the millimeter-wave region became an important issue [13]. There are two different approaches for quasi-optical power combining. One is the active antenna approach and the other is the grid approach. The coupled oscillator array integrating solid state sources in a periodic structure to combine the power spatially is an example of the active antenna approach [51]. Details of this type of approach will be discussed throughout this paper. The other approach, the grid array, is a very successful one for high power applications [14]–[21]. The grid array is a special type of active integrated antenna array of which the antenna elements are very short and the spacing of array elements is much smaller than a wavelength. Although each unit cell in the grid array can be modeled as an active antenna consisting of an active device and a short antenna, the mutual coupling of antenna elements is so strong that the grid array has to be analyzed by using the TEM waveguide mode [18]. This is the major difference between these two approaches. Each unit cell in the grid is designed and optimized by considering the plane wave incidence on an infinite grid. The grid approach therefore works well for the large array handling high power but not for each single unit. On the other hand, each unit in the active antenna array is designed and optimized independently so that the active antenna unit itself works well. The active antenna units are then integrated in an array structure to combine the power spatially. In this paper, discussion will be concentrated on the active antenna approach in which each single unit can operate by itself.

Starting from the classification, this paper goes through the active integrated antenna modules and their applications. The structures and functions of different types of active integrated antennas are reviewed. By integrating single modules in an array structure, the applications in power-combining arrays and phased arrays are discussed. Several techniques of utilizing device-circuit and device-device interactions in array structures are compared. In addition to experimental achievements, recent development in nonlinear electromagnetic simulation of active integrated antenna is also reviewed. Both time-domain and frequency-domain approaches are discussed. The simulation using the nonlinear device modeling as well as the full-wave analysis of passive structure is able to show the large-signal behavior of complex circuits and their dynamic field distributions.

II. Classification of Active Integrated Antennas

The active integrated antennas may be classified by their different applications and named as their counterparts in radio systems. Two basic categories are transmitting and receiving types active integrated antennas. The other types with both functions of transmitting and receiving are transceivers, transponders, repeaters, and so on. However, direct use of the classification for radio systems is redundant to the simple configurations of active integrated antennas. An amplifier may be integrated with antenna elements at its input port or output port to become a transmitter or receiver, respectively. It may even integrate antenna elements at both ports to become a repeater. All these combinations have a common feature: the integration of an amplifier and antenna elements.

Manuscript received April 29, 1994; revised July 14, 1994.
The authors are with the Department of Electrical Engineering, University of California, Los Angeles, Los Angeles, CA 90024-1594, USA.
IEEE Log Number 9405378.

Reprinted from *IEEE Transactions on Microwave Theory and Techniques*, Vol. 42, No. 12, pp. 2186-2194, December 1994.

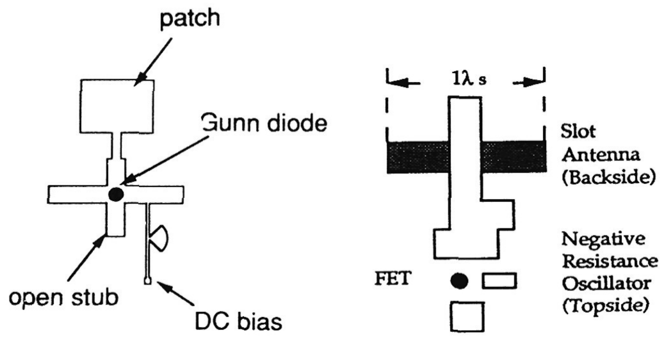

(a) (b)

Fig. 1. Oscillator type active integrated antennas. (a) Patch antenna integrates with Gunn diode [62]. (b) Slot antenna integrates with FET [64]. Both are in microstrip-line circuit configuration.

A simple and effective method of classifying active integrated antennas is to assort them by different functions of active devices they integrate. There are various definitions for active devices or active components. A general definition covering a variety of semiconductor devices is used here [12]. By this definition, the active component is the device which can be used for amplification, rectification, or to change energy from one form to another. Basic active circuits such as oscillators, amplifiers, mixers, and multipliers are all employing active devices with above functions. The active devices in these circuits generate the RF signal, amplify the RF signal, or convert the signal to different frequencies. Therefore, the basic functions of active circuits are oscillating, amplifying, and frequency converting. The active integrated antennas can then be classified into three basic groups, namely, the oscillator type [22]–[32], the amplifier type [33]–[38], and the frequency conversion type [39]–[47]. These three types of active integrated antennas may be combined further to have complex functions in a single module, e.g., the active transceiver module [48], [49]. The circuit structures of these three types of active integrated antennas are discussed in the next section.

III. Circuit Structures of Active Integrated Antennas

The active integrated antenna integrates active devices and passive antenna elements on the same substrate. Semiconductor devices and printed circuit antennas are usually used as the active devices and passive antenna elements, respectively. They have the advantages of low cost, low profile, and light weight.

A. Oscillator Type

A prototype of the oscillating active integrated antenna integrates an active device functioning as an oscillator and a passive radiating element at its output port. It is also called a quasi-optical oscillator since the generated RF power radiates into free space. Because of the strong need of compact, high power sources at millimeter wave frequencies, this type of work has received great attention recently [53]–[67].

Two terminal devices, e.g., IMPATT diodes and Gunn diodes, as well as three-terminal devices, e.g., MESFET's, HEMT's and HBT's, can be used as the active sources. The

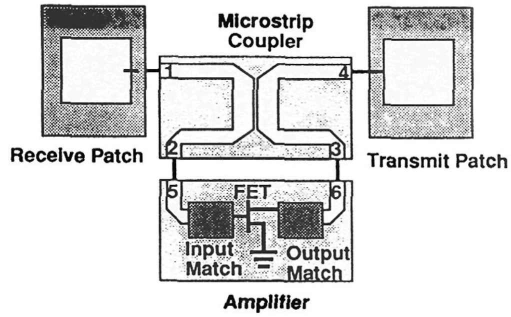

Fig. 2. Schematic of a two-port quasi-optical oscillator [31].

early development of active integrated antennas at microwave and millimeter-wave frequencies concentrated first on two-terminal devices and then moved to three-terminal devices [22]–[32]. Two-terminal devices are suitable for high power applications at millimeter-wave frequencies, but have the disadvantage of low DC-to-RF efficiency. The heat dissipation is usually an important consideration in circuit design [22]–[24]. Three-terminal devices, on the other hand, have the advantage of high DC-to-RF efficiency but are limited by the lower cutoff frequencies. Recently, however, state-of-the-art technologies of HBT and HEMT showed the great performances of high gain, high DC-to-RF efficiency, and low noise figure at millimeter-wave frequencies [68], [69]. Three-terminal devices have another advantage of easy integration with planar circuit structure, either in a hybrid or monolithic approach. The advantages and improved performance of three-terminal devices has made them important in the active integrated antennas.

Microstrip resonant antennas such as patch antennas and slot antennas are usually used as the radiating elements. They are not only the output loads of oscillators, but also serve as the resonators determining oscillation frequencies. The input impedance of the antenna element is therefore an important information for designing oscillator type active integrated antennas. In order to have a tunable quasi-optical oscillator, varactors or other tuning elements may be employed in the circuit [26]. For this type of broadband application, other antenna elements, e.g., notch and bow tie antennas, are preferred in the design [22], [30].

Two examples of oscillator type active integrated antennas are shown in Fig. 1 [62], [64]. One integrates a Gunn diode and a patch antenna. The other integrates an FET and a slot antenna. Both devices are packaged devices and the circuit patterns are fabricated on RT/duroid® substrates. These two quasi-optical oscillators serve as transmitter modules and can be integrated periodically in an array structure to increase the power.

Injection locking is an important technique in oscillator type active integrated antennas. Inter-injection-locking of coupled oscillators has been studied and applied to quasi-optical power-combining arrays as well as phased arrays [51], [54], [56]. In addition to the inter-injection-locking of one-port oscillators, two-port oscillators injection-locked by external signals also can be applied to power-combining arrays and phased arrays [28], [31]. An example of two-port quasi-optical oscillator is shown in Fig. 2. This active integrated antenna consists

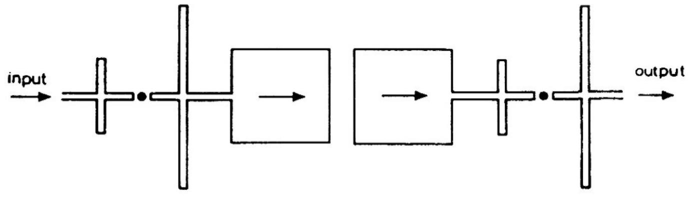

(a) (b)

Fig. 3. Amplifier type active integrated antennas [36]. (a) Transmit antenna. (b) Receive antenna. Black dots indicate the sites of two-port active devices. Arrows within the patches indicate the polarization.

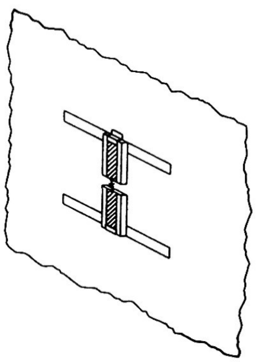

Fig. 4. Quasi-optical mixer—an example of frequency conversion type active integrated antenna [39]. Two slots coupled to the mixer diode by microstrip lines. DC and IF circuitry not shown.

of two antenna elements, one for transmitting and the other for receiving. It is capable of receiving external signals for injection locking. The radiating patch is not used as a resonator so that the Q value of the circuit is smaller than that of the one-port quasi-optical oscillator. The injection locking range is thus increased [28].

B. Amplifier Type

The amplifier type active integrated antenna integrates a two-port active device and passive antenna elements at its input or output port (Fig. 3). When the antenna is at input port only, this active integrated antenna works as a receiver [34]–[36]. The noise performance is of great importance and the low-noise amplifier (LNA) design techniques are applied [38]. When the antenna is at output port only, the active integrated antenna works as a transmitter [33], [36]. When antenna elements are integrated at both input and output ports, the circuit becomes a quasi-optical amplifier where it receives and transmits signals spatially with amplification [37]. The implementation of amplifiers in a passive antenna structure increases the antenna gain and bandwidth, and improves the noise performance. The amplifier type active integrated antenna modules can be integrated in an array structure to increase the power handling capability.

The amplifier type active integrated antenna did not receive as much attention as the oscillator type in the past few years. However, similar to the recent development of quasi-optical amplifier using grid array approach [19], research interest in the amplifier type active integrated antenna is now growing.

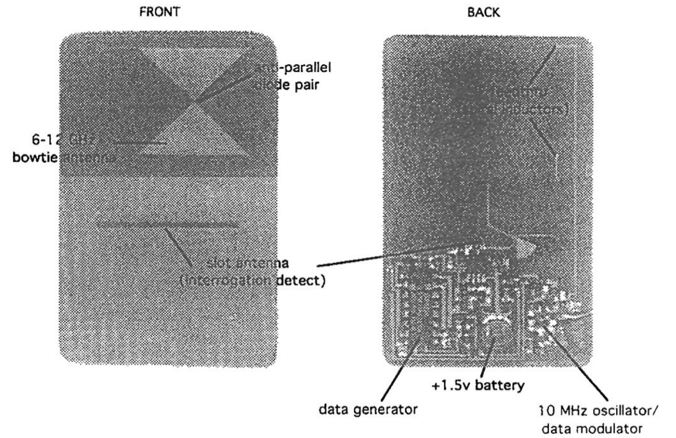

Fig. 5. A noncontact identification transponder [47]. Slot antenna is used to detect the interrogation signal at 6 GHz and turns on the IF circuitry. Bow tie antenna receives the signal at 6 GHz and responds with a modulated signal at 12 GHz.

C. Frequency Conversion Type

The development of frequency conversion type active integrated antennas can be traced back as early as 1977 [39]. A quasi-optical mixer at 100–120 GHz was invented to replace the waveguide mixer (Fig. 4). This concept of quasi-optical approach initialized the development of frequency conversion type active integrated antennas [40]–[47]. Most of the effort was concentrated on the quasi-optical mixer, but some of the works on quasi-optical multipliers were also reported [50], [52]. Recently, with interests in simple and low-cost components for intelligent highway systems and non-contact ID's, quasi-optical transponders using self-oscillating mixers or subharmonically pumped mixers became an interesting subject [46], [47].

A quasi-optical mixer integrates a receiving antenna and a mixer together, and functions as a receiver front end. The local oscillator (LO) can be integrated on the same substrate, or can be supplied by an external source through free space. Instead of using a separate LO, a self-oscillating mixer can be used, which utilizes the nonlinear property of oscillating device itself to perform the frequency conversion [42]. At millimeter-wave frequencies, LO with sufficient power level to drive the mixer is hard to achieve. In this case, a subharmonically pumped mixer using an LO frequency at one-half the value required for a conventional mixer is preferred [41]. A practical application of using the harmonically pumped mixer on a non-contact identification transponder was invented [47]. This transponder receives an interrogation signal at 6 GHz as the harmonically pumped LO power and responds with a modulated ID code around 12 GHz (Fig. 5). A broadband bow tie antenna is used for receiving as well as transmitting.

D. Transceiver Module of Active Integrated Antenna

The function of active integrated antenna is not limited in the above three basic types. Some of the oscillator type active integrated antenna circuits can be modified slightly for use as transceiver circuits [48], [49]. In these circuits, FETs perform a dual function, serving as the source for the transmitted signal

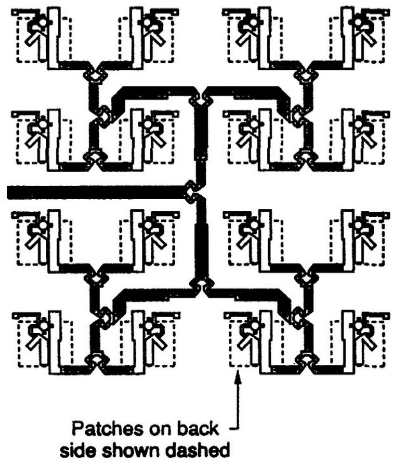

Fig. 6. A 4 × 4 FET oscillator array for power combining [55]. All 16 elements are locked in the same phase by an external signal.The radiation pattern have its main beam at broadside.

and as a self-oscillating mixer for down-conversion of the received signal [49]. This type of circuit can be used as the CW Doppler transceiver module [48].

IV. Applications of Active Integrated Antenna Array

Individual active antenna elements can be integrated in an array structure for various applications. The main advantage of doing this is to increase the power handling capability of solid state devices. By integrating numbers of active devices in the array structure for quasi-optical application, the radiated power from individual active devices can be combined in parallel. The integration of active antenna elements in arrays is not limited to power combining, however. An additional advantage from the phase relationship of array elements provides a very interesting application in active phased arrays. In this section, examples of various applications are discussed.

A. Active Integrated Power-Combining Array

Quasi-optical power combining using either the active antenna approach or grid approach has been an area of growing interest. For the active antenna approach, oscillator type of active integrated antenna arrays received most of the attention and several achievements have been reported [53]–[57], [59]–[67]. The major difficulty of this type of work is to synchronize numbers of oscillators at the same frequency as well as same phase. This technical feature makes it challenging and attractive.

There are different ways to synchronize coupled oscillators. The oscillators can be injection-locked by an external signal or by mutual synchronization of oscillators themselves. An example of externally injection-locked power-combining array is a 4 × 4 FET oscillator array [55], as shown in Fig. 6. The oscillators are all locked to the external signal at the same frequency and same phase. The power is then combined spatially in the broadside direction.

The advantage of mutually synchronized oscillator arrays is that no external source is needed. The internal mechanism of mutual synchronization is known as inter-injection locking [51]. There are two different ways for mutual synchronization.

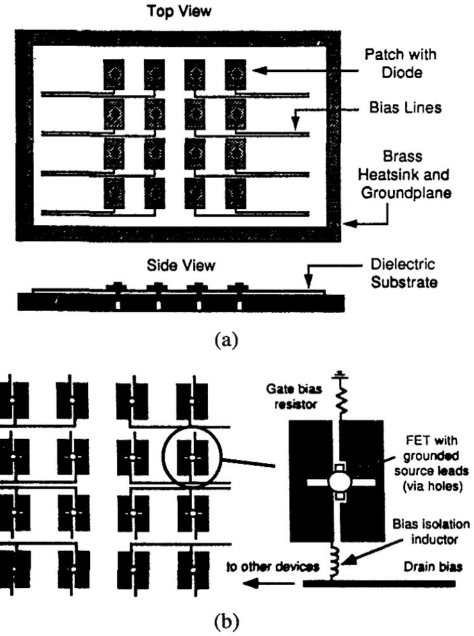

Fig. 7. 4 × 4 weakly coupled oscillator arrays [54]. (a) Gunn diodes integrate with patches. (b) FET's integrate with patches. The dielectric reflector facilitating the mutual synchronization is not shown.

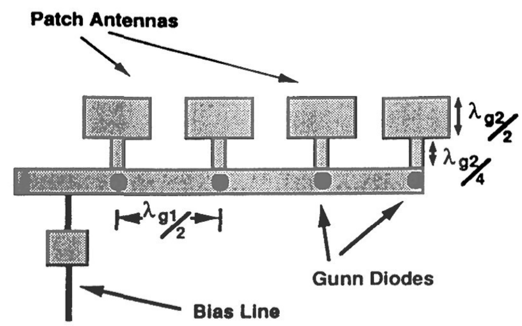

Fig. 8. A strongly coupled oscillator array for second harmonic power combining [56]. The microstrip line connecting Gunn diodes forms a strong coupling network. Packaged Gunn diodes designed to operate at X-band were used to generate second harmonic powerat 18.6 GHz.

One is to use weak coupling via radiation and the other is to use strong coupling via coupling lines connecting oscillators. An example of the weak coupling type power-combining array is a coupled oscillator array integrating patch antennas and active devices [54], as shown in Fig. 7. The weakly coupled oscillator array has the advantage of simple circuit structure. However, the coupling via radiation cannot be controlled easily. On the other hand, the strong coupling by means of connection via transmission line structures can be controlled by circuit design. An example of a strongly coupled oscillator array is a second harmonic spatial power combiner shown in Fig. 8 [56]. The circuit is designed to enhance the output power of its second harmonic component. This is a good method of obtaining high power at higher frequencies by using available active devices working at lower frequencies. In addition, the external reflector required by the weakly coupled oscillator array [54] to enhance the coupling is no longer needed in the strongly coupled oscillator array.

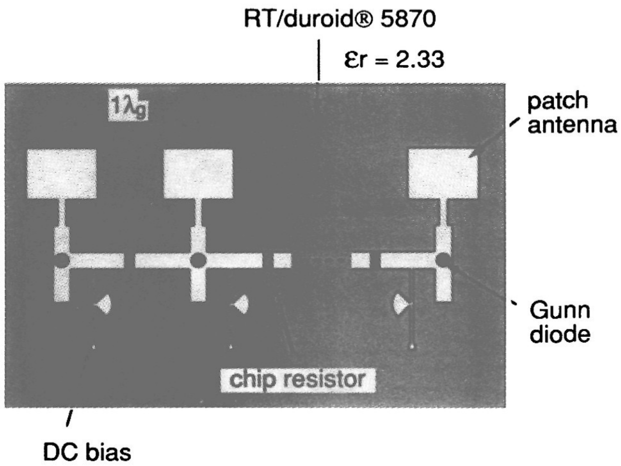

Fig. 9. A linear strongly coupled oscillator array for power combining [62]. Chip resistors are placed at the midpoints of coupling line sections to suppress undesirable modes and stabilize the in-phase mode.

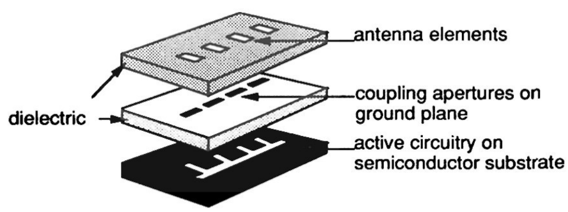

Fig. 10. Exploded view of an active integrated antenna in multilayer structure. This structure is similar to the one in [58].

A problem for a strongly coupled oscillator array is the multimoding problem. As the number of oscillators increases, the number of oscillation modes also increases so that the in-phase mode for power combining may not be achieved readily. This natural phenomenon has been a major problem hindering the development of strongly coupled type power-combining array. One solution to this problem reported recently is the introducing of resistors in the coupling line as mode suppressers [62], as shown in Fig. 9. The in-phase mode is then easily stabilized over a wide DC bias range [63]. Even when some of the devices fail, the remaining active devices still oscillate in the same phase and the power combining still works [67].

The active integrated antenna in multilayer structure is a modern trend for practical applications [58], [59], [66]. Passive antenna elements and active circuitry are designed and optimized in different substrates in this structure. The coupling between active circuitry and antennas is through the coupling apertures on the ground plane separating these two substrates (Fig. 10). The active circuitry can be fabricated on semiconductor substrate monolithically, and the antenna elements can be fabricated on another substrate with a lower dielectric constant for greater radiation efficiency [58]. This type of integration is compatible with MMIC technology.

B. Active Integrated Phased Array

The active integrated antenna array is not limited to power combining in the broadside direction. It can function as a phased array by controlling the phase relation of array elements. Traditional phased array design using phase shifters can

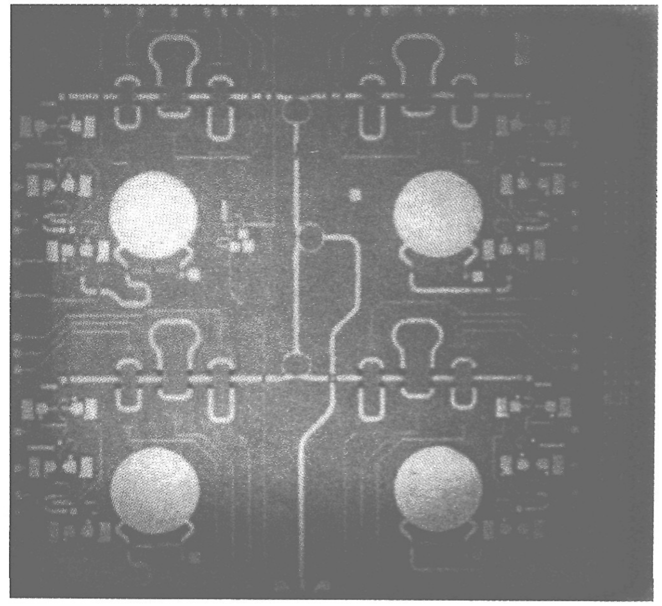

Fig. 11. Photograph of the monolithic 2 × 2 active transmittingsubarray for phased array application [69]. This circuit is designed at 44 GHz using HEMT technology.

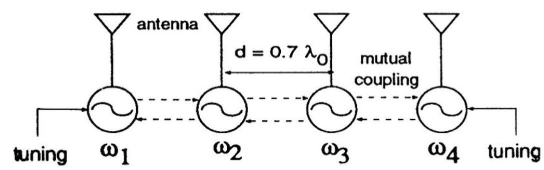

Fig. 12. Schematic of a phase-shifterless beam-scanning array [71]. Mutual coupling synchronizes the oscillators at the same frequency. A constant phase progression is created by slightly tuning the free-running frequencies of end elements.

be directly used for phase control. A monolithic 44 GHz (Q-band) active phased array was designed in this way [68], [69]. Amplifiers, phase shifters, and patch antennas are integrated on a 7 mm × 7 mm chip using pseudomorphic InGaAs/GaAs HEMT MMIC technology (Fig. 11).

Instead of using phase shifters, a method of using inter-injection locking to establish a progressive phase shift was proposed [51]. Based on this method, beam-scanning arrays using weakly or strongly coupled oscillators were demonstrated [70]–[72]. By slightly adjusting the free-running frequencies of end elements, a constant phase progression is created (Fig. 12). This simple method eliminates the use of phase shifters and makes it possible to steer the beam continuously. To increase the locking bandwidth and thus relax the frequency restrictions for mutual synchronization, strong coupling is preferred in this design [72]. However, the multimoding effect associated with strong coupling needs to be considered for large-scale arrays.

Another method of eliminating phase shifters and obtaining continuous beam scanning is to use unilateral injection locking for coupled oscillator arrays [73], as shown in Fig. 13. The inter-injection locking is a natural phenomenon for coupled oscillator arrays. To isolate the injection locking in only one direction, unilateral amplifiers are used as isolators. The multimoding problem is eliminated and the phase of each oscillator can be controlled independently. Active phased

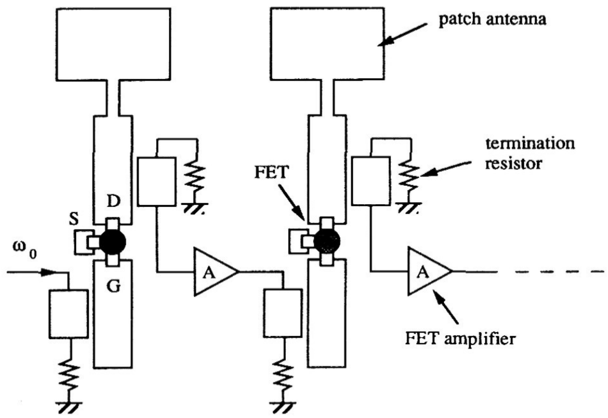

Fig. 13. A unilateral injection-locked oscillator array for beam scanning [73]. All oscillators are locked at the same frequency of the external signal. Phase of each oscillator is controlledby tuning its free-running frequency. Amplifiers are used to isolate the reverse injection locking.

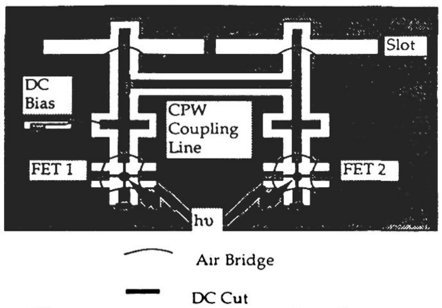

Fig. 14. An oscillator type two-element active slot antenna arrayin CPW structure [77]. The optical illumination on active devices changes the oscillation frequency.

arrays capable of scanning both difference and sum patterns were demonstrated [73]. This method provides more flexibility and controlling capability in circuit design since the injection signal propagates in one direction.

C. Optical Control of Active Integrated Antenna

The optical control of solid state device introduces additional capability of controlling active circuits. In addition to the electronic tuning, optical tuning of active integrated antennas was investigated [74]–[76]. By changing the intensity of optical illumination on the FET chip, the operating frequencies of oscillator type active integrated antennas can be tuned.

Optical tuning ranges of three different types of devices were investigated [77]. They are GaAs MESFET, AlGaAs/GaAs HEMT, and AlGaAs/InGaAs pseudomorphic HEMT. These three devices were used in a two-element CPW active slot antenna array as active sources (Fig. 14). This active integrated antenna oscillated around 10 GHz. The optical tuning ranges of using MESFET, HEMT, and pseudomorphic HEMT were about 1%, 0.1%, and 0.1%, respectively. Although the smaller tuning range using HEMT devices may be due to the thin active channel layer which is less sensitive to the optical illumination, the mixed mechanism of photovoltaic and photoconductive effects should be investigated further.

It should be noted that none of the above active devices were optimized for optical control, especially for the optical reactance control. To date, these active devices are used for

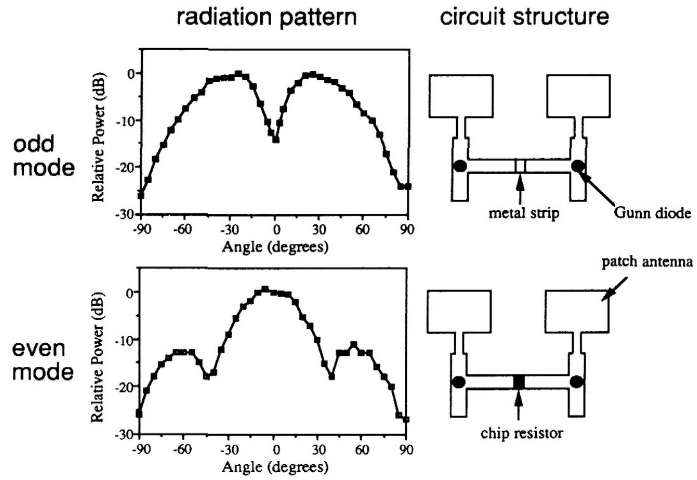

Fig. 15. A two-element mode-switching array [79]. Oscillation modes as well as radiation patterns are changed by the circuit elements at the midpoint of strong coupling line. This active antenna integrates Gunn diodes and patches in microstrip-line circuit configuration. The radiation patterns are in H-plane.

high frequency power generation or amplification and are optimized for that purpose. If active devices can be optimized for optical reactance control as well, the size and cost for active circuits can be reduced.

Small semiconductor laser diodes can be used as the source for optical illumination, and the optical fiber can be used to transmit the control signal [78]. This allows the integration of photonic circuits with microwave circuits. The control signal transmitted by the optical fiber is free from the electromagnetic interference with microwave circuits. In addition to the frequency tuning of quasi-optical oscillators, this type of technology can be applied to other active antenna circuits, e.g., active integrated phased arrays. Sophisticated functions such as the beam scanning can be controlled by optical signals.

V. Electromagnetic Characterization of Active Integrated Antenna

The active integrated antenna consists of active devices, feed networks, and radiating elements. When they are integrated in a small chip, the structure may be too complicated to be analyzed by traditional CAD tools. Even if the structure is simple, its function may be too complex to be analyzed by traditional CAD tools either. A good example is a two-element strongly coupled active antenna [79]. This circuit is composed of two identical Gunn oscillators which are connected by a coupling line, as shown in Fig. 15. Two kinds of modes, even mode and odd mode, exist in this symmetrical system. This active integrated antenna, which employs nonlinear devices and operates under large signal oscillation, cannot be simulated by frequency-domain CAD tools to predict the correct stable oscillation mode. Although this multimode oscillator can be analyzed by the averaged potential theory to predict the correct mode [79], electromagnetic characteristics of the whole circuit cannot be simulated. As the electromagnetic coupling of circuit elements becomes stronger, the circuit becomes complicated and an electromagnetic simulator is essential. Unfortunately, none of the commercially available electromagnetic CAD tools can handle the nonlinear active devices.

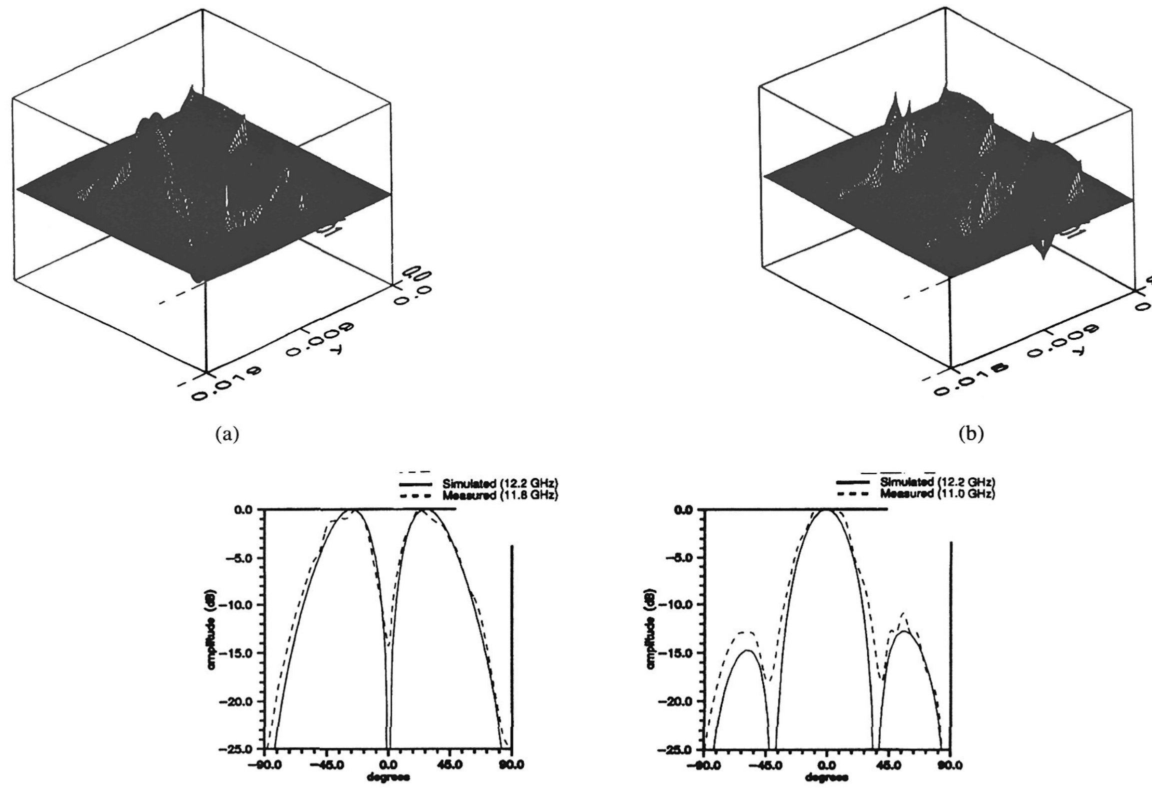

Fig. 16. FDTD simulation of the active integrated antenna in Fig. 15 [81]. (a) Steady-state oscillation with metal strip—odd mode. (b) Steady-state oscillation with chip resistor—even mode. Electric field component E_z on the substrate (dielectric-air interface) at an instant time is shown. (c) Far-field radiation patterns. Left-hand side: odd mode. Right-hand side: even mode.

The extended finite-difference time-domain (FDTD) approach is a good solution to this problem. It simulated the above example by rigorous full-wave analysis in time domain. Nonlinear device model and passive circuit elements are incorporated. The transient behavior of oscillations building up from noise level was simulated and the correct stable mode was obtained [80], [81]. The dynamic electromagnetic field distribution as well as the radiation patterns can be displayed (Fig. 16). This kind of simulator is robust and can handle complex circuit structures.

The disadvantage of FDTD method is its intensive computation time. Some efforts were made to reduce the computation time, e.g., the Diakoptics method and system identification technique [82]. On the other hand, the frequency-domain electromagnetic simulation utilizing spectral-domain approach (SDA) saves the computation time. The same example in Fig. 15 was simulated by SDA and all the possible oscillation modes were located by the rigorous full-wave analysis [83]. The oscillation frequencies were closer to the measured ones than the FDTD approach.

Whether in time domain or frequency domain, an electromagnetic simulation tool capable of simulating nonlinear active circuits is very useful in designing active integrated antennas. It will become very important for accurate design of active integrated antennas as their circuit structures and functions become complicated. In the future, with the aid of electromagnetic simulators, active integrated antennas with advanced functions can be designed more easily.

VI. Conclusion

In this paper, the progress of active integrated antennas is reviewed. A classification of active integrated antennas based on different functions of active devices is proposed. Structures of different active integrated antennas are reviewed and discussed. By integrating numbers of active modules, active integrated antenna arrays with various functions can be achieved. Applications in power-combining arrays and phased arrays are given as examples, and the application of optically controlled active integrated antenna is also discussed. A brief description of recent development of electromagnetic characterization of active integrated antenna is included in this paper. Both time-domain and frequency-domain simulations are discussed and compared.

It can be seen that the active integrated antenna will have versatile applications in the growing area of wireless communications. The key requirements for components and systems to be used in wireless communications are compactness, light weight, low cost, low DC power consumption, high DC-to-RF conversion efficiency, and high reliability. The concept of active integrated antenna satisfies the first three requirements and, with the improving performance of solid state devices, the last three requirements can also be satisfied. Some of the techniques developed for system application, e.g., active integrated phased arrays, can be foreseen to be promising candidates in the future products. The active integrated phased array technique will help lower power consumption and avoid unnecessary interference resulting from radiation in unwanted directions.

At millimeter-wave frequencies, the antenna size becomes very small so that it is possible to integrate the active antenna on a small chip [58], [69]. To optimize the antenna performance and avoid both layout and electromagnetic interference with active circuitry, the multilayer structure is a good choice for chip-level active integrated antennas. Different layers carrying different functions can be stacked together to achieve state-of-the-art performance. It is believed that the full development of active integrated antennas will bring the wireless communication technology into a new era.

ACKNOWLEDGMENT

The authors would like to thank Dr. A. R. Mickelson and Ms. K. Y. Chen in University of Colorado at Boulder for providing early literature of active antennas. Useful comments from Mr. C. W. Pobanz and Mr. S. T. Chew are appreciated.

REFERENCES

[1] H. A. Wheeler, "Small antennas," *IEEE Trans. Antennas Propagat.*, vol. AP-23, pp. 462–469, July 1975.

[2] J. R. Copeland, W. J. Robertson, and R. G. Verstraete, "Antennafier arrays," *IEEE Trans. Antennas Propagat.*, vol. AP-12, pp. 227–233, Mar. 1964.

[3] H. H. Meinke, "Active antennas," *Nachrichtentech. Z.*, vol. 19, pp. 697–705, Dec. 1966.

[4] A. P. Anderson, W. S. Davies, M. M. Dawoud, and D. E. Galanakis, "Notes on transistor-fed active-array antennas," *IEEE Trans. Antennas Propagat.*, vol. AP-19, pp. 537–539, July 1971.

[5] M. M. Dawoud and A. P. Anderson, "Calculations showing the reduction in the frequency dependence of a two-element array antenna fed by microwave transistors," *IEEE Trans. Antennas Propagat.*, vol. AP-20, pp. 497–499, July 1972.

[6] ——, "The performance of transistor fed monopoles in active antennas," *IEEE Trans. Antennas Propagat.*, vol. AP-21, pp. 371–374, May 1973.

[7] M. I. Kontorovich and N. M. Lyapunova, "Active antennas," *Radio Eng. Electron. Phys.* vol. 19, pp. 126–127, 1974.

[8] T. S. M. Maclean and P. A. Ramsdale, "Short active aerials for transmission," *Int. J. Electron.*, vol. 36, pp. 261–169, Feb. 1974.

[9] M. M. Dawoud and A. P. Anderson, "Experimental verification of the reduced frequency dependence of active receiving arrays," *IEEE Trans. Antennas Propagat.*, vol. AP-22, pp. 342–344, Mar. 1974.

[10] P. K. Rangole and S. S. Midha, "Short antenna with active inductance," *Electron. Lett.*, vol. 10, pp. 462–463, Oct. 1974.

[11] J.-P. Daniel and C. Terret, "Mutual coupling between antennas-optimization of transistor parameters in active antenna design," *IEEE Trans. Antennas Propagat.*, vol. AP-23, pp. 513–516, July 1975.

[12] B. Grob, *Basic Electronics*, 6th ed. New York: McGraw-Hill, 1959, ch. 8.

[13] J. W. Mink, "Quasi-optical power combining of solid-state millimeter-wave sources," *IEEE Trans. Microwave Theory Tech.*, vol. MTT-34, pp. 273–279, Feb. 1986.

[14] W. W. Lam, C. F. Jou, H. Z. Chen, K. S. Stolt, N. C. Luhmann, Jr., and D. B. Rutledge, "Millimeter-wave diode grid phase shifters," *IEEE Trans. Microwave Theory Tech.*, vol. MTT-36, pp. 902–907, May 1988.

[15] ——, "Millimeter-wave diode grid frequency doubler," *IEEE Trans. Microwave Theory Tech.*, vol. MTT-36, pp. 1507–1514, Nov. 1988.

[16] Z. B. Popovic, R. M. Weikle II, M. Kim, and D. B. Rutledge, "A 100-MESFET planar grid oscillator," *IEEE Trans. Microwave Theory Tech.*, vol. 39, pp. 193–200, Feb. 1991.

[17] R. M. Weikle II, M. Kim, J. B. Hacker, M. P. De Lisio, Z. B. Popovic, and D. B. Rutledge, "Transistor oscillator and amplifier grids," *Proc. IEEE*, vol. 80, pp. 1800–1809, Nov. 1992.

[18] A. Pance and M. J. Wengler, "Microwave modeling of 2-D active grid antenna arrays," *IEEE Trans. Microwave Theory Tech.*, vol. 41, pp. 20–28, Jan. 1993.

[19] M. Kim *et al.*, "A 100-element HBT grid amplifier," *IEEE Trans. Microwave Theory Tech.*, vol. 41, pp. 1762–1771, Oct. 1993.

[20] L. B. Sjogren *et al.*, "A monolithic diode array millimeter-wave beam transmittance controller," *IEEE Trans. Microwave Theory Tech.*, vol. 41, pp. 1782–1790, Oct. 1993.

[21] K. D. Stephan, P. H. Spooner, and P. F. Goldsmith, "Quasi-optical millimeter-wave hybrid and monolithic PIN diodes switches," *IEEE Trans. Microwave Theory Tech.*, vol. 41, pp. 1791–1798, Oct. 1993.

[22] D. B. Rutledge, D. P. Neikir,k and D. P. Kasilingam, "Integrated circuit antennas," in K. J. Button, Ed. *Infrared and Millimeter-Waves.* London: Academic Press, vol. 10, 1983, p. 25.

[23] H. J. Thomas, D. L. Fudge, and G. Morris, "Gunn source integrated with microstrip patch," *Microwave RF*, pp. 87–91, Feb. 1985.

[24] N. Camilleri and B. Bayraktaroglu, "Monolithic millimeter-wave IMPATT oscillator and active antenna," *IEEE Trans. Microwave Theory Tech.*, vol. MTT-36, pp. 1670–1676, Dec. 1988.

[25] R. A. York, R. M. Martinez, and R. C. Compton, "Hybrid transistor and patch antenna element for array applications," *Electron Lett.*, vol. 26, pp. 494–495, Mar. 1990.

[26] J. A. Navarro, K. A. Hummer, and K. Chang, "Active integrated antenna elements," *Microwave J.*, vol. 34, pp. 115–126, Jan. 1991.

[27] R. E. Miller and K. Chang, "Integrated active antenna using annular ring microstrip antenna and Gunn diode," *Microwave Optical Tech. Lett,* vol. 4, no. 2, pp. 72–75, Jan. 20, 1991.

[28] J. Birkeland and T. Itoh, "Two-port FET oscillators with applications to active arrays," *IEEE Microwave Guided Wave Lett.*, vol. 1, pp. 112–113, May 1991.

[29] ——, "A circularly polarized FET oscillator active radiating element," *IEEE MTT-S Int. Microwave Symp. Dig.*, vol. 3, June 10–14, 1991, pp. 1265–1268.

[30] J. A. Navarro, Y-H. Shu, and K. Chang, "Broadband electronically tunable planar active radiating elements and spatial power combiners using notch antennas," *IEEE Trans. Microwave Theory Tech.*, vol. 40, pp. 323–328, Feb. 1992.

[31] J. Birkeland and T. Itoh, "An FET oscillator element for spatially injection locked arrays," in 1992 *IEEE MTT-S Int. Microwave Symp. Dig.*, vol. 3, June 1–5, 1992, pp. 1535–1538.

[32] M. Vaughan and R. C. Compton, "Resonant-tee cpw oscillator and the application of the design to a monolithic array of MESFET's," *Electron. Lett.*, vol. 29, no. 16, pp. 1477–1479, Aug. 1993.

[33] D. J. Roscoe, A. Ittipiboon, and L. Shafai, "The development of an active integrated microstrip antenna," *IEEE AP-S Int. Symp. Dig.*, vol. 1, June 24–28, 1991, pp. 48–51.

[34] R. Gillard, H. Legay, J. M. Floc'h, and J. Citerne, "Rigorous modeling of receiving active microstrip antenna," *Electron. Lett.*, vol. 27, no. 25, pp. 2357–2359, Dec. 1991.

[35] B. Robert, T. Razban, and A. Papiernik, "Compact amplifier integration in square patch antenna," *Electron. Lett.*, vol. 28, no. 19, pp. 1808–1810, Sept. 1992.

[36] P. S. Hall, "Analysis of radiation from active microstrip antennas," *Electron. Lett.*, vol. 29, pp. 127–129, Jan. 1993.

[37] C-Y. Yu and G. M. Rebeiz, "A quasi-optical amplifier," *IEEE Microwave Guided Wave Lett.*, vol. 3, pp. 164–166, June 1993.

[38] H. An, B. Nauwelaers, and A. Van de Capelle, "On the characterization of active receiving microstrip antennas," *IEEE Trans. Antennas Propagat.*, to appear.

[39] A. R. Kerr, P. H. Siegel and R. J. Mattauch, "A simple quasi-optical mixer for 100–120 GHz," *IEEE MTT-S Int. Microwave Symp. Dig.*, 1977, pp. 96–98.

[40] K. D. Stephen, N. Camilleri, and T. Itoh, "A quasi-optical polarization-duplexed balanced mixer for millimeter-wave applications," *IEEE Trans. Microwave Theory Tech.*, vol. MTT-31, pp. 164–170, Feb. 1983.

[41] K. D. Stephen and T. Itoh, "A planar quasi-optical subharmonically pumped mixer characterized by isotropic conversion loss," *IEEE Trans. Microwave Theory Tech.*, vol. MTT-32, pp. 97–102, Jan. 1984.

[42] V. D. Hwang and T. Itoh, "Quasi-optical HEMT and MESFET self-oscillating mixers," *IEEE Trans. Microwave Theory Tech.*, vol. MTT-36, pp. 1701–1705, Dec. 1988.

[43] J. Zmuidzinas and H. G. LeDuc, "Quasi-optical slot antenna SIS mixers," *IEEE Trans. Microwave Theory Tech.*, vol. 40, pp. 1797–1804, Sept. 1992.

[44] P. A. Stimson, R. J. Dengler, H. G. LeDuc, S. R. Cypher, and P. H. Siegel, "A planar quasi-optical SIS receiver," *IEEE Trans. Microwave Theory Tech.*, vol. 41, pp. 609–615, April 1993.

[45] S. V. Robertson, N. I. Dib, G. Yang, and L. P. B. Katehi, "A folded slot antenna for planar quasi-optical mixer applications," in 1993 *IEEE AP-S Int. Symp. Dig.*, vol. 2, pp. 600–603, June 1993.

[46] K. Cha, S. Kawasaki, and T. Itoh, "Transponder using self-oscillating mixer and active antenna," to be appeared in the 1994 *IEEE MTT-S Int. Microwave Symp.*, San Diego, CA, May 23–27, 1994.

[47] C. W. Pobanz and T. Itoh, "A microwave non-contact identification transponder using subharmonic interrogation," to be appeared in the *1994 IEEE MTT-S Int. Microwave Symp.*, San Diego, CA, May 23–27, 1994.

[48] J. Birkeland and T. Itoh, "A microstrip based active antenna Doppler transceiver module," in *19th European Microwave Conf. Proc.*, Sept. 1989, pp. 172–178.

[49] ——, "FET-based planar circuits for quasi-optical sources and transceivers," *IEEE Trans. Microwave Theory Tech.*, vol. 37, pp. 1452–1459, Sept. 1989.

[50] N. Camilleri and T. Itoh, "A quasi-optical multiplying slot array," *IEEE Trans. Microwave Theory Tech.*, vol. MTT-33, pp. 1189–1195, Nov. 1985.

[51] K. D. Stephan, "Inter-injection-locked oscillators for power combining and phased arrays," *IEEE Trans. Microwave Theory Tech.*, vol. MTT-34, pp. 1017–1025, Oct. 1986.

[52] S. Nam, T. Uwano, and T. Itoh, "Microstrip-fed planar frequency-multiplying space combiner," *IEEE Trans. Microwave Theory Tech.*, vol. MTT-35, pp. 1271–1276, Dec. 1987.

[53] J. Birkeland and T. Itoh, "Spatial power combining using push-pull FET oscillators with microstrip patch resonators,"*IEEE MTT-S Int. Microwave Symp. Dig.*, vol. 3, 1990, pp. 1217–1220.

[54] R. A. York and R. C. Compton, "Quasi-optical power combining using mutually synchronized oscillator arrays," *IEEE Trans. Microwave Theory Tech.*, vol. 39, pp. 1000–1009, June 1991.

[55] J. Birkeland and T. Itoh, "A 16-element quasi-optical FET oscillator power-combining array with external injection locking," *IEEE Trans. Microwave Theory Tech.*, vol. 40, pp. 475–481, Mar. 1992.

[56] A. Mortazawi, H. D. Foltz, and T. Itoh, "A periodic second harmonic spatial power-combining oscillator," *IEEE Trans. Microwave Theory Tech.*, vol. 40, pp. 851–856, May 1992.

[57] S. Kawasaki and T. Itoh, "40 GHz quasi-optical second harmonic spatial power combiner using FETs and slots," in *1992 IEEE MTT-S Int. Microwave Symp. Dig.*, vol. 3, June 1–5, 1992, pp. 1543–1546.

[58] H. Ohmine and A. Iida *et al.*, "An MMIC aperture-coupled microstrip antenna in the 40 GHz Band," in *Proc. ISAP*, pp. 1105–1108, 1992.

[59] J. Lin and T. Itoh, "A 4×4 spatial power-combining array with strongly coupled oscillators in multilayer structure," *IEEE MTT-S Int. Microwave Symp. Dig.*, vol. 2, Atlanta, GA, June 14–18, 1993, pp. 607–610.

[60] A. Mortazawi and B. C. DeLoach, "A nine-MESFET two-dimensional power-combining array employing an extended resonance technique," *IEEE Microwave Guided Wave Lett.*, vol. 3, pp. 214–216, July 1993.

[61] S. Kawasaki and T. Itoh, "Second harmonic uniplanar active integrated antenna array with strong coupling," *23rd European Microwave Conf. Procs.*, vol. 1, Sept. 1993, pp. 204–206.

[62] S. Nogi, J. Lin, and T. Itoh, "Mode analysis and stabilization of a spatial power-combining array with strongly coupled oscillators," *IEEE Trans. Microwave Theory Tech.*, vol. 41, pp. 1827–1837, Oct. 1993.

[63] J. Lin, S. Nogi and T. Itoh, "Frequency tuning of a spatial power combining array using strongly coupled oscillators," *Proc. 1993 Asia-Pac. Microwave Conf.*, Hsinchu, Taiwan, Oct. 1993, pp. 1.26–1.29.

[64] S. Kawasaki and T. Itoh, "Quasi-optical planar arrays with FET's and slots," *IEEE Trans. Microwave Theory Tech.*, vol. 41, pp. 1838–1844, Oct. 1993.

[65] A. Balasubramaniyan and A. Mortazawi, "Two-dimensional MESFET-based spatial power combiners," *IEEE Microwave Guided Wave Lett.*, vol. 3, pp. 366–368, Oct. 1993.

[66] J. Lin and T. Itoh, "Two-dimensional quasi-optical power-combining arrays using strongly coupled oscillators," *IEEE Trans. Microwave Theory Tech.*, vol. 42, pp. 734–741, Apr. 1994.

[67] ——, "Experiment of device failures in a spatial power-combining array," *IEEE Trans. Microwave Theory Tech.*, to appear.

[68] H. C. Yen, R. Esfandiari, Y. Hwang, K. Tan, C. Liu, *et al.*, "A monolithic approach for Q-band integrated active phased array transmitting antenna," *IEEE AP-S Int. Symp. Dig.*, vol. 1, pp. 126–129, July 1992.

[69] H. Wang *et al.*, "Monolithic Q band active array module and antenna," *Applied Microwave*, vol. 5, no. 1, pp. 88, 91–94, 96, 99–100, 102, Winter 1993.

[70] J. A. Navarro and K. Chang, "Electronic beam steering of active antenna arrays," *Electron. Lett.*, vol. 29, no. 3, pp. 302–304, Feb. 1993.

[71] P. Liao and R. A. York, "Phase-shifterless beam-scanning using coupled-oscillators: theory and experiment," in 1993 *IEEE AP-S Int. Symp. Dig.*, vol. 2, Ann Arbor, MI, June 28–July 2, 1993, pp. 668–671..

[72] ——, "A six-element beam-scanning array," *IEEE Microwave Guided Wave Lett.*, vol. 4, pp. 20–22, Jan. 1994.

[73] J. Lin, S. Chew, and T. Itoh, "A unilateral injection-locking type active phased array for beam scanning," *IEEE MTT-S Int. Microwave Symp. Dig.*, vol. 2, San Diego, CA, May 23–27, 1994, pp. 1231–1234.

[74] S. Kawasaki and T. Itoh, "Optical control of active integrated antenna," *22nd European Microwave Conf. Proc.*, vol. 1, Aug. 1992, pp. 697–701.

[75] J. Lin, S. Kawasaki, and T. Itoh, "Optical control of MESFET's for active filter and active antenna," *Proc. 7th Int. MIOP '93 Conf.*, Sindelfingen, Germany, May 25–27, 1993, pp. 348–352.

[76] S. Kawasaki and T. Itoh, "Optical control of 2-element CPW active integrated antenna with strong coupling," *IEEE AP-S Int. Symp. Dig.*, vol. 3, June 1993, pp. 1616–1619.

[77] S. Kawasaki and T. Itoh, "Optical tuning range comparison of uniplanar active integrated antenna using MESFET, GaAs HEMT and pseudomorphic HEMT," *Proc. Fourth Int. Symp. Space Terahertz Technol.*, Mar. 1993, pp. 149–156.

[78] A. A. A. De Salles, "Optical control of GaAs MESFET's," *IEEE Trans. Microwave Theory Tech.*, vol. MTT-31, pp. 812–820, Oct. 1983.

[79] J. Lin, S. Nogi, and T. Itoh, "Mode switch in a two-element active array" *1993 IEEE AP-S Int. Symp. Dig.*, vol. 2, June 1993, pp. 664–667.

[80] B. Toland, J. Lin, B. Houshmand, and T. Itoh, "FDTD analysis of an active antenna," *IEEE Microwave Guided Wave Lett.*, vol. 3, pp. 423–425, Nov. 1993.

[81] ——, "Electromagnetic simulation of mode control of a two-element active antenna," in *IEEE MTT-S Int. Microwave Symp. Dig.*, vol. 2, San Diego, CA, May 23–27, 1994, pp. 883–886.

[82] T.-W. Huang, B. Houshmand, and T. Itoh, "Fast sequential FDTD Diakoptics method using the system identification technique," *IEEE Microwave Guided Wave Lett,*, vol. 3, pp. 378–380, Oct. 1993.

[83] T. S. Horng, J. Lin, and T. Itoh, "Spectral-domain approach to an active microstrip array," submitted to *IEEE Microwave Guided Wave Lett.*